博士論文

ACCELERATION MECHANISM OF VOID DEVELOPMENT IN CONCRETE SEAWALLS

（コンクリート被覆海岸堤防の空洞化の加速的進行機構）

パムク　アイクット

PAMUK AYKUT

ACCELERATION MECHANISM OF VOID DEVELOPMENT IN CONCRETE SEAWALLS

（コンクリート被覆海岸堤防の空洞化の加速的進行機構）

A dissertation submitted to the Department of Civil Engineering

in partial fulfillment of the requirements

for the degree of Doctor of Engineering

by

パムク　アイクット

PAMUK AYKUT

SEPTEMBER 2017

ABSTRACT

Among the failure modes of the seawalls, the collapse of concrete riprap seawalls due to leakage of backfill material causes destruction on the landward side of the seawall. Through holes or tears on geotextile, sheet walls or filter layers, backfill material can flow out towards the seaside or towards armor layer. Following the leakage of backfill material, the enlargement of voids continues until the soil cannot support the weight above it. Consequently, the collapse of the surface of the backfill takes place behind the seawalls.

In this study, the main objective is to confirm the acceleration of void development and to identify the void expansion mechanism after a void developed inside the backfill of the seawall due to the leakage of the backfill towards the seaside.

To confirm the acceleration of void development, laboratory experiments have been conducted in oscillatory flow tunnel to investigate the acceleration mechanism of the void development in the backfill of a seawall. Toy balloons have been used to simulate the voids that may present in a backfill. The leakage of sand through a small gap from an acrylic container under pressure oscillations have been examined. From the laboratory experiments, it is found that the rate of sand leakage is proportional to the air amount in the soil medium. The larger void appears to accelerate the further enlargement of the void. Following the leakage of soil, the voids enlarge which in turn increases the air amount in soil medium. Consequently, the void development accelerates until the subsidence of the surface of backfill.

Leakage of sand has been found to be closely related to the seepage flow due to the pressure gradient between the soil medium and the water. Therefore, propagation characteristics of the wave-induced pressure influence the leakage of sand. Compressibility and permeability of soil medium have been found to be two significant parameters for the rate of leakage. The introduction of air to the soil increases the compressibility of soil medium. As the compressibility increases, the pressure response is getting poor and high-pressure gradient can be produced. Therefore, the high-pressure gradient will cause more leakage.

As mentioned, another important parameter is the permeability of the soil medium. The pressure response becomes poorer as the permeability decrease. Therefore, similar to

the compressibility, as the soil becomes less permeable, the produced pressure gradient increases. In turn, the high-pressure gradient results in high leakage of the soil grains.

Furthermore, in this dissertation, the wave-induced pressure response has been investigated from the theoretical point of view. A numerical model has been proposed based on the quasi-static assumption on Biot's consolidation equation using finite difference method in the one-dimensional domain. In the verification of the model, earlier researchers' data on wave-induced pressure obtained from laboratory experiments have been utilized. The vertical maximum pressure distributions and instantaneous pressure amplitudes computed from the developed model has been used for the validation.

Moreover, the numerical model has been tested with the parameters of present laboratory experiments. The results from the developed model using appropriate permeability and compressibility values have been compared with the leaked sand and displacements measured during the laboratory experiments. The amount of leaked sand has found to be strongly correlated with the maximum pressure gradients computed near the surface. Also, the displacements in the soil medium due to the pressure oscillations have been found to be related to both pressure gradients and compressibility of balloons.

On the basis of both laboratory experiments and the theoretical approach, the acceleration mechanism of void development has been confirmed. Two mechanisms that accelerate the void development are the pressure gradient between water and soil interface and displacements due to the compressibility of air content. The intensity of these two mechanisms increases as the voids enlarge which further accelerates the void development. Also, a good correlation between model and experiments have been obtained according to the reasoning of this study.

ACKNOWLEDGEMENTS

Firstly, I would like to thank my supervisor Prof. Shinji Sato for his supervision, patience, and encouragement since the beginning of my graduate studies. I enjoy every part of my studies in Coastal Engineering Laboratory of The University of Tokyo, as being the result of his kind-hearted and surely his precious experiences.

I would like to thank Prof. Yoshimitsu Tajima and Assoc. Prof. Takenori Shimozono for their valuable comments, sharing their experiences and knowledge and for their strong contribution to my graduate studies and support.

I would like to thank the committee members Prof. Reiko Kuwano and Prof. Akio Kobayashi for their valuable guidance and comments.

I want to express my deepest gratitude to Ms. Müge Kuleli for her involvement in all parts of my doctoral study and my life as a motivator and supporter.

I want to express my gratitude to my associates and all of my friends in Coastal Engineering Laboratory of The University of Tokyo.

I would like to thank my parents for their supports and everlasting encouragements.

Finally, I gratefully acknowledge Ministry of Education, Culture, Sports, Science, and Technology - MEXT for providing the scholarship which turns a lifelong dream into reality.

TABLE OF CONTENTS

LISTS OF FIGURES

LISTS OF TABLES

I. INTRODUCTION

Seawalls are one of the most common artificial structures that are built around the coasts. They are built to protect the coastal community against stormy conditions. Also, they prevent erosion for the area behind it.

Among the failure modes of the seawalls, the collapse of the filled area due to leakage of backfill material causes destruction on the landward side of the seawall. The general man-made structures constructed just behind the seawalls such as roads, recreational areas or buildings are subjected to the subsidence type of destruction because of the failure of the surfaces of the backfills being a result of the void development and the leakage of the backfill material of the seawalls.

Surfaces of backfills are usually paved with asphalt or concrete. The collapses of these pavements are generally sudden, without giving a warning. Therefore, the subsidence of the pavements due to leakage of backfill causes great threat for the living, as the areas behind seawalls are highly populated considering the attractiveness of the coastal zone.

To protect the backfill material from leakage, in engineering practice, filter layers, sheet walls or geotextile materials are widely used. However, through holes, tears or imperfections on geotextile, sheet walls or filter layers, backfill material can flow out towards the seaside or towards armor layer. Wave pressures, forces or chemical deteriorations on a seawall can create these holes and tears. Also, during the construction stage, the integrity of geotextile can be spoiled during placement of large rocks. Consequently, repeated wave attacks cause the backfill material to leak towards the seaside of the seawall through small imperfections.

As an example, in June 2015, a collapse has been encountered in Zonguldak, Turkey, which is located on the coast of Black Sea (Figure 1). The destruction in the backfill had created nearly 3.5 meters deep and 9 meters wide cave in just behind the seawall. The pavement and a small part of the road have been damaged. From the right picture of Figure 1, it is necessary to see that there is no protection in front of the seawall

Figure 1 The Subsidence of Road and Sidewalk behind a Concrete Seawall in Zonguldak, Turkey (CNN TURK, June 25, 2015)

where the collapse has occurred. Due to lack of protection, backfill material has been leaked easily towards sea side. However, natural rocks have prevented such destruction at the other parts of the seawall. Thus, subsidence of the road and the pavement has occurred just behind the section where there is no natural protection against the effects of strong wave attacks. To the author's knowledge, the presence of a measure against the leakage of backfill material such as geotextile or filter layer is unknown. However, according to the interviews with the authorities, this part of the road has been collapsed 3 times in 10 years. So, even if a measure against the leakage of backfill material is present, there is a problem with the protection of backfill material.

One year later, a site visit to this location has revealed that instead of protecting the backfill material to leak, the municipality has decided to repair only the road and the pavement. Therefore, following the leakage of backfill under wave action, another subsidence failure in the pavement of this section of the seawall can be anticipated.

In the literature, only a handful of studies has focused on especially the leakage of backfill material for the seawalls. From their laboratory experiments, Takahashi et al. (1997) revealed the stages that lead to settlement of backfill pavement (Figure 2). According to the laboratory experiments in a wave flume, at the first stage, the leakage of sand starts (Figure 2a), then the generation of caves observed (Figure 2b). Enlargement of the caves continues until the soil cannot support the weight of soil above developed cave (Figure 2c). Consequently, the collapse of the pavement takes place (Figure 2d).

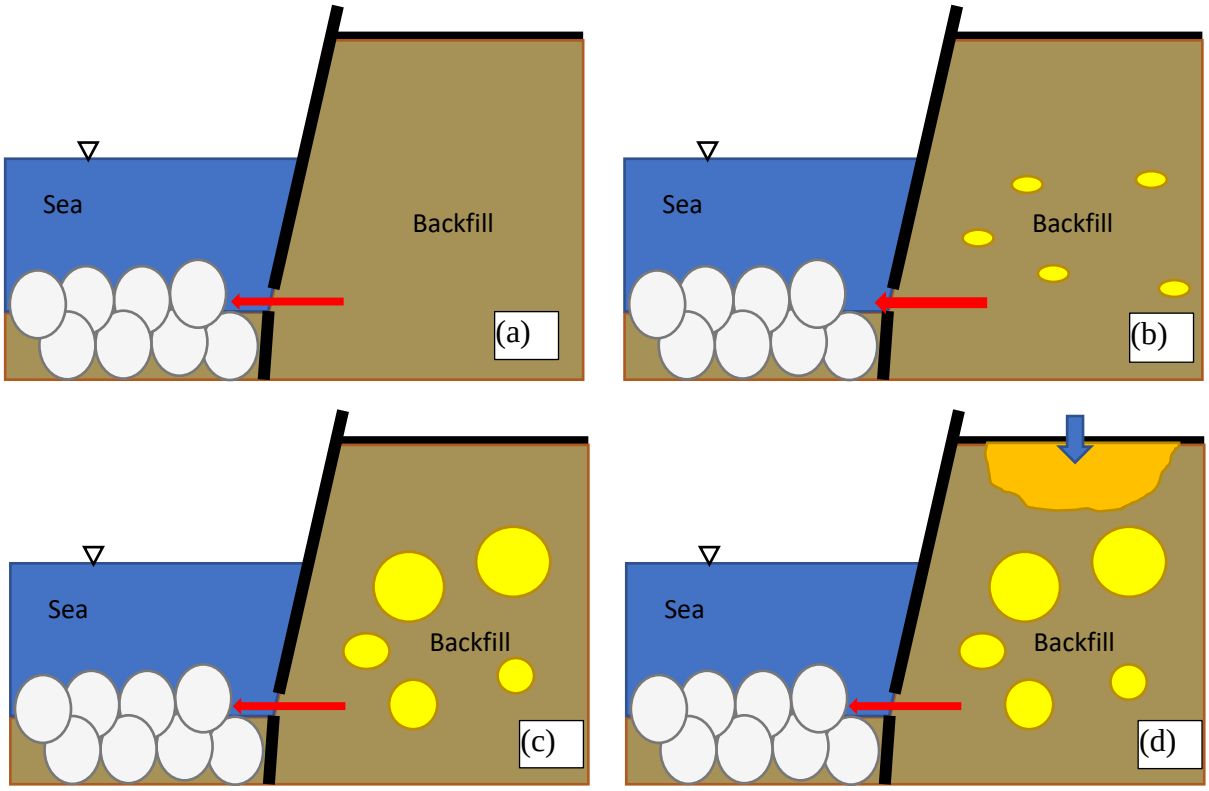

Figure 2 Stages that lead to subsidence of surface of a backfill

Bierawski et al. (2002) noted that the backfill leaks from behind a seawall due to pressure oscillations. Also, they noted that leakage of the backfill starts very slowly and leads to failures in the seawalls. Nakamura et al. (2008) have also reported that the leakage of the backfill phenomenon is closely related to the wave-induced pressure response. Later, Hur et al. (2007) studied the sand suction mechanism. Findings from the experiments agreed with Takahashi et al. (1996). A similar mechanism has been described for the destruction of the subsidence of backfill.

In this study, the main objective is to identify the void expansion mechanism after a void developed inside the backfill of the seawall due to the leakage of the backfill towards the seaside. In other words, the study aims to elucidate the time between Figure 2b to Figure 2c. The motivation of this thesis is whether during the enlargement of voids, the rate of leakage increases or not. And, if the rate of leakage increases with the enlargement of the void, what is the mechanism that accelerates the void development in the seawalls?

As pointed out by the earlier researchers, the sand leakage phenomenon is closely related to the wave-induced seabed response. As wave pressure propagates in the soil

medium, pore pressure and effective stresses change and cause displacements and seepage flow due to pressure gradients in the soil. The difference in pressures and displacements near the water-soil interface may generate the leakage of backfill material through imperfections in the geotextile materials, filter layer or from the foundation. As stated in the previous studies (Sumer, 2014), the presence of air in seabed causes high-pressure gradients near the water-soil interface of soil layer due to the exceptionally high compressibility of air comparing with water and soil skeleton. This phenomenon may enhance the soil leakage and accelerate the void development. Another mechanism that may cause the leakage of sand is the displacement of the soil due to contraction and expansion of developed voids in a backfill by pressure fluctuations.

Therefore, in this study, laboratory experiments have been carried out and leakage of sand through a small gap under pressure fluctuations have been investigated. Instead of a scaled model of a seawall, water flow has been applied to an acrylic container filled with sand and water to have a better control on the important parameters such as the volume of voids. In order to simulate the voids in the soil medium, small balloons filled with air have been used. After the confirmation of acceleration of the rate of leakage through laboratory experiments, the theoretical approach to the process of void development has been examined with a numerical model.

Earlier experimental studies mostly considered the end results of laboratory experiments with a scaled hydraulic model under the exposure of a sequence of waves. In this study, the movement of soil during one cycle is also examined with video analysis which gives the opportunity to examine the instantaneous conditions of the leakage of soil grains

The outline of this dissertation is as follows: In Chapter 2, the literature review on the sand leakage phenomenon behind the seawalls and the wave-induced soil response will be presented with more detail. In Chapter 3, methodology and results of the laboratory experiments that have been performed in the oscillatory flow tunnel will be explained to demonstrate the mechanism that accelerates the rate of leakage of sand grains. In Chapter 4, the theoretical approach in which a numerical model with finite difference model will be presented. And, validation and results from the developed numerical model will be demonstrated. In Chapter 5, the comparison of the results of the developed numerical

model with the results of the laboratory experiments. Also, the topics for further studies based on the shortcomings of the current study will be explained. In Chapter 6, the conclusion will be presented. Furthermore, the recommendations to future researchers will be given.

II. LITERATURE REVIEW

In this part of the dissertation, a literature review on the leakage of sand from the back of a seawall, void development in the backfill, the wave-induced soil response and related parameters such as compressibility and permeability of soil is introduced to demonstrate theories, laboratory experiments, and numerical and analytical investigations that have been carried out by the earlier researchers.

Even though the sand suction leads to a dangerous subsidence of the backfill surface, in the literature, only a handful of research studies exists about this phenomenon. A likely reason of this can be due to the complex soil structure near the seawalls, difficulties in the physical modeling in the laboratory, and challenges in field study because the location of the failure and the time span needed to collapse a seawall is still unknown. However, valuable studies that approach to the sand leakage behind the seawall from various perspectives can be found in the literature. Firstly, the studies on particularly the leakage of the backfill material from behind the seawalls will be explained.

A. The Leakage of Backfill Material behind the Seawalls

From the laboratory experiments at a wave flume, Takahashi et al., (1997) have found out that in the case of an opening or a hole in the geotextile sheet, the backfill soil behind a caisson-type seawall leaks towards the seaward side. The mechanism of subsidence of backfill surface has also been revealed in the study. Following the leakage of sand through a small opening in the geotextile or filter layer, voids are generated in the backfill soil. With the application of waves on the physically modeled seawall, voids enlarge in the backfill and when the soil cannot support the void, the backfill surface collapses and subsidence destruction is observed. Also, the location of void development has been observed to take place near the hole in the laboratory experiments. Another important measurement in this study was the pressure related to the saturation of backfill soil. The transmission of pressure acting on the backfill soil has been measured to be better in the case of saturated soil rather than unsaturated soil.

Bierawski et al., (2002) has conducted investigations with both hydraulic experiments and numerical modeling approach to assess the motion of backfill soil of a fixed vertical revetment under cyclic pore water pressure changes. From the study, it has been

concluded that even a small amount of leakage leads to failure of a seawall. As the leakage of soil starts slow, the destruction in the surface of backfill is inevitable. The sensitivity analysis on the leakage rate of soil has also been studied. And, the height of the wall, soil and wave characteristics have been found to be effective in the intensity of the leakage. In their numerical model with combining distinct element and finite element method, pressure gradients have been found to be causing a seepage force which generates the leakage of soil from the back of seawall towards the seaside.

In the laboratory experiments, Hur et al., (2007) have modeled a rubble mound breakwater and backfill soil in a wave flume to reveal the sand leakage mechanism. A void development mechanism that is similar to Takahashi et al., (1997) has been confirmed in the experiments. Generated cave formations in the backfill enlarge due to wave attacks and consequently, cave-ins (subsidence on top of the backfill) have been observed. In their laboratory experiments, typical subsidence on the surface of the backfill has been observed like the subsidence cases near the actual seawalls. Furthermore, the Ursell number and the relative breakwater width have been found out to be effective in the sand leakage process. For numerical modeling part of the study, Biot's consolidation equations, which governs the displacement and pressure transmission in the seabed, have been employed with partly dynamic assumption and solved with finite element method.

Nakamura et al., (2008) have presented a couple of real examples of subsidence of backfill surface from Japan, following the both toe scouring and leakage of backfill material towards the seaside. In their hydraulic experiments, sand leakage has been investigated through a small gap under a vertical revetment in a wave flume. A special attention has been given to the seaward velocity of the flow and leakage is found out to be correlated with the maximum seaward velocity of the flow. Also, the gap dimensions and the steepness of waves have been identified as very influential parameters. Furthermore, a numerical model which is similar to Hur et al., (2007), has been developed in this study to model the effective stresses and pore water pressures in the soil.

Looking at the given examples from the literature, in general, the experiments focusing on, especially the leakage of backfill from a seawall or a rubble mound breakwater have been conducted in wave flumes. And, waves attack to the physically modeled seawalls which have a backfill sand in order to observe the mechanisms that

may lead to subsidence of backfill surface. However, due to the scale of the experiments, the leakage rate estimations are inadequate to apply in a real seawall. Also, the backfill of seawalls is much more complex locations in terms of soil and flow conditions (e.g. degree of saturation) which are hard to achieve in a laboratory study. Still, valuable information such as the important parameters, the mechanism of subsidence of backfill surface and the governing equations that control the sand leakage process have been understood from the laboratory experiments and numerical model studies.

As pointed out, the wave-induced soil response is one of the key aspects to consider which control the leakage of soil and the void development in the backfill of the seawalls. Therefore, the experimental, theoretical, and field studies that have been carried out by the earlier researchers about the wave-induced soil response will be explained in the next section.

B. Wave-Induced Soil Response

The physical modeling of the wave-induced soil response covers the topics including the laboratory experiments and the field studies. The data collected from such studies usually used to verify the developed theoretical models. Also, to elucidate the process of the wave-induced soil response, the laboratory experiments have been conducted extensively by the researchers.

As the wave-induced soil response in the marine environment is concerning both geotechnical and coastal engineers, there are two distinct types of experimental approach by these researchers. The geotechnical engineers use a special equipment filled with the soil. And, directly apply the wave load upon the soil. In these experiments, it is easier to control the soil properties. For example, Chowdhury et al. (2006) have used an equipment filled with soil about 1.41 m height and measured the pressures at various depths due to the wave loading. The damping of the wave and phase lag have been observed in the study. In another study, Nago (1982) has used a similar equipment in the laboratory experiments related to the wave-induced soil response. In this study, it has been realized that the pressure acting on the soil propagates with attenuation in magnitude and a lag in the phase. Also, volume of air in the soil layer significantly has affected the attenuation in the magnitude of pressure and the phase lag

However, in the experiments of geotechnical engineers, the loading is much different than water waves that propagate over the seabed. Therefore, the coastal engineers, on the other hand, use wave flume experiments to assess the wave-induced soil response. For instance, Tsui and Helfrich (1983) have conducted series of experiments in a wave flume. The soil has been placed on the bottom of the flume, and pressure sensors have been installed in the soil in various depths and the water waves have been applied to the soil layer. With using two types of soil, the results revealed the vertical distribution of the maximum pressure oscillation with damping. Also, some phase lag between the wave-induced pore pressure in the seabed and the wave pressure on the top of seabed has been observed in the study.

The field measurements for the wave-induced soil response can be carried out by measuring the pressures inside soil medium. However, in the case of field studies, it is hard to control the important parameters in the pressure propagation. For example, the degree of saturation is most important parameters in the wave-induced soil response. Although there are some field studies to detect air content with the geo-endoscopy technique in the seabed (Mory et al., 2007), the degree of saturation is still very hard to measure with both in-situ or laboratory measurements.

Earlier researchers investigating the wave-induced soil response have considered the flat seabed without structures in the vicinity. Figure 3 shows a definition sketch of the problem. Waves traveling in the sea affects the seabed by changing the pore water pressure and effective stresses and inducing displacements in the seabed. For example, the crest and the trough of wave increases and decreases the pore pressure inside seabed, respectively. Many researchers studied the wave-induced seabed response, especially after the late 1970s.

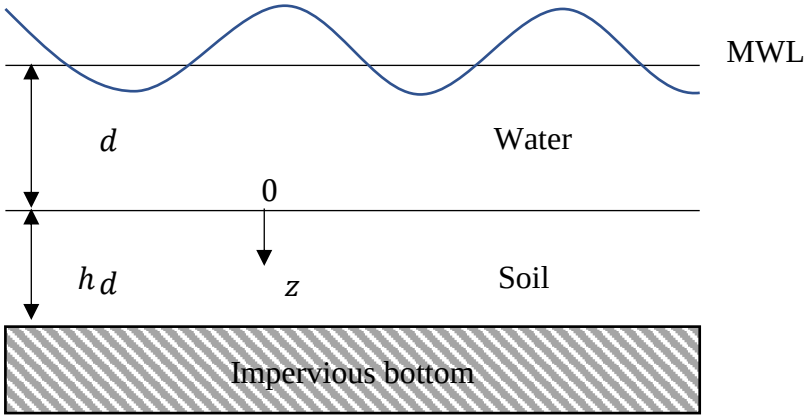

Figure 3 A definition sketch to wave induced-seabed response

In this research area, a large amount of work has been done in the theoretical and numerical studies. In his famous studies, Biot (1941, 1956) has introduced the governing equations for the pore water pressure, effective stresses, and displacements in a soil medium under the wave action. For the two-dimensional domain, hydraulically isotropic, and compressible pore fluid in a compressible porous medium (soil), including the accelerations due to both sediment and fluid, the full set of governing equations have been defined by Jeng et al. (2000) as follows:

$$k\left(\frac{\partial^2 p}{\partial x^2}+\frac{\partial^2 p}{\partial z^2}\right)-n\beta\gamma_w\frac{\partial p}{\partial t}=\gamma_w\frac{\partial}{\partial t}\left(\frac{\partial u_x}{\partial x}+\frac{\partial u_z}{\partial z}\right)-\rho_w k\frac{\partial^2}{\partial t^2}\left(\frac{\partial w_x}{\partial x}+\frac{\partial w_z}{\partial z}\right) \quad 1$$

where k is hydraulic conductivity of soil, p is wave-induced pore pressure, n is soil porosity, γ_w is the unit weight of the water, ρ_w is the density of the water, and u_x and u_z are the displacements of soil in x and z directions, respectively. Also, w_x and w_z are the displacements of pore fluid in x and z directions, respectively. The equation of motion in x direction is

$$G\left\{\left(\frac{\partial^2 u_x}{\partial x^2}+\frac{\partial^2 u_x}{\partial z^2}\right)+\frac{1}{1-2\mu}\frac{\partial}{\partial x}\left(\frac{\partial u_x}{\partial x}+\frac{\partial u_z}{\partial z}\right)\right\}-\frac{\partial p}{\partial x} = n\rho_w\frac{\partial^2 w_x}{\partial t^2}+(1-n)\rho_s\frac{\partial^2 u_x}{\partial t^2} \quad 2$$

And the equation of motion in z direction is

$$G\left\{\left(\frac{\partial^2 u_z}{\partial x^2}+\frac{\partial^2 u_z}{\partial z^2}\right)+\frac{1}{1-2\mu}\frac{\partial}{\partial z}\left(\frac{\partial u_x}{\partial x}+\frac{\partial u_z}{\partial z}\right)\right\}-\frac{\partial p}{\partial z} = n\rho_w\frac{\partial^2 w_z}{\partial t^2}+(1-n)\rho_s\frac{\partial^2 u_z}{\partial t^2} \quad (3)$$

where μ is the Poisson's ratio and ρ_s is the density of the sand grains. And the momentum equation in x direction can be defined as

$$\rho_w\frac{\partial^2 w_x}{\partial t^2}=-\frac{\partial p}{\partial x}-\frac{\gamma_w n}{k}\left(\frac{\partial w_x}{\partial t}-\frac{\partial u_x}{\partial t}\right) \quad (4)$$

The momentum equation in z direction is

$$\rho_w\frac{\partial^2 w_z}{\partial t^2}=-\frac{\partial p}{\partial z}-\frac{\gamma_w n}{k}\left(\frac{\partial w_z}{\partial t}-\frac{\partial u_z}{\partial t}\right) \quad (5)$$

β is the compressibility of pore fluid which is related to the compressibility of water and air inside the soil and calculated as (Verruijt, 1969)

$$\beta=\frac{1}{K_w}+\frac{1-S_r}{P_{abs}} \quad (6)$$

where K_w is the bulk modulus of water and S_r is degree of saturation and P_{abs} is the absolute pressure.

1. The Assumptions on the Governing Equations of Wave-Induced Soil Response

In the literature, there are analytical or numerical models in which the researchers have made some assumptions to solve the governing equations. First of these models is the so-called uncoupled model, in which the accelerations of fluid and soil grains are ignored. However, depending on the choice, either the fluid is considered as compressible or the porous medium considered as compressible. The models with uncoupled assumption are not very good at representing dynamic processes like wave-soil interaction inside soil medium. However, this model has been used in soil mechanics to assess the consolidation process which takes place over a longer period (Terzaghi, 1943).

The second model to solve the governing equations is the quasi-static model. In this model, the accelerations due to fluid and soil grains are also ignored. However, the compressibility of soil and pore fluid is included in the quasi-static model. This method is proven to be better an estimation of pressure transmission inside a soil medium for relatively slow processes.

The third approach for the wave-induced soil response is the partly dynamic formulation which has been introduced by Zienkiewicz et al. (1980). This model is also called as 'u-p approximation'. In this model, the accelerations due to the soil particles are included in the governing equations. However, the accelerations due to fluid are ignored. According to Jeng (2013), the relative difference between the quasi-static model and the u-p approximation can be maximum 17% of the amplitude of wave pressure.

The fourth model is so called dynamic model which includes all the terms to solve the governing equations. Specifically, in this model, accelerations due to both pore fluid and the soil grains and the compressibility of both soil and pore fluid are included in the computation. Ulker et al. (2009) have compared the results of dynamic, partly dynamic, and quasi-static assumptions and for the wave-induced seabed response in the marine environment, the quasi-static assumption is sufficient to use except for soils with high permeability.

Also, Sakai et al. (1988) have investigated the effects of acceleration terms in the wave-induced soil response for the ocean waves. According to their results, they have confirmed that the acceleration terms can be ignored in the normal wave conditions except for breaking waves.

2. The Methodologies to Solve the Governing Equations

The researchers have solved the governing equations for the wave-induced soil response based on these assumptions (uncoupled, quasi-static, partly dynamic and dynamic) with different approaches. For example, Yamamoto et al. (1978) have introduced the analytical solution to the wave-induced soil response based on the quasi-static assumption. Since then, difference approaches, such as boundary layer approximation, finite element method, finite difference approximation have been used to solve the governing equations.

In their paper, Mei and Foda (1981) have introduced an approximate analytical solution to the wave-induced soil response with the quasi-static assumption based on the boundary layer theory in which the laws of elasticity govern the motion of the fluid and solid particles outside the boundary layer. On the other hand, Magda (1996), Magda et al. (1997) have developed a finite element model to solve the governing equations of the wave-induced soil response based on the quasi-static assumption where compressibility of pore fluid and soil is included.

In order to assess the wave-induced soil response near the coastal structures, numerical models combining the water flow models with the finite element method for the soil response. For example, Mizutani et al. (1998) and Mostafa et al. (1999) have developed a model based on combining the boundary element method and finite element method (BEM-FEM model) where the quasi-static assumption has been used for the wave-induced soil response. In another example, Hur et al. (2007) have used the volume of fluid method for the water flow model and finite element method for the wave-induced soil response in their numerical model in which the partly dynamic assumption has been utilized for the governing equation of soil response to pressure oscillations.

A detailed review of the wave-induced soil response has been carried out by Jeng (2003) explaining the studies based on the assumptions (uncoupled, quasi-static, partly dynamic and dynamic assumptions) and the numerical and the analytical methods to solve the governing equations based on these assumptions.

3. Discussions on the Wave-Induced Soil Response based on the Literature

The pressure oscillations by the waves are not transmitted simultaneously to the soil. There is a damping in pressure amplitudes and phase lag. As going further away from the wave-soil interface, the pressure amplitude attenuates and phase lag increases. Therefore, pressure differences develop in the soil medium.

Due to the pressure difference, a seepage flow is observed from high pressure to low pressure in soils. Along with the seepage flow, the seepage force is exerted on the soil grains in the flow direction. Accordingly, a seepage flow either towards water (leakage) or towards soil (compaction) can be observed. Any pressure difference between the soil

and water can trigger this process. Rainfall, overtopping, tidal changes in water level or the pressure fluctuations due to waves can create such pressure differences near the seawalls.

The magnitude of the seepage force is a function of the generated pressure gradient. Therefore, the response of soil to the pressure changes during a wave passage is very important for the assessment of the seepage flows. In case the damping in pressure amplitude is large between two points, then, the generated pressure gradient is also large.

Jeng (2013) has discussed the effects of important soil and flow characteristics on the wave-induced soil response based on dynamic, partly dynamic, and quasi-static assumptions. The results have revealed that the degree of saturation is one of the most important parameters that affect the response of soil to pressure fluctuations. The degree of saturation is the ratio of the volume of water to the volume of voids inside the soil. In other words, it describes how much space in the voids of soil is occupied by the water. It is a measure of the relative quantity of water and gas within a soil medium. If the soil is not fully saturated, then, inside the voids, some air content can be expected. Even a small amount of air existing in the soil medium blocks the pressure from reaching to lower levels in the seabed by dissipating the pressure at the top levels of the seabed. In sand with low permeability, this effect is more notable than in sand with high permeability. Therefore, the permeability of the soil medium has also very significant effects on the pressure response. Also, in the marine environment, Wheeler (1986) noted that air can present like bubbles which are much greater than the soil grains.

The permeability of a soil is a measure of how easy the pore water can move through pore spaces between soil grains. For soils consisting of sand grains, the coefficient of permeability depends on the particle sizes. In the case of fine grain sands, the permeability is much lower than the case of coarse grain sand. According to Jeng (2013), under the same degree of saturation, coarse grain sand transmits the applied pressure at top of the seabed surface better to the lower levels of the seabed. However, in fine grain sand, the reduction in pressure is larger against the soil depth. Consequently, under the same degree of saturation, the developed pressure gradient due to wave action is higher in fine grain soil rather than coarse grain soil.

Another important parameter for the pressure response has been confirmed by Jeng (2013) as the thickness of the seabed. However, considering the same degree of saturation for various seabed thicknesses resulted in similar pressure responses at the top layers of the seabed where the pressure gradients are also similar. It would also be helpful to see if the air amount kept same in the various depths rather than keeping a constant degree of saturation. However, it can also be expected that as the seabed thickness increases, the degree of saturation will decrease due to constant air amount in the soil and increasing soil volume. Therefore, as the thickness of seabed increases, the transmission of pressure to the lower levels of seabed will be improved if the air amount is constant.

Furthermore, the effects of the period of waves on the pressure response are examined in Jeng (2013). According to the results, for both coarse and fine grain sand, the transmission of pressure is better in larger period waves. Therefore, the generated pressure gradients in are higher in small period waves comparing with the large period waves.

The effect of shear modulus of soil on the pressure response has also been investigated by Jeng (2013). In a saturated seabed, the effect of shear modulus is comparatively lower than in an unsaturated seabed.

Also, from the results obtained from the sensitivity analysis of Jeng (2013), the quasi-static assumption gives comparable results to the partly dynamic and dynamic assumptions for the selected wave and soil characteristics. Also, the author has provided a method when the dynamic assumption should be used in the response of pressure for the soils.

C. Liquefaction

Liquefaction is a form of instability in the soil as the effective stress goes to zero, the soil loses its strength and acts like a liquid. Therefore, the soil can be transported easily by the flow. Thus, the liquefaction phenomenon is quite dangerous for the marine environment and structures. There are many studies for the wave-induced liquefaction phenomenon such as Ishihara and Yamazaki (1984), Tsotsos et al. (1989), Maeno and Nago (1983) and Kirca et al. (2013).

Sumer (2014) has pointed out that there are 2 distinct mechanisms that lead to liquefaction of soils by the waves. One of them is called residual liquefaction and is related to the development of pore pressure. The second type of liquefaction is related to the vertical gradient of the pressure. This type of liquefaction is called momentary liquefaction and can occur in mostly unsaturated soils due to high-pressure gradients. As Sumer (2014) points out that for fully saturated soil, the lift force causing the momentary liquefaction cannot be developed because the generated pressure gradients are not large in fully saturated soils. However, in the unsaturated soils, the pressure on the soil cannot penetrate towards the bottom of the soil and dissipates near the water-seabed interface due to high compressibility of air (Figure 4). Therefore, high-pressure gradients can be observed from soil towards the water under negative oscillatory pressure which

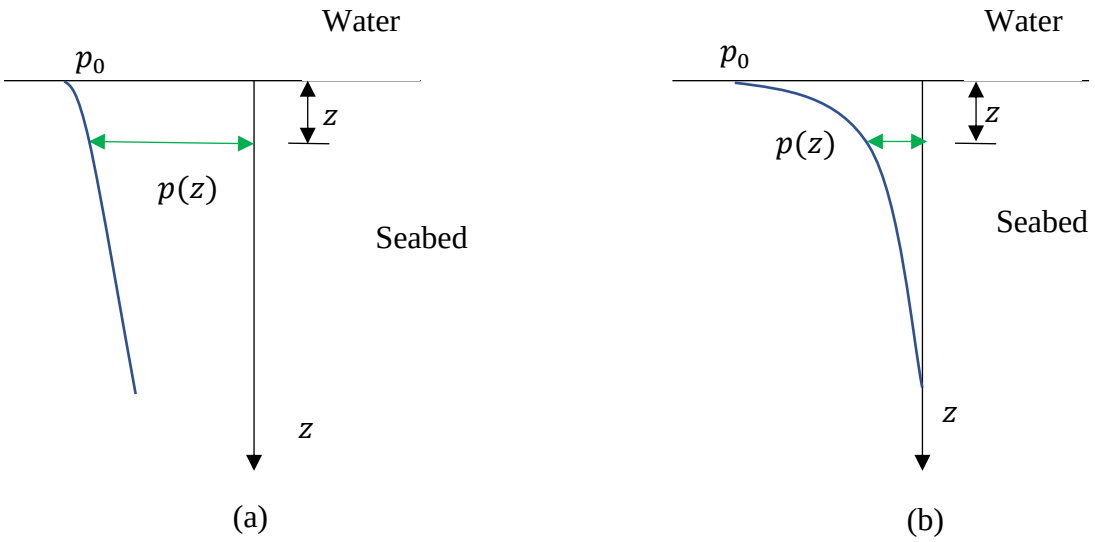

Figure 4 The pore pressure transmission in the soil due to pressure oscillations during the wave attacks for saturated soil (a) and for unsaturated soil (b) (Sumer, 2014)

corresponds to the trough of waves. If the pressure difference between the applied pressure to the top of the soil and the transmitted pressure at a depth, d, exceeds the initial vertical effective stress at depth, d, then the soil loses its strength up to depth, d that is called the depth of momentary liquefaction (Chowdhury et al. (2006)). Zen and Yamazaki (1990) has mentioned that the wave-induced liquefaction is closely related to seepage flow from soil to water under wave trough. Therefore, the momentary liquefaction can be

considered as an ultimate case of vertical seepage from soil towards the water where the seepage force exceeds the weight of the soil.

So, the summary of the literature review is as follows.

- The void development in seawalls is related to the leakage of sand through imperfections in the geotextile or filter layer.
- Pressure gradient near the water-soil interface causes sand to leak.
- Wave-induced soil response determines the pressure transmission. Poor response results in high-pressure gradient, good response results in low-pressure gradient
- High-pressure gradients near soil-water interface can induce large amount of leakage
- The compressibility and permeability of soil are the main parameters in the wave-induced soil response
- Entrapped air bubbles due to wave action can drastically change the compressibility and permeability of the soil. The assessment and control of these parameters are very hard in both field and laboratory.
- The air content near the marine environment is in form of air bubbles.
- The momentary liquefaction is an instability generated by large pressure difference where the soil loses its integrity and starts to float.

III. THE LABORATORY EXPERIMENTS

In this section of the dissertation, the laboratory experiments that have been conducted to investigate the leakage of sand through a small gap under pressure oscillations will be presented.

A. Oscillatory Flow Tunnel

To examine the mechanism of void development inside backfill of seawalls, a set of laboratory experiments have been conducted in an oscillatory flow tunnel (OFT) at the University of Tokyo. The schematic view of the OFT is given in Figure 5. The top view and the side view are shown in Figure 5a and Figure 5b, respectively. The test section is 600 cm long, 7 cm wide and 28 cm deep and one side is made up of glass to observe experimental developments inside the OFT (Figure 6). Back and forth motion of the piston type wave maker generates the water flow inside the tunnel under pressurized environment.

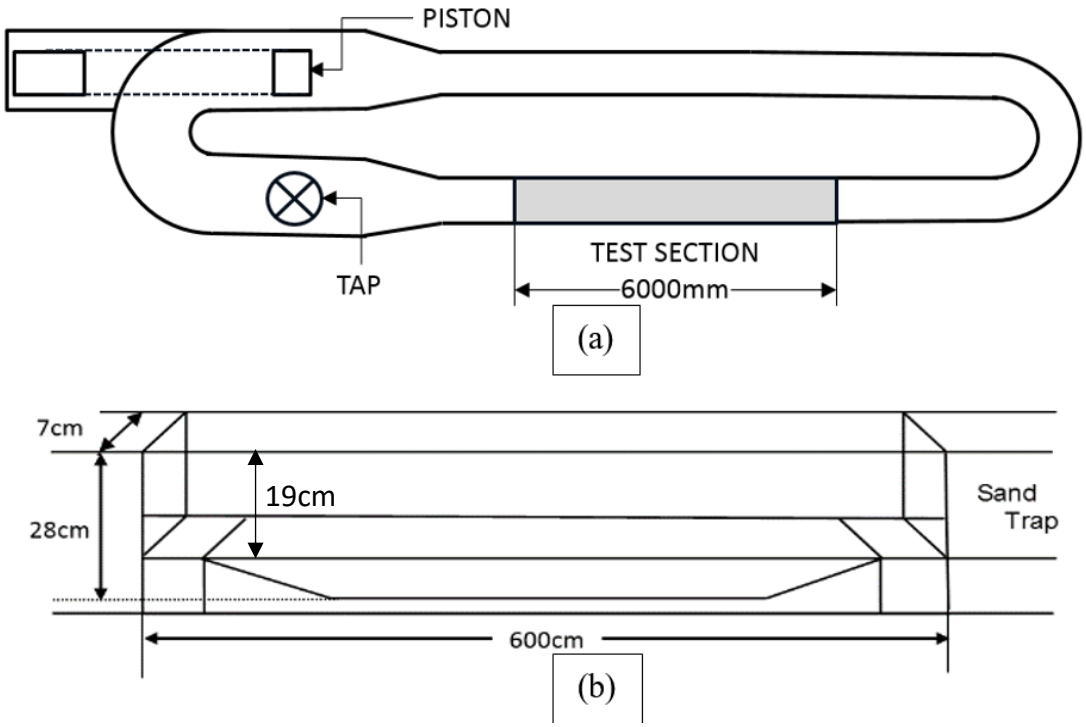

Figure 5 The schematic view of the Oscillatory Flow Tunnel. (a) is the top view, (b) is the test section from the side

Figure 6 A photograph of the oscillatory flow tunnel

OFT is generally used to investigate sediment transport processes under sheet flow conditions (Dong et al., 2013). Therefore, to place the sediment to the bottom of the tunnel for the laboratory experiments of sediment transport, the bottom of the tunnel is not flat. However, in the following experiments, an acrylic container has been used. To have a smooth flow around the container, the bed is raised to the container level. So, the depth inside the OFT is no longer 28 cm, but it is 19 cm.

The water flow characteristics in the OFT are controlled with the movement of the circular piston type wave maker. The displacement and the period of the piston can be adjusted from the computer as electric signals. As the piston and test section dimensions are known, horizontal displacement amplitude, a in the test section can be found. Thus, the water particle displacement is calculated as,

$$\xi = a\,cos\,\omega t \tag{7}$$

in which $\omega = 2\pi/T$ is the angular frequency of the oscillatory flow, T is the period of the flow, and t is time. Then, the velocity, u is calculated as,

$$u = \frac{\partial \xi}{\partial t} = -a\omega\,sin\,\omega t \tag{8}$$

From the Eq. 8, the velocity of the flow is not affected by the spatial coordinate. Therefore, inside the test section, the velocity is uniform.

Later, the pressure oscillations due to the generated water flow is calculated from the relationship with velocity,

$$\rho \frac{\partial u}{\partial t} = -\frac{\partial p}{\partial x} \quad (9)$$

By integrating the equation of motion,

$$p = \int_{x_0}^{x} \rho a \omega^2 cos(\omega t) dx = \rho a \omega^2 (x - x_0) \cos \omega t \quad (10)$$

And, the amplitude of pressure oscillation is expressed as,

$$\hat{p} = \rho a \omega^2 (x - x_0) \quad (11)$$

where ρ is the density of water, x is the spatial coordinate in horizontal direction and x_0 is the location where the pressure fluctuation becomes zero. From Eq. 11, the magnitude of pressure oscillation decreases linearly from left end to right hand throughout the test section.

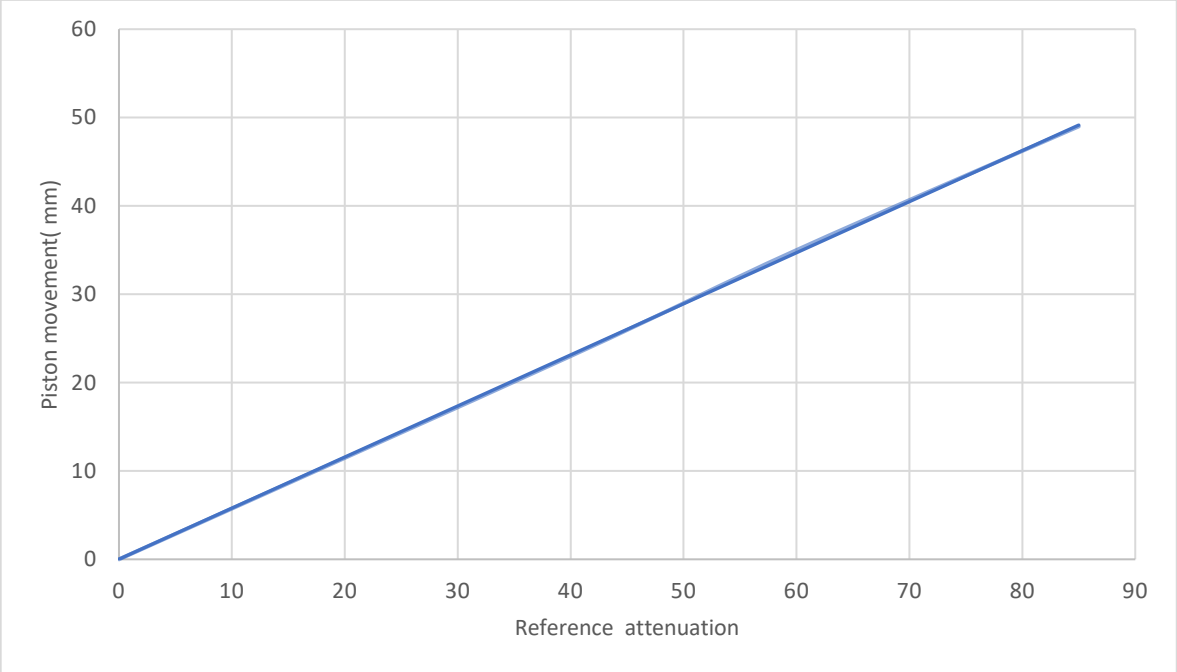

Figure 7 The movement of piston type wave maker according to the input of reference attenuation

The water flow characteristics have been defined as electrical inputs to the piston of oscillatory flow tunnel. The reference attenuation which controls the displacement of the piston and the period are the two inputs to the system. In the experiments, the reference

attenuation has been set to 40 and period has been set to 2 seconds. To calculate the flow velocity and pressure oscillations inside the tunnel, the dimensions of piston and tunnel and the movement of the piston are needed. Therefore, the movement of the piston has been observed under different reference attenuation values. Figure 7 shows the observed piston movements under different reference attenuation values.

According to Figure 7, the movement of the piston under reference attenuation under 40 has been found as 23 mm. In other words, in 2 seconds, the piston travels 23 mm forth and 23 mm back. The diameter of the circular piston wave maker is 389 mm, the width of the tunnel is 70 mm, and depth of the tunnel is 190 mm when there is the container. So, the relation of flow flux can be written from the mass conservation as,

$$U_p A_p = u A_t \tag{12}$$

where U_p and u are the amplitude of the velocity of the piston and the water flow, respectively. A_p and A_t are the cross-sectional areas of the piston and the tunnel, respectively. Considering the angular frequencies of the piston and water flow are same ($\omega_p = \omega$), the horizontal excursion length of the piston,

$$a_p = \frac{U_p}{\omega_p} \tag{13}$$

and the excursion length of the water particles,

$$a = \frac{u}{\omega} \tag{14}$$

So, the Equation 12 becomes,

$$a_p \omega_p A_p = a \omega A_t \tag{15}$$

From the Figure 7, the amplitude of horizontal displacement of the piston has been found as, $a_p = 23/2 = 11.5\ mm$. Thus, the amplitude of horizontal displacement of the water flow in the OFT can be found as,

$$a = \frac{a_p A_p}{A_t} = 102.76\, mm \tag{16}$$

Therefore, the velocity of water flow can be found as,

$$u = a\omega \sin \omega t = 322.83 \sin \omega t \ \ mm/s \tag{17}$$

The equation of pressure is determined as,

$$p = \rho a \omega^2 (x - x_0) \cos \omega t = 1014.2\ (x - x_0) \cos \omega t \ \ Pa \tag{18}$$

Between the pressure oscillations and the velocity of the water flow, a phase difference of $\pi/2$ is noted due to the trigonometric functions. When the velocity is maximum, the pressure is near to zero. And when the pressure is maximum, the velocity of the water flow approaches to zero. The phenomenon of phase difference has been illustrated in Figure 8 for wave with a period of 2 seconds. Note that the magnitude of both pressure and velocity have not been considered while drawing this graph.

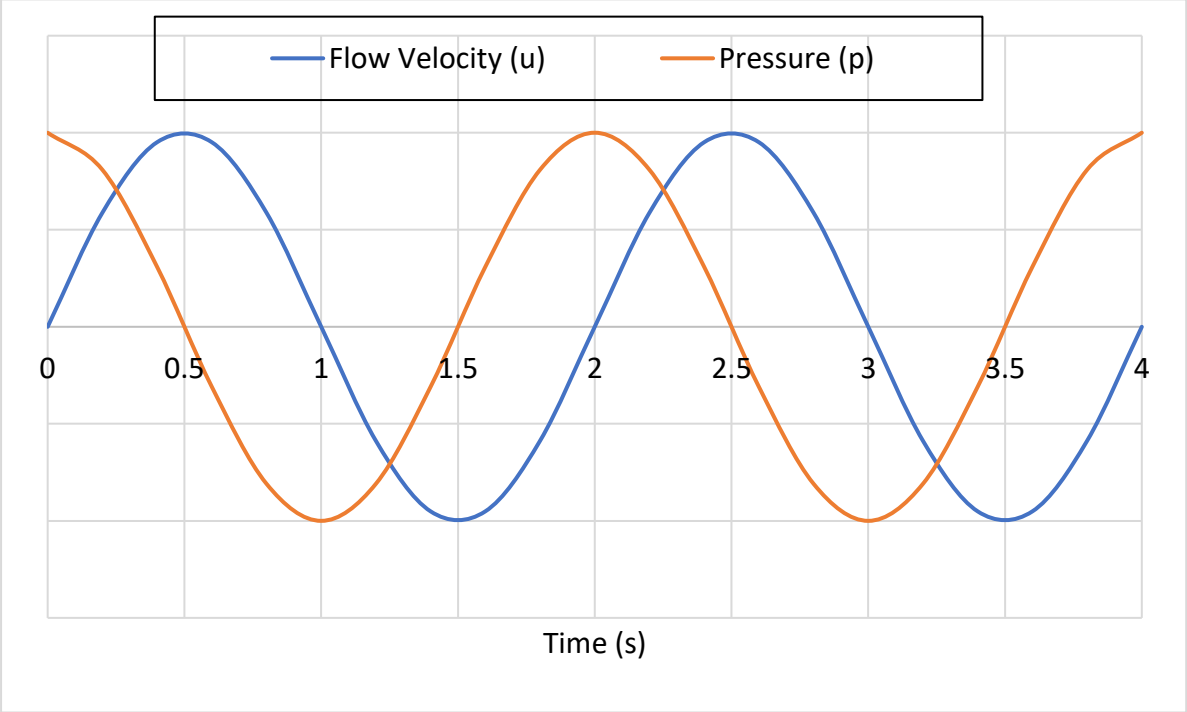

Figure 8 The phase difference between flow velocity and pressure

B. Experimental Equipment

To simulate the leakage through a small gap like the real seawall environment, an acrylic rectangular parallelepiped-shaped container with a small gap on the top has been prepared and leakage of sand has been observed under oscillatory flow. The container has been 30 cm long, 6 cm wide and 8 cm deep. The material of the acrylic container has been moderately rigid to conserve the soil inside the container from water flow other than the provided gap on the top.

As one of the purposes of this study is to examine the void development mechanism and how the leakage rate is affected by the presence of air void, air has been introduced to the soil medium with small toy balloons (Figure 9) to simulate the voids in the backfill of a seawall. They have been prepared by placing 40 ml of air and sealing carefully to have the same compressibility in each balloon. It is very important to keep the same pressure level inside the balloons from the compressibility point of view because the main contribution of the air balloons is to change the compressibility of the soil medium. Such increase in compressibility may happen in a backfill of a seawall due to successive soil losses through the imperfections in the protection elements of the backfill.

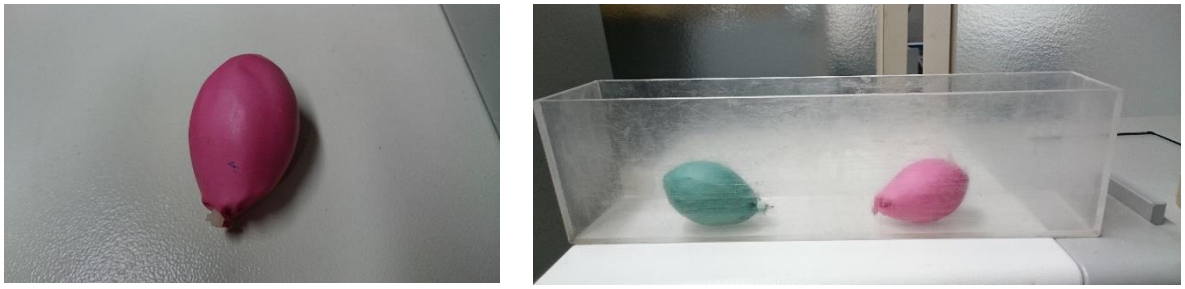

Figure 9 The balloons to simulate the voids in soil medium and the acrylic container

Two types of sand have been used with different grain sizes in the experiments. They are named as fine grain ($d_{50} = 0.25$ mm) and coarse grain ($d_{50} = 0.89$ mm). The grain size analysis has been conducted with a laser diffraction particle size analyzer. The importance of using two various sand is to examine the effect of soil permeability on the rate of leakage of sand. In the laboratory experiments, the fine grain sand will represent the less permeable and the coarse grain sand will represent the more permeable soil medium.

C. Preparation of the Experiments

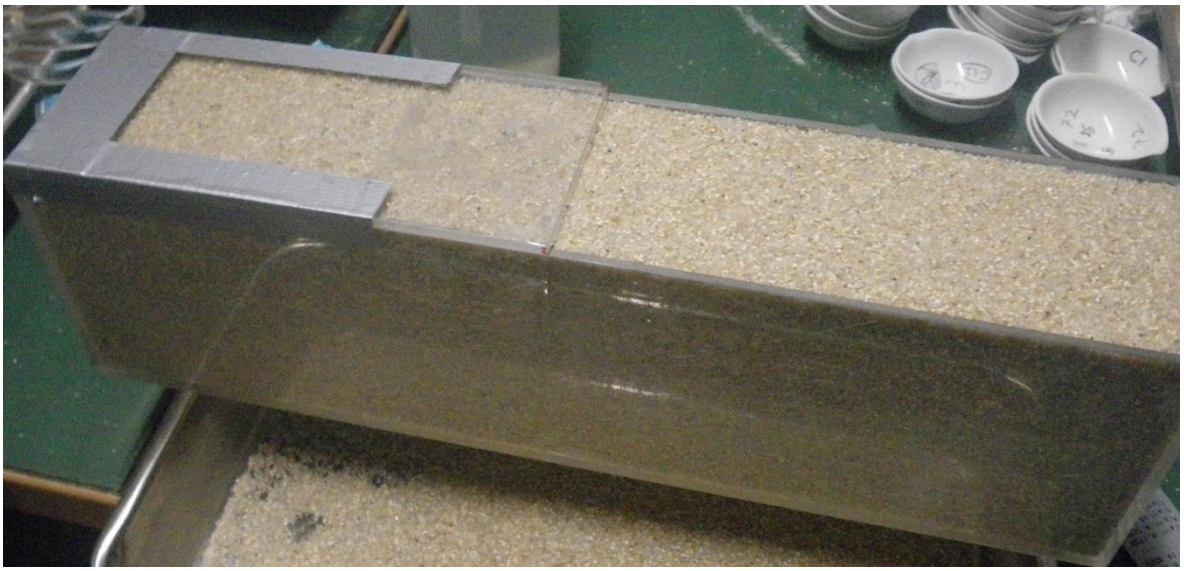

Figure 10 The acrylic container after filling the sand

Due to unique nature of the laboratory experiments, the details about the preparation of the experiments will be presented. Firstly, the prepared balloons are placed to the bottom of the acrylic container (Figure 9). Then, sand is filled with hitting from the sides to have similar porosity in each experiment (Figure 10). Then, the top of the container is closed with two acrylic plates just providing a small gap on top. Afterward, the plates are attached to the container with waterproof tape to make sure the only the flow on top of the small gap affects the soil medium. Then, the container is placed and kept under water to make the sure inside the container there is no air except the provided balloons.

Later, the container is put to the bottom of the OFT, which is leveled beforehand for the container to have a smooth water flow on top of it without any eddies. After that, the OFT is filled with water and the lids of the OFT are closed. The filling of water is continued until the tunnel is pressurized. Under pressurized environment, the experiment is started with setting up the period and the horizontal displacement of the piston, which creates the oscillatory flow inside the tunnel (Figure 11). Sand leakage through the small gap under oscillatory flow (Figure 12) is observed and recorded with video cameras. After several trial experiments, it has been realized that 3 minutes later, the soil profile reaches a relatively stable condition. Therefore, the oscillatory flow has been applied for 3 minutes for each experiment.

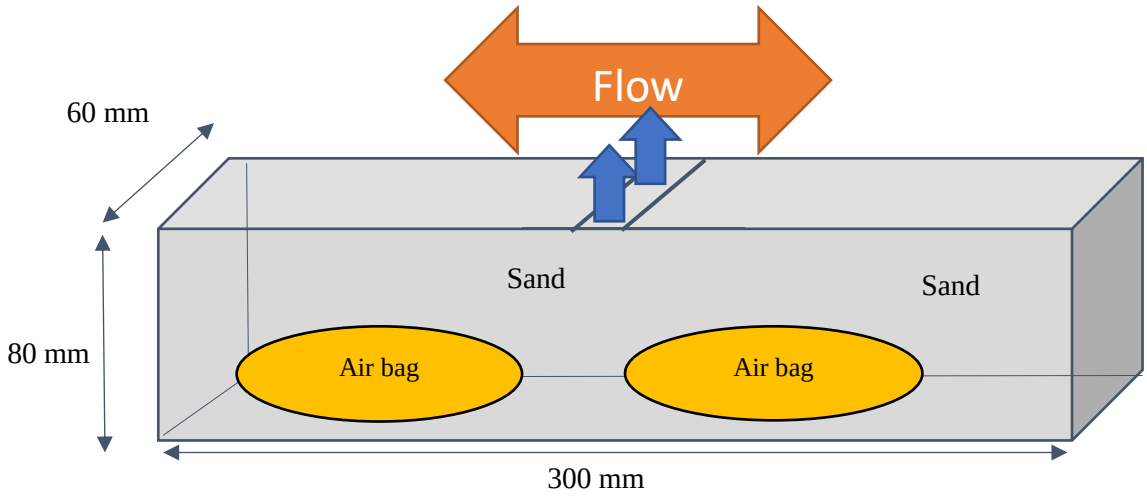

Figure 11 The schematic view of the laboratory experiment

In the preliminary experiments, the volume of leaked sand has been determined by the weight of the container before and after the experiments. However, since the weight of leaked sand after the experiments is very limited (5 to 20 grams), the measurement on weighing the container, before and after the experiments, is prone to operational errors during taking out the container from the OFT and putting the sand into an oven to dry. Therefore, a different approach has been performed. The recorded videos during the experiments have been used to assess the leakage of sand. The difference between the

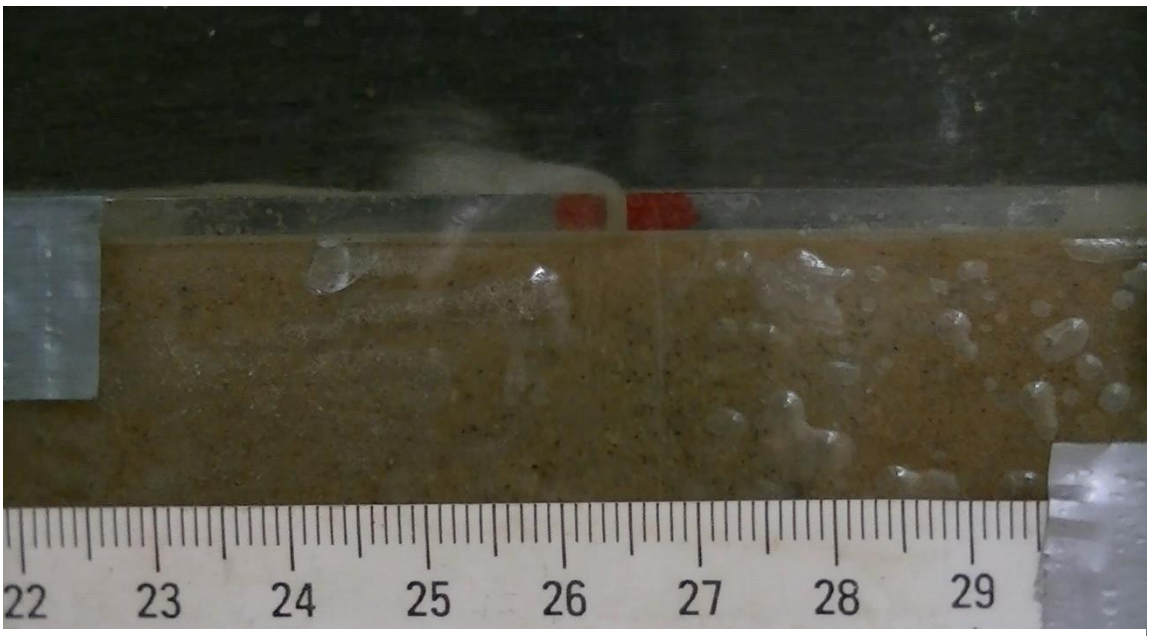

Figure 12 Leakage of sand through a small gap under pressure oscillations

scoured portion of soil before and after the experiment considered as the leaked sand from the container.

The procedure of image analysis as follows: Firstly, the scoured area near ±3 cm from the provided gap in the horizontal direction is selected. Then, the number of pixels in the selected area are counted and converted into scoured area, A_s, with the help of scale which is taped on the glass of OFT. Applying this procedure both before and after the experiment, the difference of the scoured areas gives the leaked sand amount. Furthermore, the displacements in the soil medium during the oscillatory flow application have been measured from the videos after 1 minutes starting of the experiments. Since, it is hard to account for a displacement during the experiments by the videos from a common point for all experiments, the measured displacements are away from gap. The

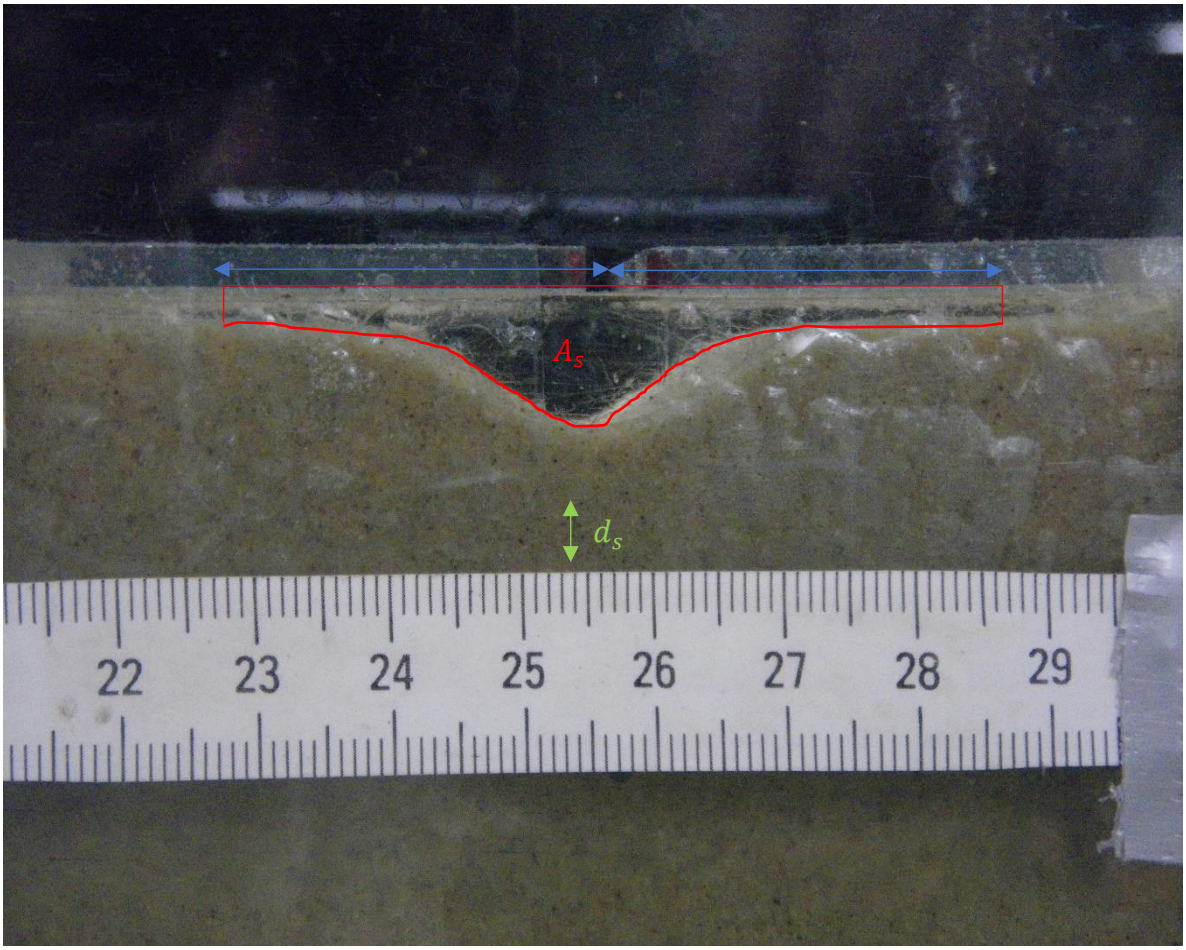

Figure 13 The leaked sand area and the displacements in the sand away from the gap

difference of pixels in the vertical direction during the pressure oscillations inside the soil medium has been recorded as the displacements away from the gap, d_s (Figure 13).

D. Results

The pressure amplitude along the OFT have been measured with three manometers that are placed on top of the lids of the OFT (Figure 14). The pressure amplitude decreases as the manometer goes to the right from the left for 4 different experiments with different water flow conditions, according to the Figure 15. This graph matches well with the

Figure 14 A manometer placed on the lid of OFT

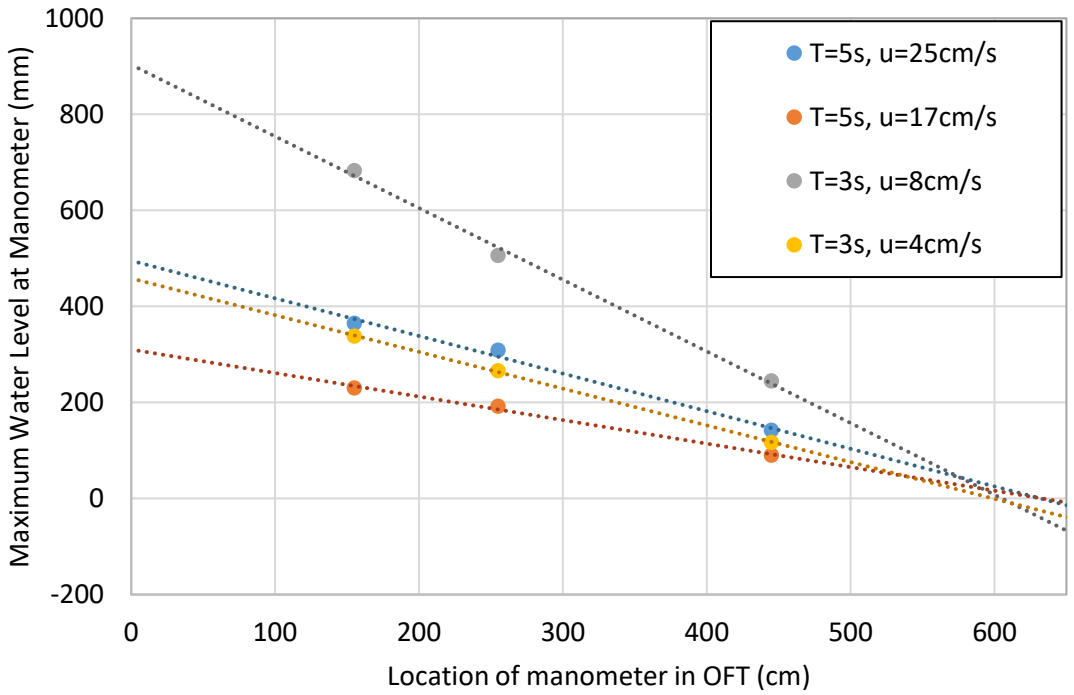

Figure 15 Measurement of pressure fluctuations along the oscillatory flow tunnel

calculation for pressure theoretically in Eq. 11, where it is suggested that the amplitude of the pressure oscillations decrease along the OFT. Note that the velocity of the flow is same at every location for the same experiment. Also, the term x_0, which defines the location where the pressure fluctuation is zero has been found as approximately 600 cm.

In the preliminary experiments, the container has been divided into two parts. In the first part, there is only soil and water mixture. In the other part of the container, an air pocket has been introduced to the water and soil mixture (Top panel of Figure 16). Then, the container has been placed at various locations along the OFT under same water flow conditions. The experiments revealed that the measured leakage decreased as the container placed towards the right side where the magnitude of pressure oscillation decreases despite the flow velocity remains same (Bottom panel of Figure 16). Also, it is observed that the rate of sand leakage from the part where the balloon has been introduced into the soil medium is considerably larger than the other part where there is only soil and water. So, from these experiments, it can be concluded that the magnitude of pressure oscillations and the response of the soil to these pressure oscillations are responsible for the leakage of the sand. Furthermore, it has been understood that there is a mechanism

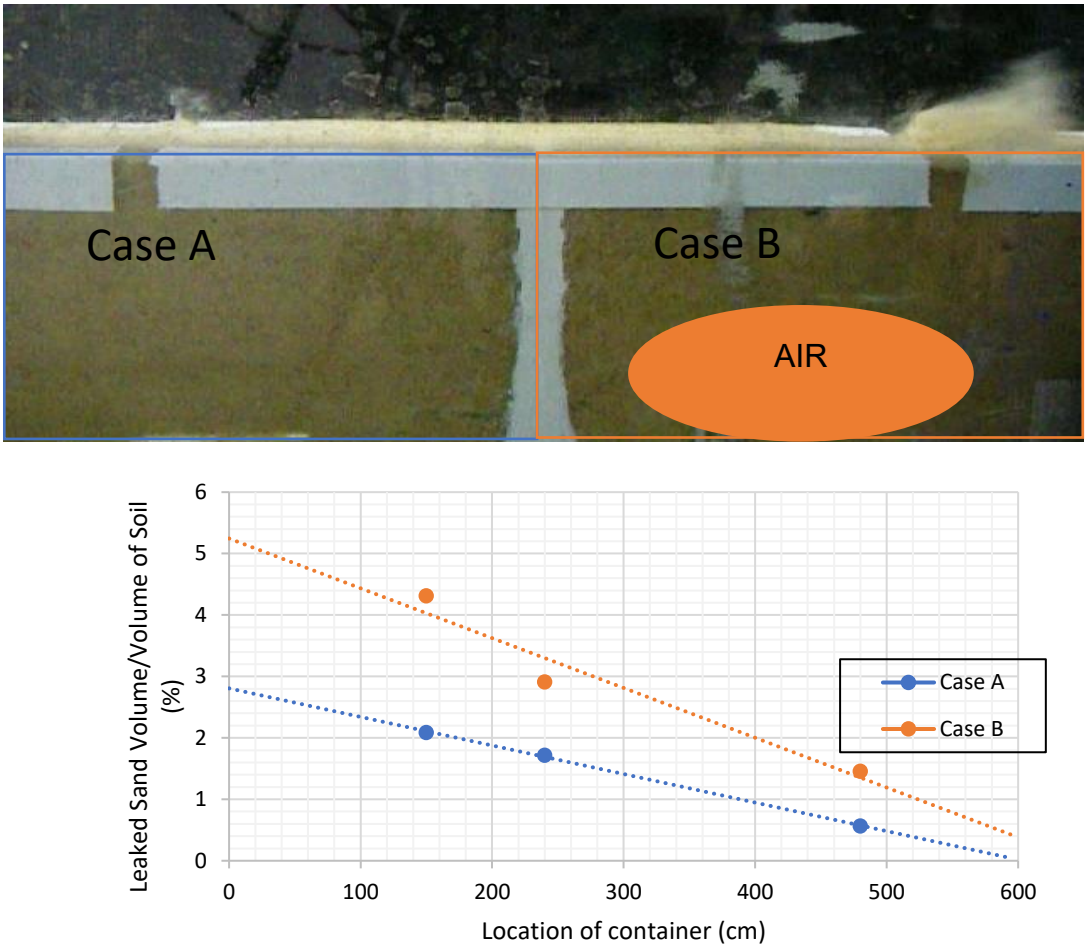

Figure 16 Comparison of experiments with air and no-air under different amplitude of pressure

which accelerates the void development as the rate of leakage of sand is much larger in the case where the balloon is introduced i.e., the compressibility of soil medium increased.

Furthermore, the frame-by-frame analysis of the video revealed that the leakage is highest during the pressure is minimum and velocity is near zero. Figure 17shows the images from the experiments while the flow is towards the right side. The velocity is negative and the pressure is decreasing to minimum from maximum. In this time sequence, the soil medium migrates towards the gap (Image A-B-C-D of Figure 17) and at the end when the pressure is minimum (Image D of Figure 17) a high leakage is observed. When the pressure is minimum in the water flow, it can be expected that the upward pressure gradient and accordingly, the seepage force is close to its highest value.

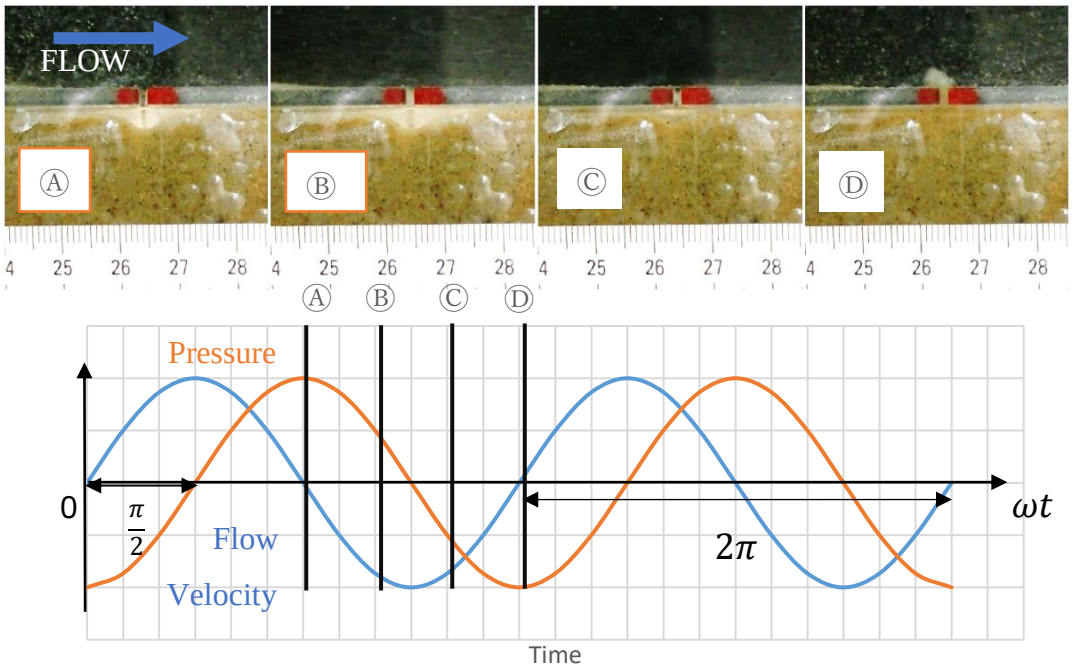

Figure 17 Recordings from the experiments while flow is towards right (velocity is negative)

Figure 18 shows the images from the experiments while the flow is towards the left side. The velocity is positive and the pressure is increasing to maximum from minimum. In this time sequence, the soil medium goes down, away from the gap by the effect of pressure increase (Image D-E-F-G of Figure 18). Also, during this time sequence, the downward pressure gradient is effective which will generate the downward seepage flow. Furthermore, when the pressure is above zero, very low leakage has been observed.

So, it was noted that during the laboratory experiments, the soil medium moves towards and against the gap based on the pressure oscillations. When the pressure oscillation is low in the water flow, the soil medium moves towards the gap because of both pressure gradients and the expansion of the volume of air. However, when the pressure oscillation is the highest point, the soil medium is pushed to bottom because of both pressure gradients and the contraction of the volume of air (Figure 19).

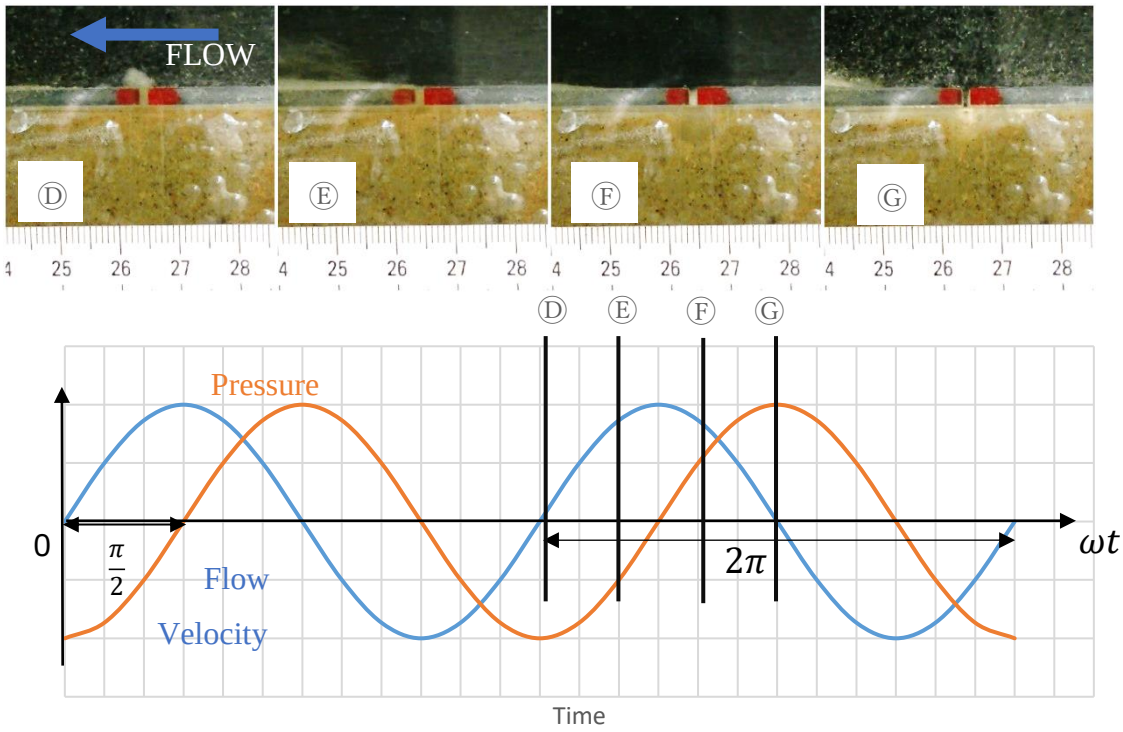

Figure 18 Recordings from the experiments while flow is towards left side (velocity is positive)

Additionally, an experiment with two small pressure sensors has been carried out. One pressure sensor has been placed on top of the container near the gap, and the other one has been positioned to the inside of a balloon (Figure 20). Figure 21 shows the measurements between 20-40 seconds from this experiment. According to the result, damping in the pressure amplitude and a slight time lag have been observed. Pressure amplitude has attenuated around 20-30%. And, around 10 degrees of phase lag has been

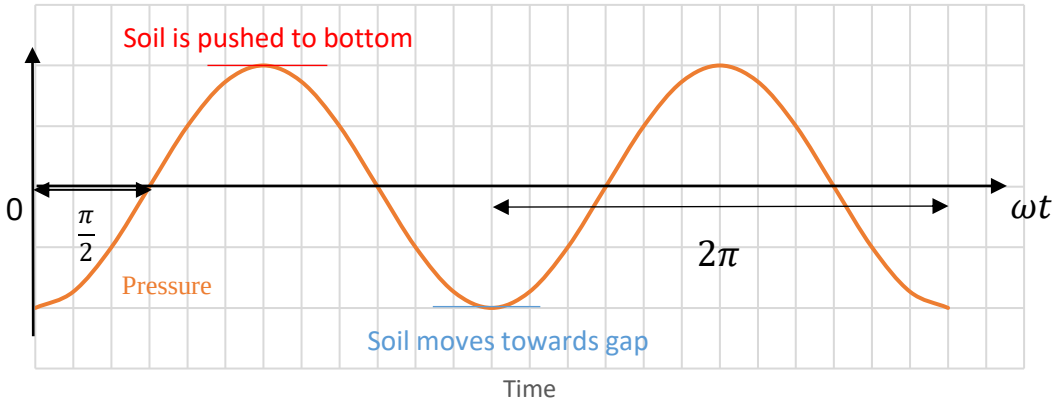

Figure 19 Pressure oscillations at the top of the container

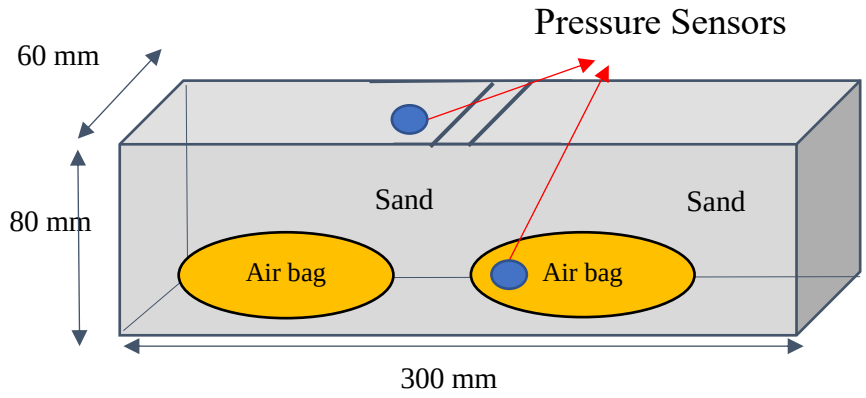

Figure 20 Laboratory experiments using pressure sensors

noticed. The pressure measurement with the sensors has not been carried out in the other experiments due to the fragility of the sensors.

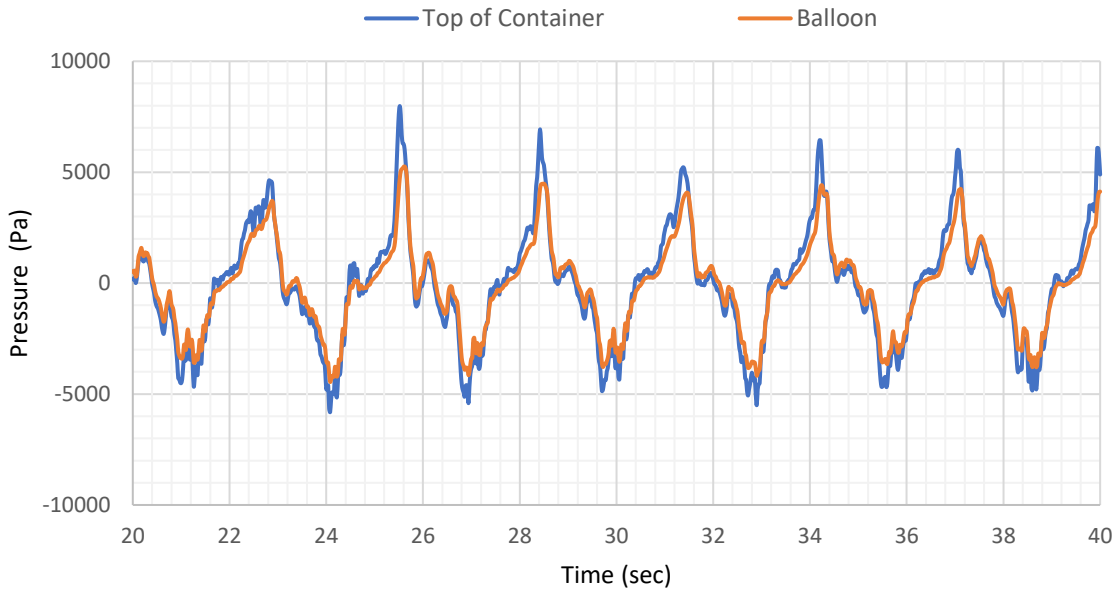

Figure 21 Pressure oscillations on top of the container and inside a balloon

As it is seen by the previous experiments, the sand leakage is associated with the pressure fluctuations in the water flow rather than the flow velocity. Therefore, under same flow conditions, a sensitivity analysis on the amount of air placed in soil medium and grain size has been performed. Fundamentally, inserting balloons changes the compressibility of the soil medium. As sand grains and water are incompressible comparing with the air, putting more air will increase the overall compressibility of the soil medium. So, this analysis can be seen also as the effect of the compressibility on the

leakage of soil. As pointed out in the chapter on literature review, previous studies on wave-induced soil response (Jeng 2013, Sumer 2014) reveal that the pressure response is getting poorer when the compressibility increases. It is because the pressure on the soil surface dissipates rapidly near the upper region of soil because air mitigates the pressure by expansion or contraction.

Also, the permeability can affect the pressure response of the soil. According to the study of Jeng (2013), with the same degree of saturation, the transmission of pressure oscillation is better in the more permeable soil. Therefore, in the coarser sand, it is expected that the magnitude of the generated pressure gradients is comparatively small.

From the image analysis on the laboratory experiments, the leaked sand area depending on gap width and volume of air for coarse grain sand and for fine grain sand has been presented in Table 1 and Table 2, respectively.

Table 1 Leaked Sand Area depending on gap width and air amount for the coarse grain sand

Coarse Grain Sand				
Volume of Air	**Gap Width**			
	3 mm	**5 mm**	**7 mm**	**Average**
0 ml	13.2	12.5	16.3	14.0
80 ml	35.0	21.5	34.7	30.4
160 ml	50.7	65.5	34.1	50.1

Table 2 Leaked Sand Area depending on gap width and air amount for the fine grain sand

Fine Grain Sand				
Volume of Air	**Gap Width**			
	3 mm	**5 mm**	**7 mm**	**Average**
0 ml	28.5	15.8	17.2	20.5
80 ml	163.1	127.6	132.1	140.9
160 ml	224.6	215.5	186.5	208.9

From the measurements of the laboratory experiments with 4 balloons (160 ml), 2 balloons (80 ml) and no balloon, the average leaked sand area (combining the results from the laboratory experiments with gap width of 3 mm, 5 mm, and 7 mm) for both fine grain and coarse grain sand are given in Figure 22. According to the graph, the sand leakage rate is proportional to the air amount in the soil medium. Introducing more air into the container increases the rate of leakage. Already stated acceleration mechanism of void development has been confirmed with this result. Especially, in the fine grain soil, the sand leakage rate is influenced more from the air amount. Though there is a slight increase, this effect is not as much conspicuous in coarse grain sand. There can be several reasons for this outcome. As the movement of soil grains out of the container is related to the pressure and the pressure gradient between soil inside the container and the flow above the container, the pressure gradient in fine grain soil is much higher than in the coarse grain. Also, the reduction in pressure disturbs the soil medium to displace the soil closer to the gap. Another reason might be the generated force on soil grains cannot lift the heavier coarse grain soil. Consequently, the leakage of sand in the coarse grain sand is not as much as the leakage in fine grain soil.

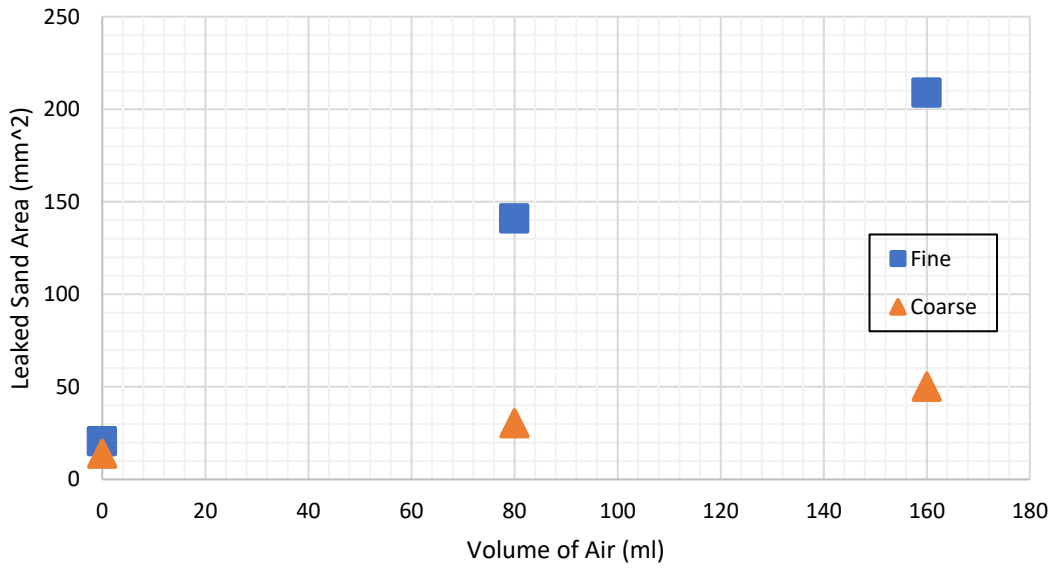

Figure 22 The leaked sand area depending on the air content

The sand leakage depending on the gap width with the fine grain soil experiments is given in Figure 23. In these experiments, 4 balloons have been placed to the bottom of

the container which is filled with fine grain sand. As gap width increases, the point of application of the pressure oscillations and the gap from which the sand leaks change.

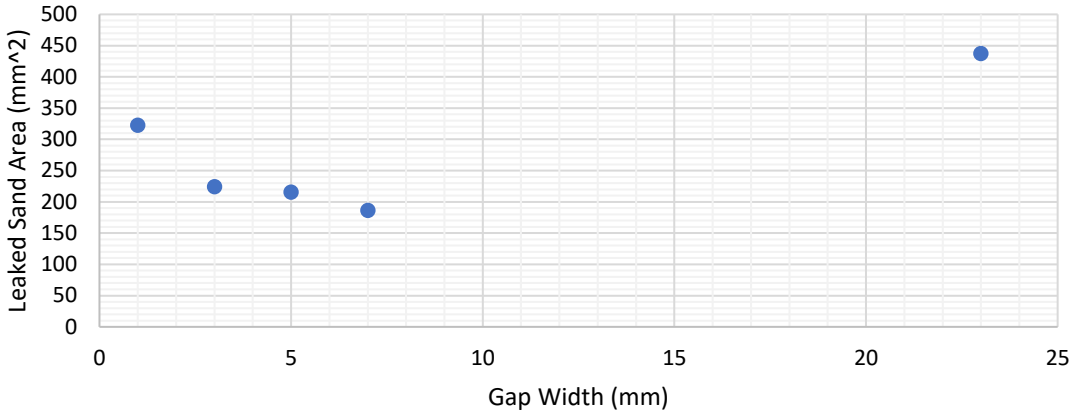

Figure 23 The leaked sand area depending on the gap width (4-balloons, fine grain)

While the gap gets wider, the leakage amount would be expected to increase with the increasing exposed area of soil to shear stress and regular sediment transport processes. Therefore, the experiment with 23 mm gap caused a large amount of leakage due to the large exposed area to shear stress. However, when the gap is very small (1 mm), it is observed that the leakage amount is also very high. The reason behind this might be explained with the poor pressure transmission when the gap is very small. With a limited area of application, the pressure could not be transmitted towards the bottom of soil and this generates a large pressure gradient near the water-soil interface. With larger pressure gradient, the amount of sand leakage is also large. As explained before, poor transmission of pressure oscillations leads to high-pressure gradient and intensify the amount of leakage. However, as the gap gets wider, the pressure can be transmitted better and the magnitude of the pressure gradient gets lower; however, the shear stress turns into more effective in the leakage of sand due to the larger application area of the water flow. Around 5-7 mm gaps, a minimum is observed. The reason behind this result might be the summation of the effects of shear stress and pressure transmission makes a minimum around a gap width of 5 to 7 mm. It is also worth noting that from the experiments of Takahashi et al. (1996), when the gap is too small, it may get blocked by the soil grains

and no leakage can be observed. Although in the current experiments, blockage of the gap has not been observed, this condition may happen in a real seawall environment.

The results on the displacements away from the gap are given as average for the gap widths of 3 mm, 5 mm, and 7 mm in Table 3. The relation between the amount of air introduced by the balloons to the soil medium and the displacements away from the gap for coarse and fine grain sand is given in Figure 24.

Table 3 The displacements away from the gap inside the soil medium (Average of experiments with a gap width of 3 mm, 5 mm, and 7 mm)

Volume of Air	Fine Grain	Coarse Grain
0 ml	0.0312 mm	0.0000 mm
80 ml	0.1288 mm	0.0189 mm
160 ml	0.2924 mm	0.1809 mm

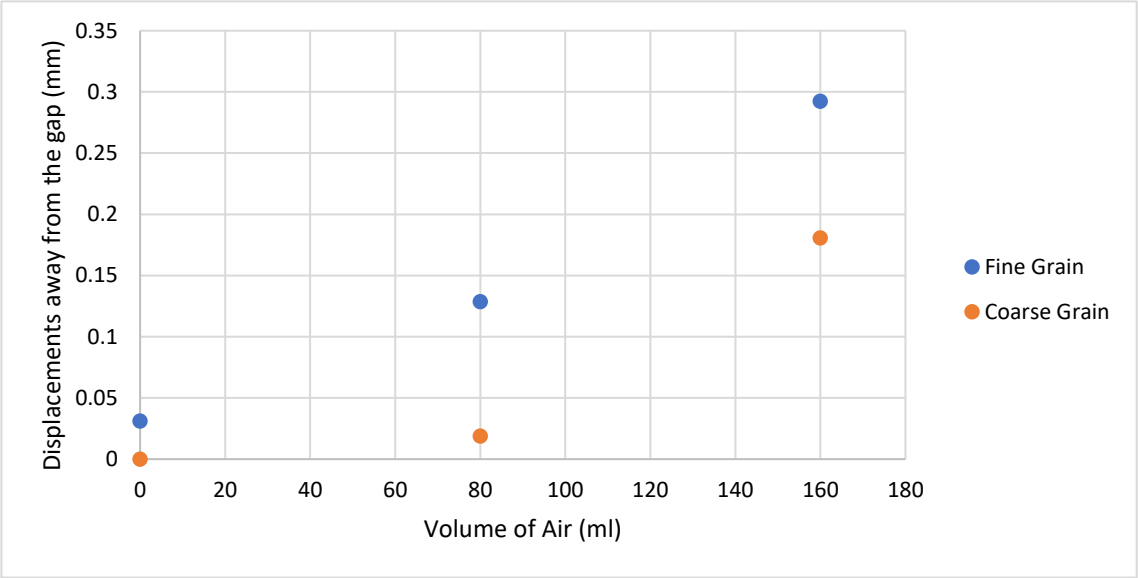

Figure 24 The relation between the volume of air and the displacements

E. Discussion of results of the laboratory experiments

In the current laboratory experiments, a larger void in the soil medium causes a faster rate of leakage of sand from the container which confirms the acceleration in the void development. As the compressibility of soil increases due to the leakage of sand, the

enlargement of the void will accelerate. One of the reasons for the large leakage when the amount void inside the soil is large is the pressure gradient between soil medium and the water flow. The pressure gradient, which enhances the leakage of the soil particles with higher inertia and drag forces, depends on the soil response. As the pressure response is getting poorer, the pressure gradient increases. And, high-pressure gradient results in an increase in the rate of leakage of soil grains.

Another reason for the large leakage under large void is due to the high compressibility of the soil medium, the displacement of soil particles near the gap is higher. This enlarged displacement of soil near the gap may also contribute to the leakage rate of sand.

These reasons reveal that as the air amount increases in the soil medium, the rate of leakage of the soil grains also increases. In other words, the rate of void development is proportional to the volume of a void in the soil medium. Therefore, the rate of void development can be written as,

$$\frac{dV_{air}}{dt} = \alpha V_{air} \tag{19}$$

Therefore, the volume of a void in soil is exponential with time, based on the following equation:

$$V_{air} = ce^{\alpha t} \tag{20}$$

where the α and c are relevant coefficients.

Therefore, the laboratory experiments have confirmed the acceleration mechanism of the void development in the backfill of a seawall. The leakage of sand through a small gap has been found out to be closely related to the upward seepage flow due to the pressure gradient between soil medium and water flow. Therefore, the response of the soil medium to the pressure oscillations is the key in this process.

The compressibility and the permeability of the soil affect the leakage of sand through a small gap. This condition is similar to the effects of compressibility and the permeability of the soil on the wave-induced soil response based on the literature review. In short, if soil response to pressure fluctuation gets worse, it is likely to have a greater soil leakage.

As the behavior of soil changes depending on the compressibility of air, it is important to know in the coastal environment which type of air present. Sumer (2014) and Wheeler (1986) have reported that in the sea environment, air is in the shape of bubbles which are much larger than the grain size of soil particles. Therefore, the experimental setup in this study may provide a soil medium which has mechanics like real sea environment. However, the condition in seawall environment can be very different. Therefore, a field study is strongly recommended for the air presence in backfill of seawalls.

The soil permeability is a measure of how rapidly fluid is transmitted between grains. Also, it is generally related to the grain size of the soil particles for sands and gravel. In coarse grain sand (high permeability), the pressure gradient is rather low. In other words, pressure transmission is better in coarse grain sand. Therefore, as observed in the experiments, the rate of leakage with coarse grain sand has not been affected by the placement of balloons as much as fine grain sand. As stated in Jeng (2013), under the same degree of saturation, pressure gradient near the soil surface is smaller for more permeable material. This explains the effect of air balloons in the coarse sand is not as much as the fine sand.

IV. THE THEORETICAL APPROACH TO THE LEAKAGE OF SAND

In the previous chapter, the laboratory experiments that have been conducted to observe the leakage of sand through a small gap under oscillatory flow has been demonstrated. In this chapter of the thesis, a theoretical approach to the sand leakage phenomenon through wave-induced soil response under oscillatory flow will be investigated. Based on the governing equations of wave-induced soil response, a numerical model has been developed. Later, the results of the numerical model will be presented and discussed.

From both the laboratory experiments and the literature survey, the leakage of sand from the backfill of seawalls has been found to be strongly related to the wave-induced sand response. The governing equations have been introduced firstly by Biot (1941, 1956). Since then, researchers tried to solve these equations in their models based on several assumptions and with several methods. An extensive review on some of these models has been already summarized in the literature review part (Chapter 2) of this thesis.

A. The Numerical Model

To model the laboratory experiments, the quasi-static assumption has been employed in this study as the difference between dynamic and quasi-static assumption is relatively low for the water wave conditions based on the studies by Ulker et al. (2009), Sakai et al. (1988), Jeng (2013), Sumer (2014).

1. Applicability of Quasi-Static Assumption

Furthermore, a method has been explained by (Jeng & Cha, 2003) about depending on the soil and wave characteristics, if it is acceptable to use quasi-static assumption in the wave-induced soil response. From the developed analytical solution, two dimensionless parameters have been introduced. Based on these non-dimensional parameters, Π_1 and Π_2, the applicable range of quasi-static assumption can be found. Π_1 is calculated as

$$\Pi_1 = \frac{\rho k V_c^2 \left(\frac{2\pi}{L}\right)^2}{\rho_w g \omega} \quad (21)$$

where ρ and ρ_w are densities of soil and water, respectively. k is the permeability of soil, L is the wave length, g is the gravitational acceleration and ω is the wave frequency $(2\pi/T)$ and V_c is the speed of compressive wave and calculated as,

$$V_c^2 = \frac{\left(\frac{G}{1-2\mu} + \frac{1}{\beta n}\right)}{\rho} \quad (22)$$

where n is soil porosity, $G$is the elastic shear modulus, and μ is the Poisson's ratio and β is the compressibility of soil medium. The other non-dimensional parameter, Π_2 is calculated as,

$$\Pi_2 = \frac{\rho \omega^2}{\left(\frac{G}{1-2\mu} + \frac{1}{\beta n}\right)\left(\frac{2\pi}{L}\right)^2} \quad (23)$$

Table 4 The soil and wave parameters of the laboratory experiments

Parameter	**Value**
Density of Sand Grains	2650 kg/m^3
Porosity	0.47
Shear Modulus	5 MPa
Permeability (Fine)	0.337 mm/s
Permeability (Coarse)	4.265 mm/s
Poisson's Ratio	0.33

The relationship limit between Π_1 and Π_2 has been given by the following equation.

$$\Pi_{2(\text{limit})} = 0.0298(k)^{0.5356}\Pi_1 \quad (24)$$

If the Π_2 calculated from the wave and soil parameters is lower than the $\Pi_{2(limit)}$, then it can be said that the quasi-static assumption is reasonable over the dynamic assumption for the wave-induced soil response.

Based on the soil and wave parameters of the laboratory experiments (Table 4), the dimensionless parameters Π_1, Π_2, and $\Pi_{2(limit)}$ have been calculated for coarse grain and fine grain sand based on the degree of saturation of the soil.

Table 5 The non-dimensional parameters Π_1, Π_2 and $\Pi_{2(limit)}$

	Coarse Grain			Fine Grain		
Degree of Saturation	100%	88%	77%	100%	88%	77%
Π_1	3000	10	10	200	1	1
Π_2	$1\ x\ 10^{-6}$	$2\ x\ 10^{-4}$	$2\ x\ 10^{-4}$	$1\ x\ 10^{-6}$	$2\ x\ 10^{-4}$	$2\ x\ 10^{-4}$
$\Pi_{2(limit)}$	5	$2\ x\ 10^{-2}$	$2\ x\ 10^{-2}$	$1\ x\ 10^{-1}$	$4\ x\ 10^{-4}$	$4\ x\ 10^{-4}$

From Table 5, in all cases, Π_2 is lower than $\Pi_{2(limit)}$. Therefore, it can be said that for the current wave and soil parameters, the quasi-static assumption on the governing equations of the wave-induced soil response is applicable.

2. Governing Equations and Finite Difference Scheme

In the quasi-static assumption to the poroelasticity equations, the compressibility of soil and pore fluid are considered. However, the accelerations due to both soil and fluid are ignored. The governing equations in 3D based on the quasi-static model treating the soil hydraulically anisotropic as follows;

$$\frac{\mathrm{K_x}}{K_z}\frac{\partial^2 p}{\partial x^2}+\frac{K_y}{K_z}\frac{\partial^2 p}{\partial y^2}+\frac{\partial^2 p}{\partial z^2}-\frac{\gamma_w n\beta}{K_z}\frac{\partial p}{\partial t}=\frac{\gamma_w}{K_z}\frac{\partial}{\partial t}\left(\frac{\partial u_x}{\partial x}+\frac{\partial u_y}{\partial y}+\frac{\partial u_z}{\partial z}\right) \quad 25$$

$$G\nabla^2 u_x+\frac{G}{1-2\mu}\frac{\partial}{\partial x}\left(\frac{\partial u_x}{\partial x}+\frac{\partial u_y}{\partial y}+\frac{\partial u_z}{\partial z}\right)=\frac{\partial p}{\partial x} \quad 26$$

$$G\nabla^2 u_y+\frac{G}{1-2\mu}\frac{\partial}{\partial y}\left(\frac{\partial u_x}{\partial x}+\frac{\partial u_y}{\partial y}+\frac{\partial u_z}{\partial z}\right)=\frac{\partial p}{\partial y} \quad 27$$

$$G\nabla^2 u_z+\frac{G}{1-2\mu}\frac{\partial}{\partial z}\left(\frac{\partial u_x}{\partial x}+\frac{\partial u_y}{\partial y}+\frac{\partial u_z}{\partial z}\right)=\frac{\partial p}{\partial z} \quad 28$$

where K_x, K_y, and K_z are the permeability of the soil in x-, y- and z-directions, respectively. Also, p is water pressure inside soil, γ_w is the unit weight of water. And, u_x,

u_y, and u_z are the displacements of soil in the $x-$, $y-$ and $z-$ directions, respectively. $\beta$is the compressibility of pore fluid and calculated as,

$$\beta = \frac{1}{K_w} + \frac{1 - S_r}{P_{abs}} \quad (29)$$

In the numerical modeling of the pressure transmission and the displacements in the soil medium, the 1D approach has been used for simplicity in this study. Therefore, the governing equations change as follows,

$$k\frac{\partial^2 p}{\partial z^2} - n\beta\gamma_w\frac{\partial p}{\partial t} = \gamma_w\frac{\partial}{\partial t}\left(\frac{\partial u_z}{\partial z}\right) \quad (30)$$

$$G\left\{\frac{\partial^2 u_z}{\partial z^2} + \frac{1}{1-2\mu}\frac{\partial}{\partial z}\left(\frac{\partial u_z}{\partial z}\right)\right\} - \frac{\partial p}{\partial z} = 0 \quad (31)$$

In order to solve the governing equations, following boundary conditions have been introduced. Firstly, the pressure at the top of soil layer has been calculated from the water flow equation. That is:

$$p = p_0\cos(\omega t), \text{ at } z = 0 \quad (32)$$

Also, at the water-soil interface, effective normal and shear stress should be equal to zero.

$$\sigma_z' = \tau_{xz} = 0, \text{ at } z = 0 \quad (33)$$

Then, at the bottom of the soil layer, due to impervious layer, the pressure gradient and the displacement is equal to zero.

$$u = 0 \text{ and } \frac{\partial p}{\partial z} = 0, \text{ at } z = -h \quad (34)$$

The finite difference method has been used to approximate the differential terms in the governing equations. As can be seen in the governing equations, the pressure and displacement terms are coupled in each time step. To overcome with this complexity, Equation 31 has been integrated over the whole depth.

$$\int_{-h}^{0} G\left(\frac{\partial^2 u}{\partial z^2} + \frac{1}{1-2\mu}\frac{\partial}{\partial z}\left(\frac{\partial u}{\partial z}\right)\right)dz = \int_{-h}^{0}\frac{\partial p}{\partial z}dz \quad (35)$$

From the top layer, the derivative of displacement is zero due to no vertical effective stress. After the integration, the simplified equation is,

$$p = G\left(1 + \frac{1}{1-2\mu}\right)\frac{\partial u}{\partial z} + p_0\cos(\omega t) \quad (36)$$

And, Equation 30 becomes,

$$k\frac{\partial^2 p}{\partial z^2} - n\beta\gamma_w\frac{\partial p}{\partial t} = \gamma_w\frac{\partial}{\partial t}\left(\frac{p - p_0\cos(\omega t)}{G\left(1 + \frac{1}{1-2\mu}\right)}\right) \quad (37)$$

Arranging the equation gives,

$$k\frac{\partial^2 p}{\partial z^2} - \frac{\gamma_w\omega p_0\sin(\omega t)}{G\left(1 + \frac{1}{1-2\mu}\right)} = \left(n\beta\gamma_w + \frac{\gamma_w}{G\left(1 + \frac{1}{1-2\mu}\right)}\right)\frac{\partial p}{\partial t} \quad (38)$$

With the central difference for spatial second order derivative and forward difference for first-order temporal derivative, the finite difference scheme becomes,

$$k\frac{p_{i+1}^n + p_{i-1}^n - 2p_i^n}{\Delta z^2} - \frac{\gamma_w\omega p_0\sin(\omega t)}{G\left(1 + \frac{1}{1-2\mu}\right)} = \left(n\beta\gamma_w + \frac{\gamma_w}{G\left(1 + \frac{1}{1-2\mu}\right)}\right)\frac{p_i^{n+1} - p_i^n}{\Delta t} \quad (39)$$

Here, the subscript i shows the spatial location and the superscript n shows the time step. The pressure at each time step is calculated explicitly, then the displacement in vertical direction u_z is computed implicitly.

3. Compressibility of Soil

Sand grains and water have very low compressibility values comparing with the air. In the laboratory experiments, with introducing air into the soil medium by balloons, the compressibility of the soil medium has been increased, significantly. However, the air inside the balloons cannot dissipate into the sand-water mixture. From the literature review, it is already known that, in the marine environment, the air can present like bubbles which are much greater than the soil grains (Wheeler, 1986). However, in the complex and undiscovered seawall environment, how air would behave is still unknown. Therefore, at this point, it is important to stress that there is a need for research in the field to assess the void presence and the degree of saturation in the seawall environment.

To model the laboratory experiments, it is needed to know how compressible is the soil medium. In the governing equations (Eq. 25), the term, β determines the compressibility which is the relative volume change as a response to pressure change. It can be calculated as,

$$\beta = -\frac{1}{V}\frac{dV}{dp} \tag{40}$$

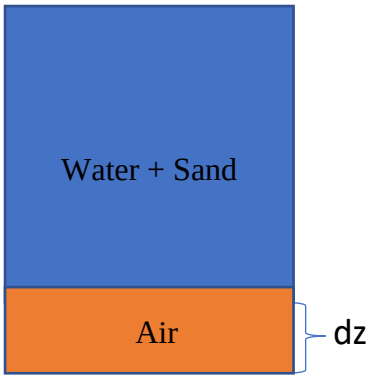

Figure 25 Hypothetical Drawing for Compressibility in 1D

Furthermore, from the Boyle's Law, in an adiabatic condition

$$P_{abs} * V_{initial}^{\gamma} = (P_{abs} + P_c) * V^{\gamma} = p * V^{\gamma} \approx Constant \tag{41}$$

where P_{abs} is the absolute pressure of air before any pressure oscillations, P_c is the magnitude of pressure oscillation applied on the air. Following the hypothetical drawing

for the compressibility (Figure 25), the initial volume of air $V_{initial} = dzdxdy$ and the instantaneous volume, $V = (dz + u_{bottom})dxdy$ can be found where u_{bottom} is the vertical displacement of air-soil contact and P is the instantaneous pressure, which is the summation of absolute pressure at the beginning and pressure oscillations. So, for the volume, it can be written as,

$$V^{\gamma} = \frac{P_{abs} * V_{initial}^{\gamma}}{p} \Rightarrow \frac{dV^{\gamma}}{dp} = -\frac{1}{p^2}\left(P_{abs} * V_{initial}^{\gamma}\right) \quad 42$$

So, the compressibility of air in the soil medium can be found as,

$$\beta = -\frac{1}{V^{\gamma}}\frac{dV^{\gamma}}{dp} = -\frac{1}{V^{\gamma}}\left(-\frac{V_{initial}^{\gamma} * P_{abs}}{p^2}\right) \quad 43$$

So, at the beginning, it is known that the volume of air, $V^{\gamma} = V_{initial}^{\gamma}$ and the pressure, $p = P_{abs}$. Therefore, the compressibility of air at the beginning of the experiment can be found as,

$$\beta = \frac{1}{P_{abs}} \quad 44$$

Due to the very low compressibility of the sand grains, only water and air can be considered as compressible. And, relative values of water and air can be determined from the degree of saturation. Therefore, the compressibility equation that will be used in the numerical model can be calculated as,

$$\beta = \frac{1}{K_w} + \frac{1 - S_r}{P_{abs}} \quad 45$$

where K_w is the bulk modulus of water and S_r is the degree of saturation. The Equation 45 is extensively used in wave-induced soil response models. In fact, the compressibility of air decreases and increases as the pressure of the air increase and decrease, respectively. So, during the pressure oscillations, the compressibility of air changes. However, as the magnitude of the pressure oscillations are very low than the absolute pressure, in this study, Equation 45 will be used like the former researchers for the wave-induced soil response.

B. Validation of the Numerical Model

In order to validate the developed 1D Quasi-static model, experimental results from previous studies have been used. Comparison with five different data sets from experimental work and with an analytical solution will be presented here.

Tsui and Helfrich (1983) have carried out laboratory experiments in a wave flume with a soil layer, in which there are pressure sensors installed throughout the depth of soil layer. Figure 23 shows the comparison of the vertical distribution of the maximum normalized pressure calculated from the present QS model and laboratory experiments of Tsui and Helfrich (1983). The input values for this computation are given in Table 6.

Table 6 Input values for computation of pressure response for the study of Tsui and Helfrich (1983)

Period, T	1.5 sec
Depth of soil layer, h	0.33 m
Porosity of soil medium, n	0.3
Poisson's Ratio, μ	0.3333
Shear Modulus, G	5 MPa
Water level above the soil, d	0.488 m

The permeability and the degree of saturation of the soil medium have been assigned proper values according to the trials. According to the computations, for the loose sand, the degree of saturation has been calculated as 0.996, and the permeability has been calculated as 5 mm/s. On the other hand, for the dense sand, the degree of saturation has been calculated as 0.975, and the permeability has been calculated as 2.5 mm/s

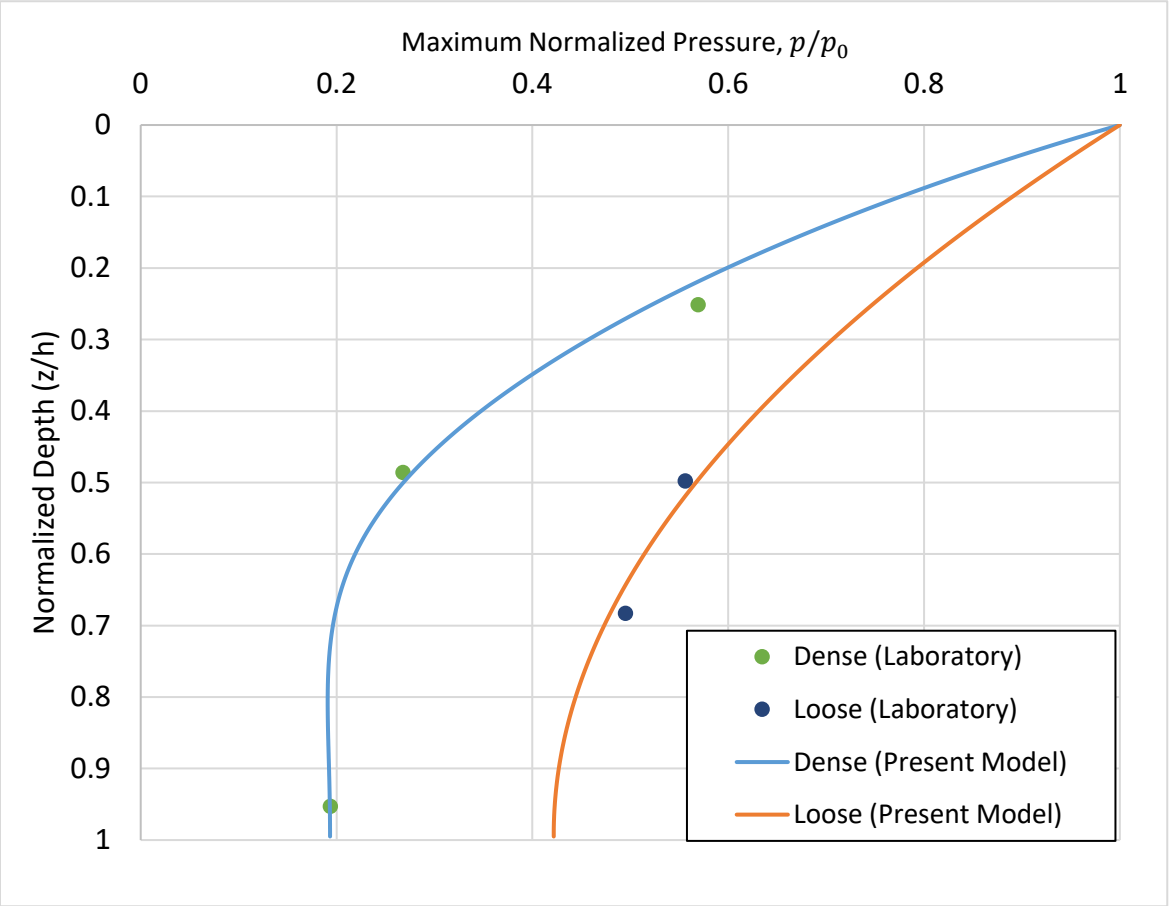

Figure 26 Comparison of the vertical distribution of maximum normalized pore pressure oscillation, p/p_0. (Tsui and Helfrich, 1983)

It can be seen from the Figure 26; the present model agrees well with the experimental data for each case with the suitable degree of saturation and permeability values.

Furthermore, the data from two laboratory experiments from the study of Maeno and Hasegawa (1985) will be presented. They have conducted the experiments under different wave conditions. In these modeling study, for the first experiment, the input values are given in Table 7.

Table 7 Input values for computation of pressure response for the first experiment of Maeno and Hasegawa (1985)

Period, T	0.96 sec
Depth of soil layer, h	0.36 m
Porosity of soil medium, n	0.4
Poisson's Ratio, μ	0.495
Shear Modulus, G	2 MPa
Water level above the soil, d	0.41 m
Degree of Saturation, S_r	0.996
Permeability of soil, k	0.23 mm/s

The comparison of the vertical distribution of maximum pressure between the experimental study of Maeno and Hasegawa (1985) and the presented model for the first case is given in Figure 27. From this figure, with the relevant parameters, the laboratory measurements and the developed quasi-static model results agree well.

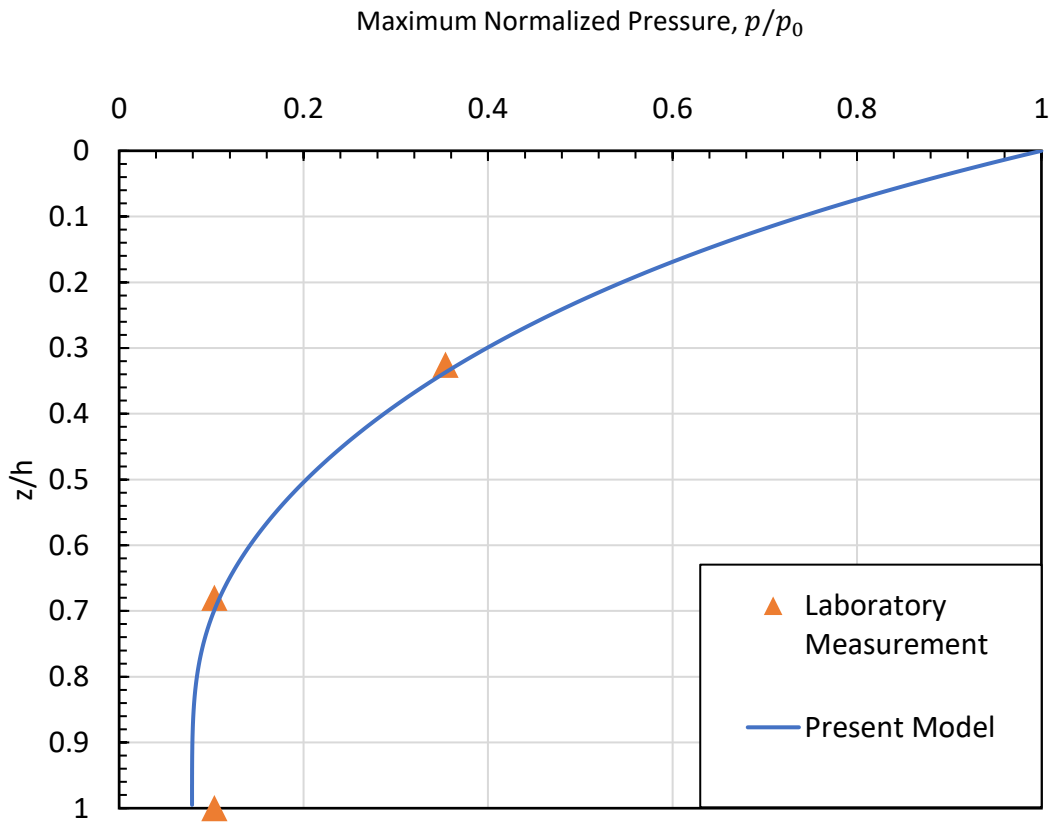

Figure 27 Comparison of the vertical distribution of maximum normalized pore pressure oscillation, p/p_0. First Experiment (Maeno and Hasegawa, 1985)

And for the second experiment, the input values are given in Table 8.

Table 8 Input values for computation of pressure response for the second experiment of Maeno and Hasegawa (1985)

Period, T	1.92 sec
Depth of soil layer, h	0.36 m
Porosity of soil medium, n	0.4
Poisson's Ratio, μ	0.495
Shear Modulus, G	2 MPa
Water level above the soil, d	0.41 m
Degree of Saturation, S_r	0.95
Permeability of soil, k	0.23 mm/s

The comparison of the vertical distribution of maximum pressure between the experimental study of Maeno and Hasegawa (1983) and the presented model for the second case is given in Figure 28. It can be seen from the figure, the results from the present model match well with the laboratory measurements of Maeno and Hasegawa (1983).

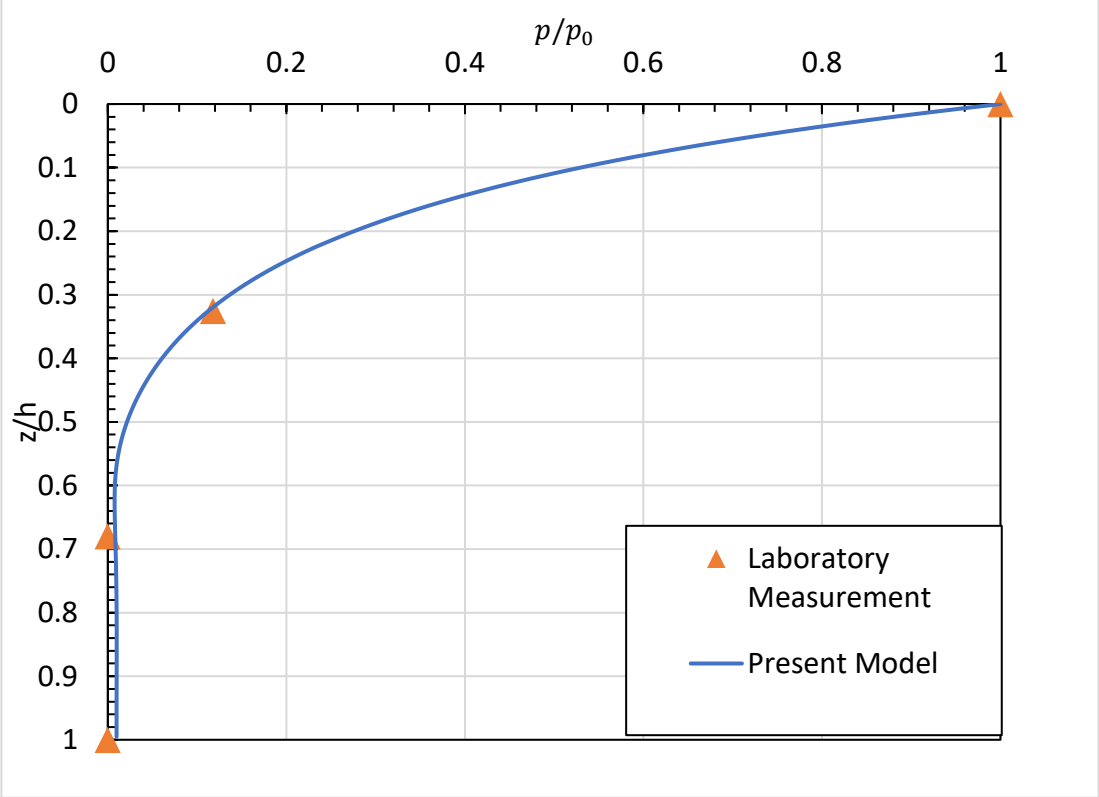

Figure 28 Comparison of the vertical distribution of maximum normalized pore pressure oscillation, p/p_0. Second Experiment (Maeno and Hasegawa, 1985)

Also, Jeng (2013) has also validated his analytical solution in 2D with the quasi-static assumption with the vertical distribution of maximum pressure values measured in the studies of Tsui and Helfrich (1983) and Maeno and Hasegawa (1983). The results of this analytical solution and experimental work of Tsui and Helfrich (1983) and Maeno and Hasegawa (1983). have agreed well. Therefore, the present quasi-static model gives a similar result with the analytical solution of quasi-static assumption.

Furthermore, to validate the numerical model for the instantaneous pressure transmission in a soil medium, the laboratory measurements of Chowdhury et al. (2006) has been used. In their laboratory experiments, rather than a wave flume, and equipment to test the pressure transmission due to wave has been utilized to examine liquefaction potential of the soil. The parameters that have been used in the model are presented in Table 9. Even though the initial degree of saturation before the experiment has been given as 96%, it has been assumed as 99.9% in the developed numerical model following the trials with several values of the degree of saturations. This may be because after starting the experiment, the soil gets compacted following the pressure oscillations.

Table 9 Input values for computation of pressure response for the experiment of Chowdhury et al. (2006)

Period, T	9 seconds
Depth of soil layer, h	1.41 m
Porosity of soil medium, n	0.46
Static Pressure of water	49 kPa
Permeability of soil, k	2.9 mm/s
Pressure amplitude p_0	9 kPa

From the Figure 29, the input pressure oscillation to the model can be seen in the upper left panel for z=0. The pressure response of the soil has been estimated reasonably well, except the normalized depth of z=0.86. However, the input wave motion in the model is triangular, while the wave in the laboratory experiments is rather irregular. Also, in the laboratory experiments of Chowdhury et al. (2006), the pressure appears linear at the top layer. However, as the depth increases, there are noises in the pressure oscillations. It may be due to the heterogeneity in the soil structure which may be the reason for the difference between the model and the measurements towards the bottom.

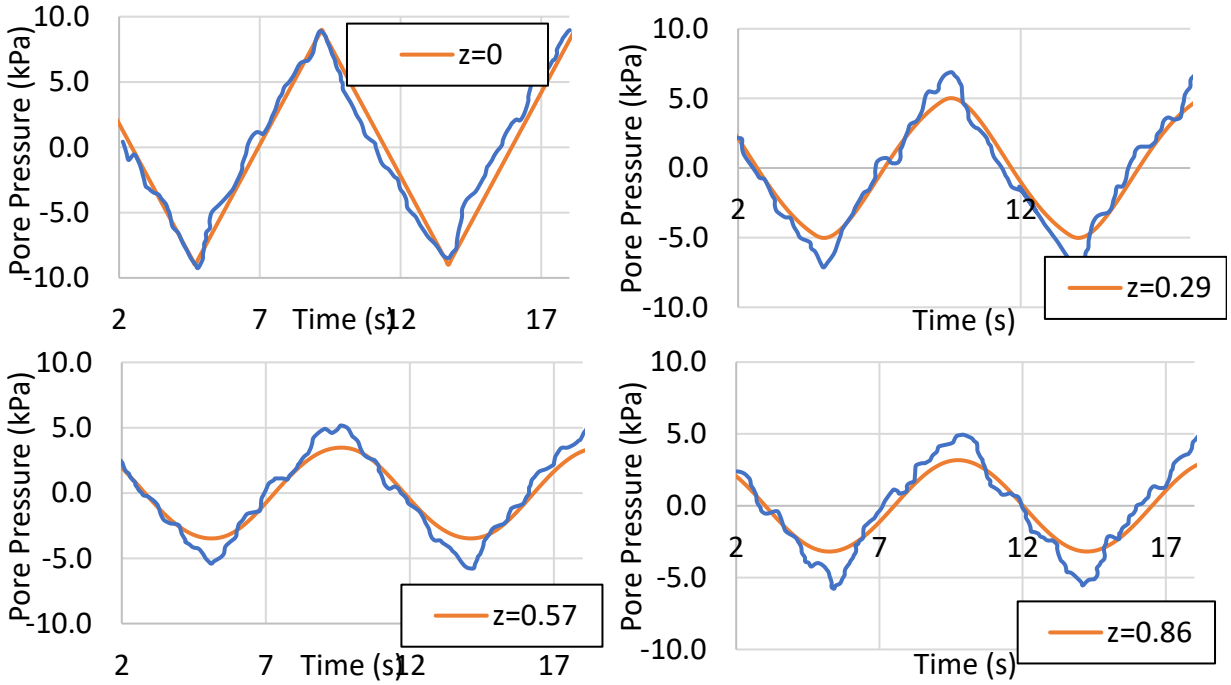

Figure 29 Instantaneous pressure fluctuations for the normalized depths of, $z = 0$, $z = 0.29$, $z = 0.57$, and $z = 0.86$

Finally, the developed numerical model based on the quasi-static assumption has been validated by the laboratory experiments of Tsui and Helfrich (1983), Maeno and Hasegawa (1983), Chowdhury et al. (2006), and by the analytical solution of Jeng (2013). According to the validation, the developed numerical model is applicable to the wave-induced pressure response.

C. Quasi-Static Model Results

After the verification analysis, the results from the numerical model will be explained. The soil properties from the laboratory experiments that have been used in the numerical

modeling are given in Table 10. In the laboratory experiments, as the balloons included inside the soil medium, the compressibility has increased significantly. Therefore, to account the effect of compressibility is one of the main objectives. Furthermore, in the experiments, two various kinds of sand have been used. Coarse and fine grain soils had different leakage rate under same oscillatory flow. Therefore, the permeability of these soils has also an important effect on the wave-induced pressure response.

From the measurements of laboratory experiments, the degree of saturation for 2 balloons has been found as 88%. Also, in the experiments with 4 balloons, the degree of saturation has been calculated as 77%.

Table 10 Soil properties for numerical modeling

Parameter	**Value**
Density of Sand Grains	2650 kg/m^3
Porosity	0.47
Shear Modulus	5 MPa
Permeability (Fine)	0.337 mm/s
Permeability (Coarse)	4.265 mm/s
Poisson's Ratio	0.33

For the case of sand grains in the marine environment, the permeability is strongly correlated to the median diameter of the sand grains. Through the sand particle analysis in the laser particle size analyzer, the median diameter size of coarse and fine grain sand has been measured as $0.89\,mm$ and $0.25\,mm$, respectively. The permeability values have been calculated from the following equation,

$$k = \frac{k_i \rho_w g}{\mu} \tag{46}$$

where k_i is intrinsic permeability, μ is the dynamic viscosity of water, ρ_w is the density of water and g is the gravitational acceleration. The intrinsic permeability, k_i, is calculated according to Harleman et al. (1963),

$$k_i = C d_{50}^2 \tag{47}$$

where C is a dimensionless constant and it can be assumed as $5.5 * 10^{-4}$ for the sand grains and d_{50} is median grain size diameter (in cm). Solving the equations, the

permeability of fine grain sand is found as 0.337 mm/s. And, the permeability of coarse grain sand is calculated as 4.265 mm/s. Sand can show anisotropic characteristic for the hydraulic conductivity. In other words, the permeability of a soil can be different in each direction. However, in this study, the permeability of soil is assumed as isotropic due to the one-dimensional model.

Also, in the calculations, the shear modulus, density of sand grains and the Poisson's ratio have been assumed based on the general sand properties in the marine environment.

Using the soil and wave parameters from the laboratory experiments, the quasi-static model gives the following results for the vertical distribution of maximum normalized pore pressure (p/p_0) values for coarse grain (Figure 30) and for fine grain sand (Figure 31). (p_0 is the applied maximum pressure oscillation at the top of the soil layer)

In the coarse grain, it is obvious that the pressure transmission (Gray line in Figure 30) is very good when there is no air inside soil medium, i.e., the degree of saturation is 100. In other words, the pressure applied to the top surface of the soil is transmitted to the bottom of the container without much damping. However, when the air is introduced to

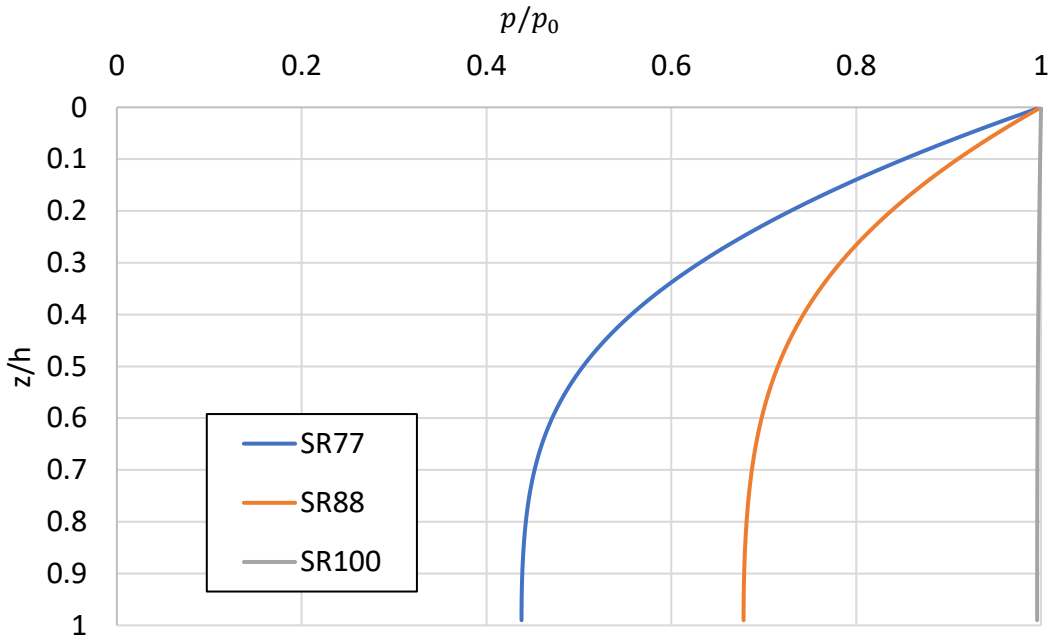

Figure 30 The vertical distribution of maximum normalized pore pressure, p/p_0 for coarse grain sand

the soil, due to the rapid dissipation of the pressure oscillation at the top layer of the soil, a large pressure gradient is created. So, the pressure reaching to the bottom of the container is much less than the case when the soil is fully saturated. Also, the pressure response is getting poorer as the degree of saturation decreases.

In the fine grain sand, from Figure 31, the pressure transmission is poorer than in the coarse grain sand for the same degree of saturation. Also, as the degree of saturation decreases, the pressure response of the soil gets poorer and poorer. Especially, at the top layer of the soil, the rapid dissipation is again observable for the fine grain sand.

At this point, using the developed numerical model, the maximum pressure gradients at the top layer of the soil for both fine and coarse grain under different degree of saturation values are calculated. Since, in the laboratory experiments, pressure gradients near the top layer of the soil have been found responsible for the large leakage.

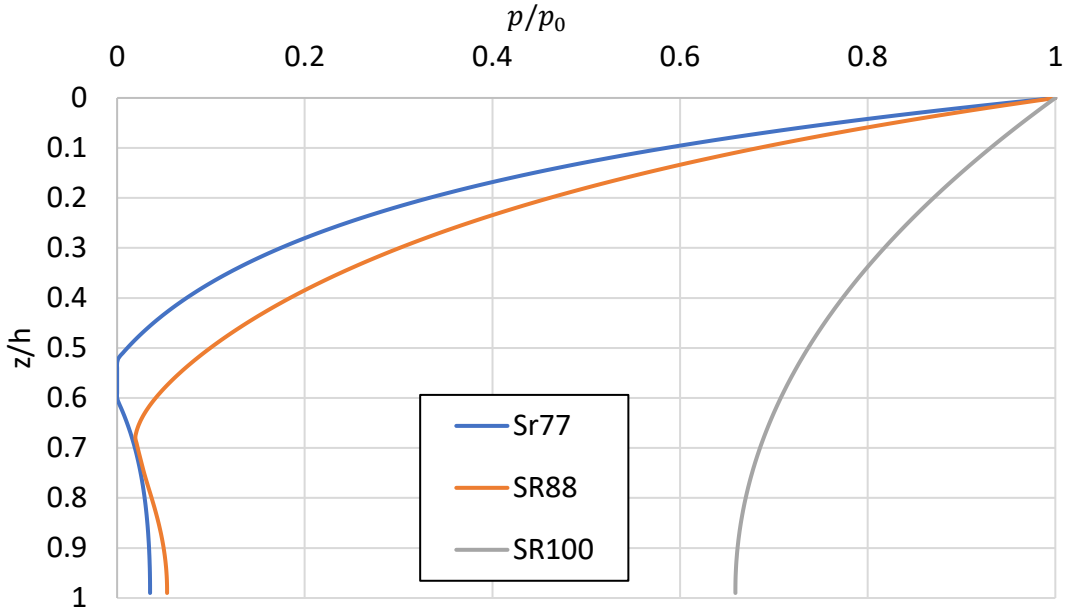

Figure 31 The vertical distribution of maximum normalized pore pressure, p/p_0 for fine grain sand

As can be seen from the Figure 30 and Figure 31, at the top layers of the soil, there is a clear pressure gradient due to the oscillations in the pressure. The normalized pressure gradient has been calculated as

$$NPG = \frac{\frac{p_{i+1} - p_i}{p_0}}{\frac{z_{i+1} - z_i}{h}} \quad (48)$$

where i+1 subscript denotes the next spatial coordinate and i subscript denotes the current spatial coordinate. The normalized pressure gradient is a dimensionless parameter and in the numerical model, it is calculated in each time step. So, it has been calculated separately from the normalized pore pressure. And, the largest normalized pressure gradient during the model run has been determined as the maximum normalized pressure gradient.

Figure 32 shows the maximum normalized pressure gradients of the top layer of soil for fine and coarse grain sand while the degree of saturation is 77%, 88%, and 100%.

It is already clear from Figure 30 and Figure 31 that the decrease in the degree of saturation causes high-pressure gradients at the top soil layer. From the maximum normalized pressure gradient perspective, Figure 32 brings the similar conclusion. In

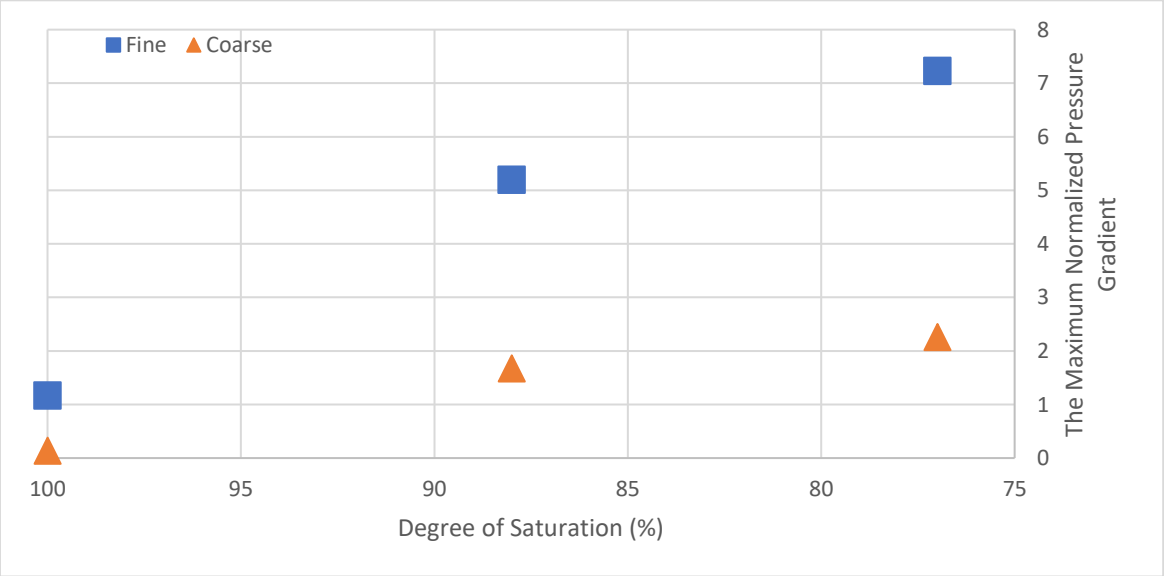

Figure 32 The maximum normalized pressure gradient at the top layer of soil medium depending on the degree of saturation and grain size of the soil

other words, as the compressibility of the soil medium increases, the pressure response is getting poorer.

Also, from Figure 32, the maximum pressure gradient increases due to decreasing degree of saturation for both coarse and fine grain sand. However, for the coarse grain sand, the maximum pressure gradient at the top layer is smaller than for the fine grain under the same degree of saturation which is similar to the measurements of the leakage of sand in the laboratory experiments.

Therefore, if there is a positive correlation between pressure gradient and the leakage of sand, from Figure 32, the acceleration of the void development can be confirmed by the validated numerical model. Since, in a real seawall, the leakage rate would be expected to have an exponential correlation with the time due to decreasing degree of saturation following the leakage of sand. Due to sharper increase in the pressure gradient for the fine grain sand, as the filler soil getting finer, the leakage rate will increase faster. In other words, finer sand will be more susceptible to air content rather than coarser sand.

Also, in Figure 33, the relation between the maximum pressure gradient at the top layer and the degree of saturation has been given for the permeability value of 0.337 mm/s (fine grain soil from the laboratory experiments). As the coarser sand (more permeable) has a better response to the pressure oscillations, the maximum pressure gradient for the same degree of saturation will be lower for the coarse grain sand. Likewise, the maximum

pressure gradient at the top layer for the same degree of saturation will be higher in a finer grain soil (less permeable) due to poor response to pressure oscillations

From the compressibility point of view, one thing to consider in a real seawall environment is that the developed voids may fill with air or water. If air fills the developed voids, the pressure response of the soil will get poorer due to high compressibility of air.

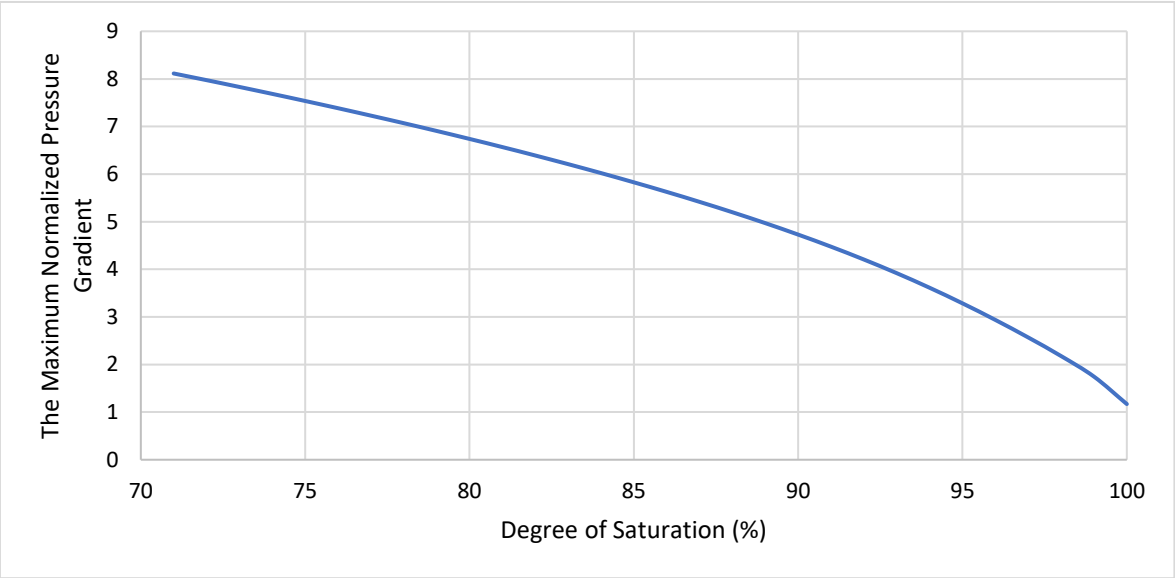

Figure 33 The maximum normalized pressure gradient according to the degree of saturation of the soil

However, if water fills the voids, then the pressure response will not be affected too much by this change due to the low compressibility of water. Therefore, it is also very important to consider the type of fluid is entering in the developed voids inside the backfills of the seawall. The lack of field study in the void development behind seawalls limits the knowledge about the void filler material. However, from the laboratory experiments of Hur et al. (2007), the first void developed around the still water level. Therefore, in a real seawall, the void development can take place around the mean water level and the voids filled with both air and water at the same time. Also, wave attacks may trap some air below the sea level. This condition can also be dangerous as it may accelerate the void development further.

Another important parameter in wave-induced soil response is the permeability of the soil. Figure 34 shows the maximum pressure gradients near the top layer depending on the permeability of soil under the same degree of saturation, which is assumed 88% in this computation.

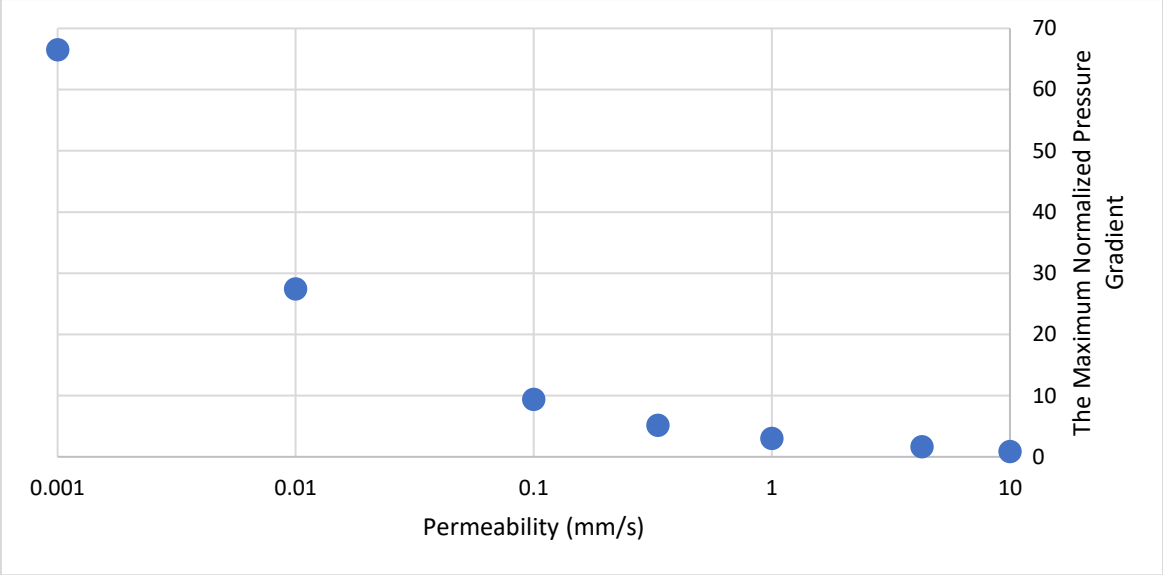

Figure 34 The maximum normalized pressure gradient according to the permeability of the soil

Note that the horizontal axis is in the logarithmic scale in Figure 34. As it was also obvious from the Figure 32, the maximum pressure gradient decreases as the permeability increases. If the pressure gradient is the main force leading to the leakage of sand, the movement of sand grains from the container through the gap to the outside of container intensifies as the permeability decreases. As it has been found out, in the laboratory experiments of the fine grain soil, the leaked sand was larger than in the laboratory experiments of the coarse grain soil. Therefore, the result of numerical model agrees with the interpretation of the results of the laboratory experiments

Next, Figure 35 and Figure 36 show the time variation of pressure and pressure gradient throughout the depth of soil layer for one period of oscillatory flow, respectively. The time variation of pressure and pressure gradient have revealed that between the maximum pressure and the maximum pressure gradient, there is a phase difference.

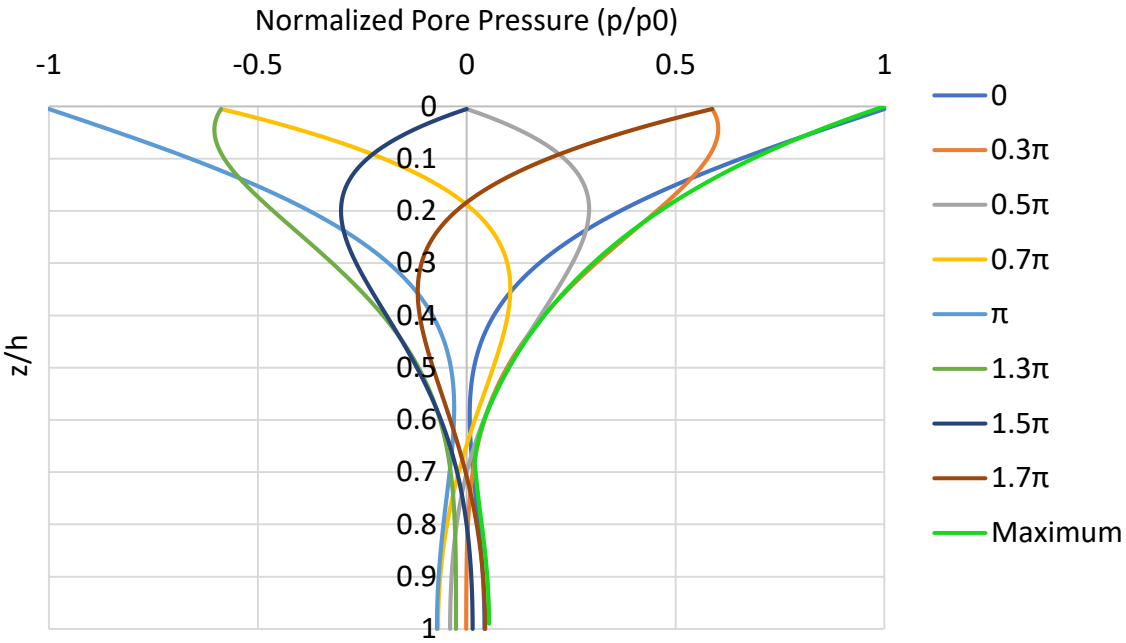

Figure 35 Time variation of normalized pore pressure oscillation throughout the depth of soil medium

These graphs have been drawn for the case of fine grain soil and the degree of saturation of 88%. The time difference between the maximum pressure and the maximum pressure gradient at the top layer is around 0.25π. Therefore, an investigation on the

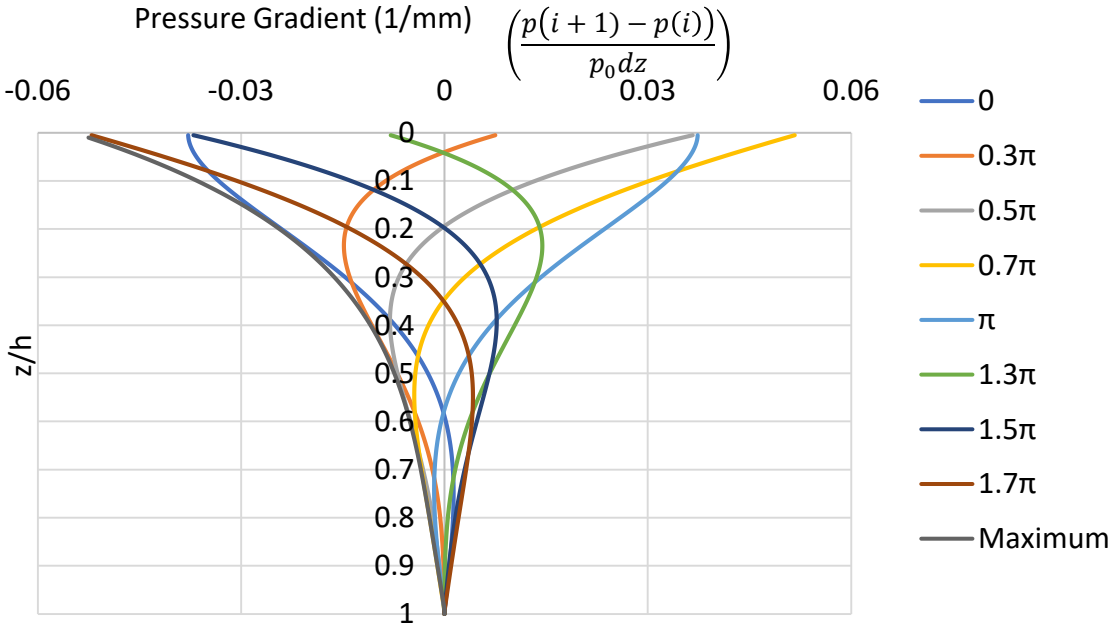

Figure 36 Time variation of pressure gradient throughout the depth of soil medium

phase difference has been conducted. The dependency on the degree of saturation has been studied. The Figure 37 shows the phase difference between the maximum pressure and the maximum pressure gradient at the top layer for various degree of saturation values when the period of flow is 2 seconds. In Figure 37, different permeability values have been tested when the degree of saturation is 77%, 88% and 100%. Therefore, the permeability of soil also affects the phase difference between the maximum pressure and the maximum pressure gradient.

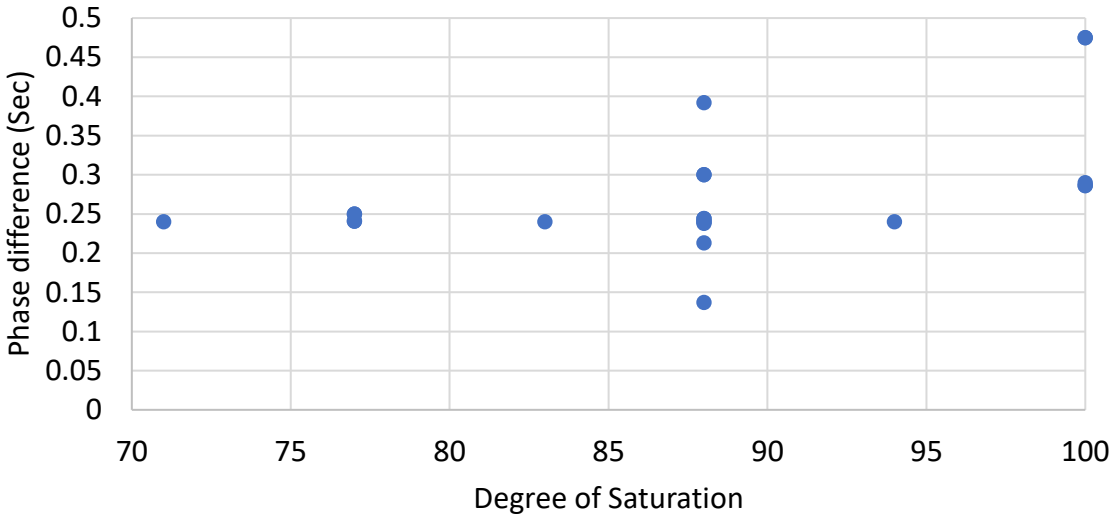

Figure 37 Phase difference between maximum pressure and maximum pressure gradient depending on degree of saturation

From the Figure 37, it can be said that the degree of saturation is not very effective on the phase difference unless the soil is fully saturated under same permeability. Phase difference increases as the soil get fully saturated. Figure 38 shows the dependency of phase difference on the permeability when the degree of saturation is 88% based on the numerical model.

Figure 38 shows that as the permeability increases, the phase difference between the maximum pressure and the maximum pressure gradient for the top layer also increases. So, it can be concluded that as the pressure response is getting better the phase difference increases. However, if the soil is not fully saturated, as the degree of saturation decreases the phase difference does not show a notable change. So, it is hard to say that there is a

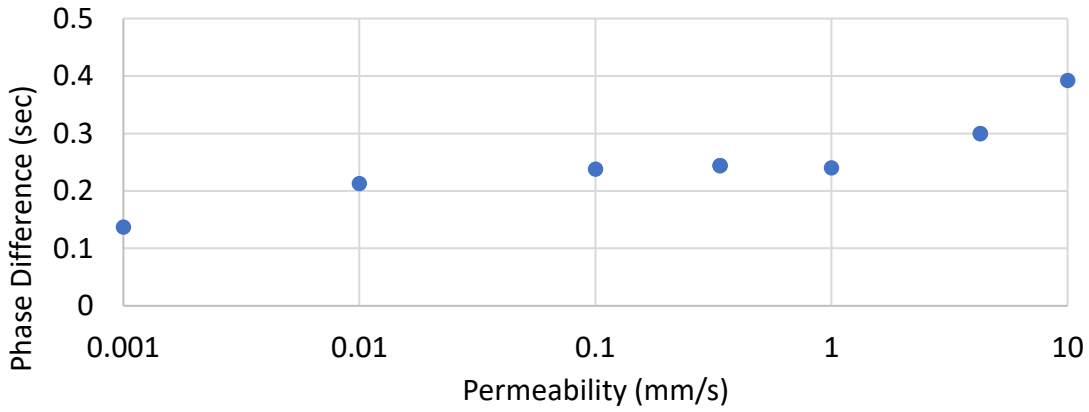

Figure 38 Phase difference between maximum pressure and maximum pressure gradient depending on the permeability of soil

correlation between the phase difference of maximum pressure and maximum pressure gradient and pressure response.

D. Phase Lag due to Progression of Pressure to Deeper Levels of Soil Medium

According to the experiments using the pressure sensors and the literature review, while the pressure is transmitted to the deeper levels of the soil medium, not only the magnitude of the pressure oscillation attenuates, but also a phase lag is observed. The phase lag during the progression of the pressure oscillations to the deeper levels of soil has been investigated based on the developed numerical model. Following figures show the pressure fluctuations through time in the whole soil layer. Figure 39 shows the pressure fluctuations for 5 seconds in the soil medium for fine grain sand and saturated case ($S_r = 100\%$).

Figure 40 and Figure 41 show the pressure fluctuations for 5 seconds in the soil medium for fine grain sand and the degree of saturation of $S_r = 88\%$ and the degree of saturation of $S_r = 77\%$, respectively.

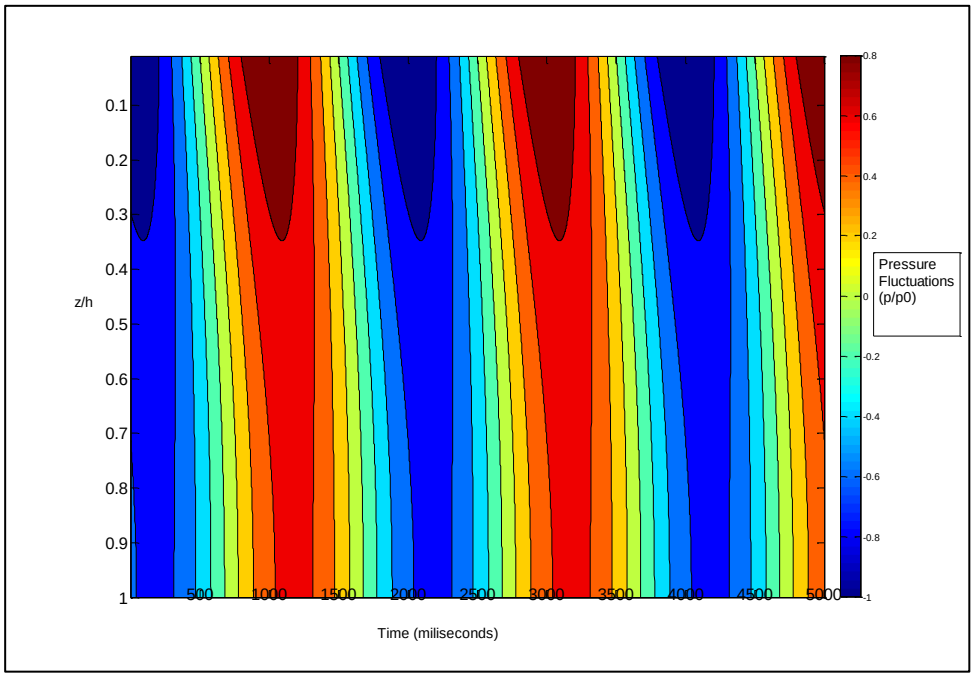

Figure 39 The pressure fluctuations for 5 seconds in the soil medium for fine grain sand and saturated case ($S_r = 100\%$)

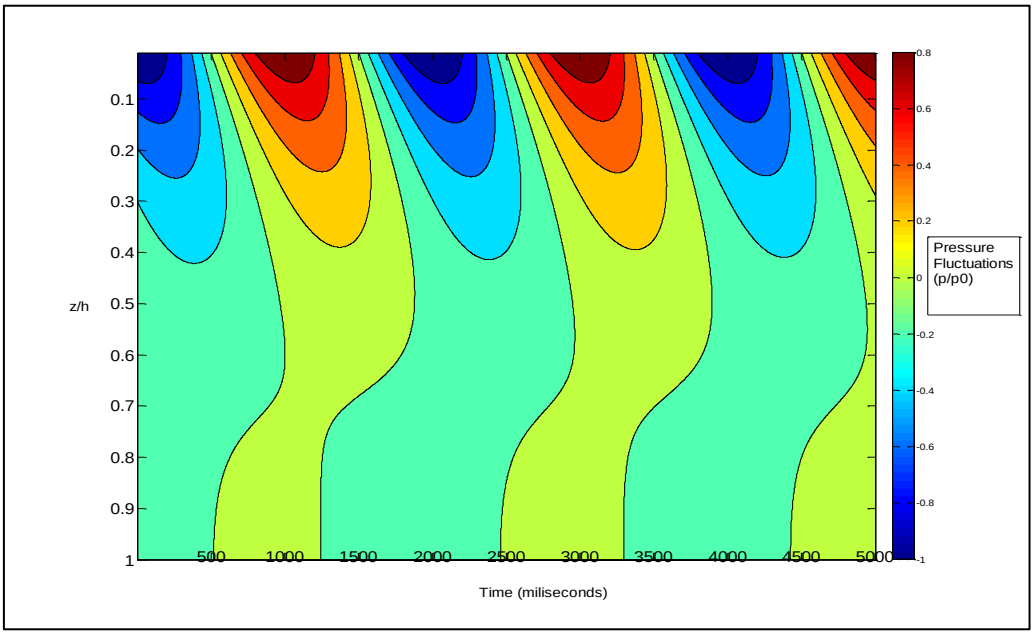

Figure 40 The pressure fluctuations for 5 seconds in the soil medium for fine grain sand and the degree of saturation of $S_r = 88\%$

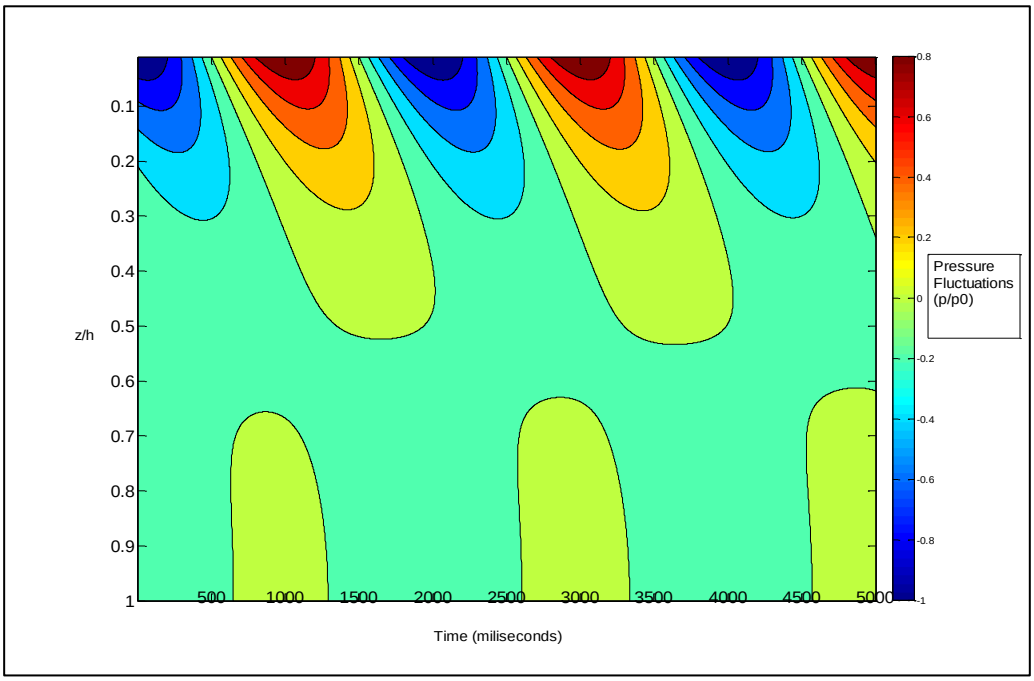

Figure 41 The pressure fluctuations for 5 seconds in the soil medium for fine grain sand and the degree of saturation of $S_r = 77\%$

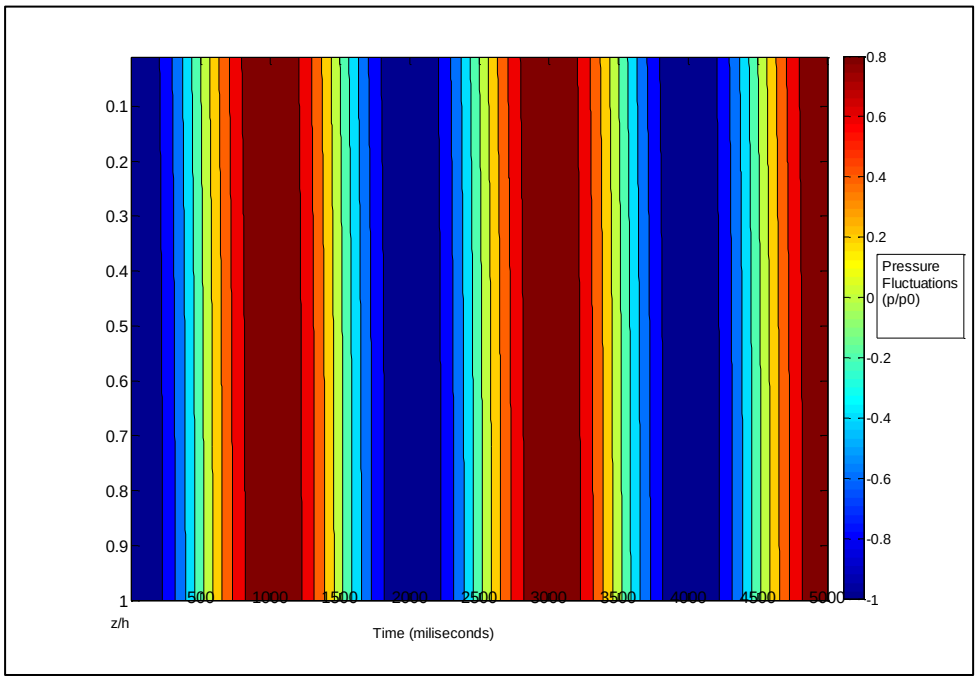

Figure 42 The pressure fluctuations for 5 seconds in the soil medium for coarse grain sand and saturated case $(S_r = 100\%)$

Figure 42 shows the pressure fluctuations for 5 seconds in the soil medium for coarse grain sand and saturated case ($S_r = 100\%$).

Figure 43 and Figure 44 show the pressure fluctuations for 5 seconds in the soil medium for coarse grain sand and the degree of saturation of $S_r = 88\%$ and the degree of saturation of $S_r = 77\%$, respectively.

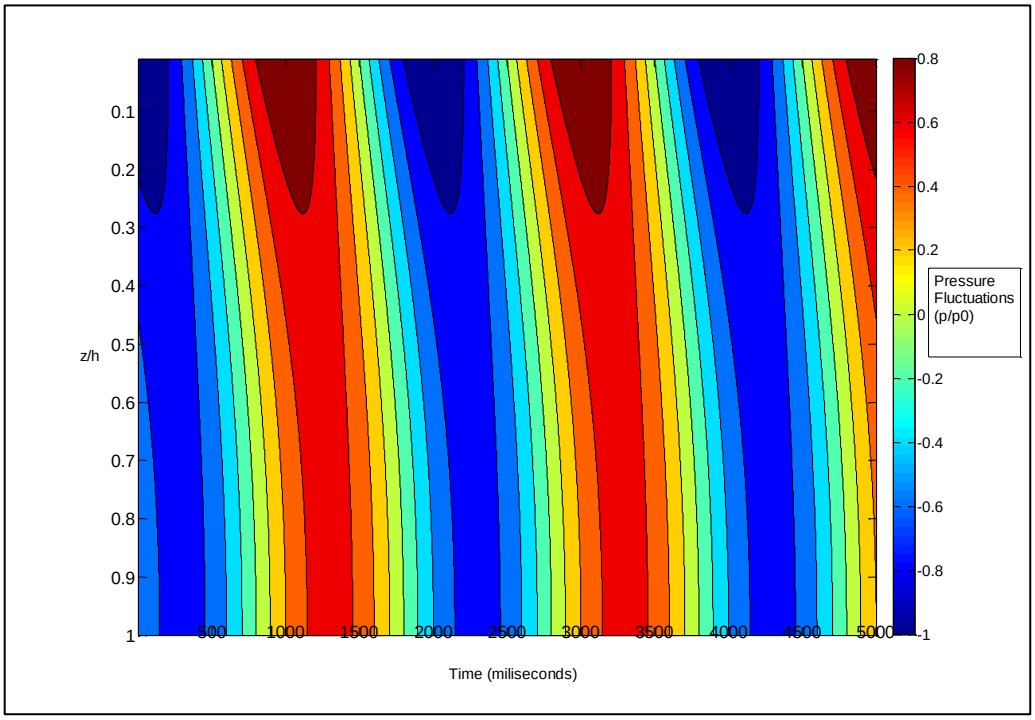

Figure 43 The pressure fluctuations for 5 seconds in the soil medium for coarse grain sand and the degree of saturation of $S_r = 88\%$

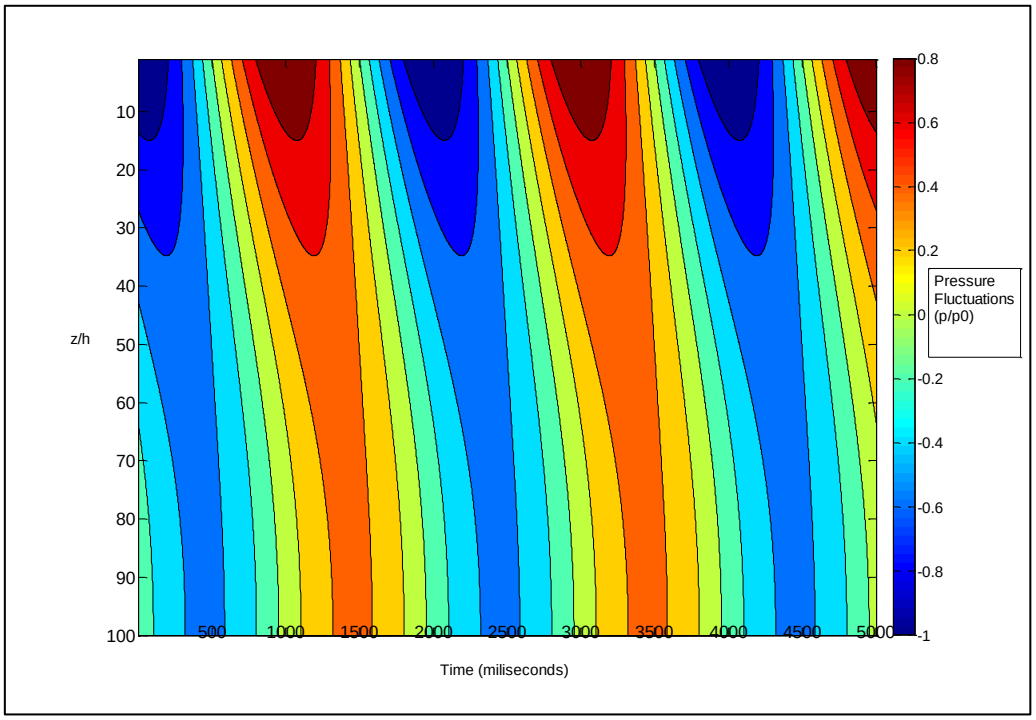

Figure 44 The pressure fluctuations for 5 seconds in the soil medium for fine grain sand and the degree of saturation of $S_r = 77\%$

From the figures above, it is clear that the phase lag increase with the decreasing degree of saturation. Also, for the same degree of saturation, coarse grain sand has less phase lag compared with the fine grain sand. Figure 45 shows the phase lag and degree of saturation relation for coarse grain and fine grain sand based on the developed numerical model.

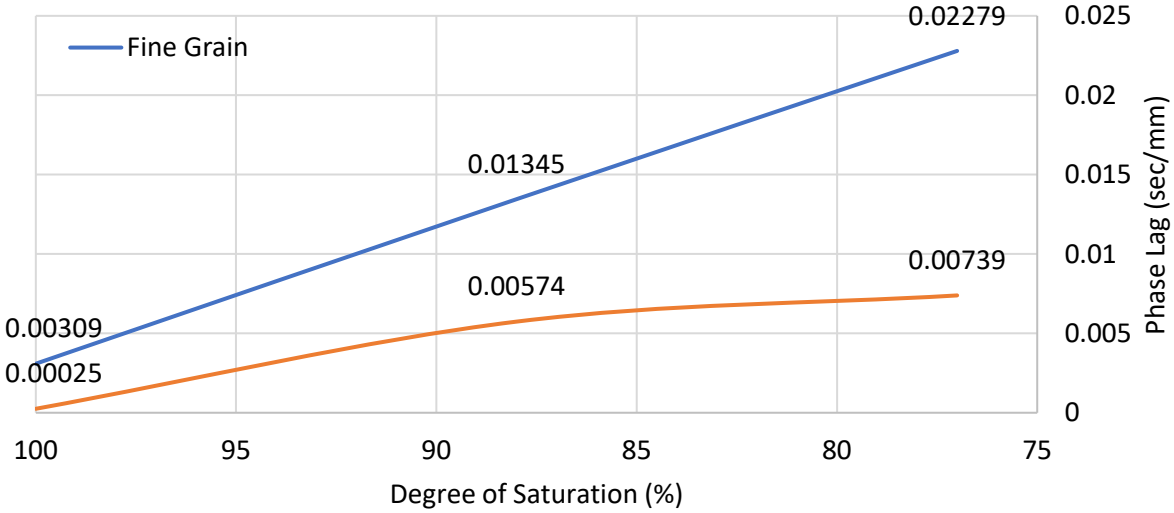

Figure 45 The phase lag and degree of saturation relation for coarse grain and fine grain sand

E. The Effects of Some Wave and Soil Parameters on the Pressure Response of Soil

Until now, the effects of compressibility and the permeability of soil on the pressure response have been demonstrated. In this part of the dissertation, the effects of soil depth, shear modulus and period on the wave-induced soil response will be presented based on the developed numerical model.

Also, it is noticed that the magnitude of pressure oscillation does not change the response of the pressure. In other words, the normalized pressure distributions remain similar with the varying magnitude of pressure fluctuations. However, if the magnitude of the pressure fluctuation increases, the magnitude of pressure gradients also increases. Therefore, under larger pressure fluctuations, the resulted sand leakage would be expected to be larger.

1. The Effect of Soil Depth on the Pressure Response of Soils

In order to assess the effect of soil depth on the wave-induced soil response to the pressure fluctuations, with the developed numerical model, 3 different model runs have

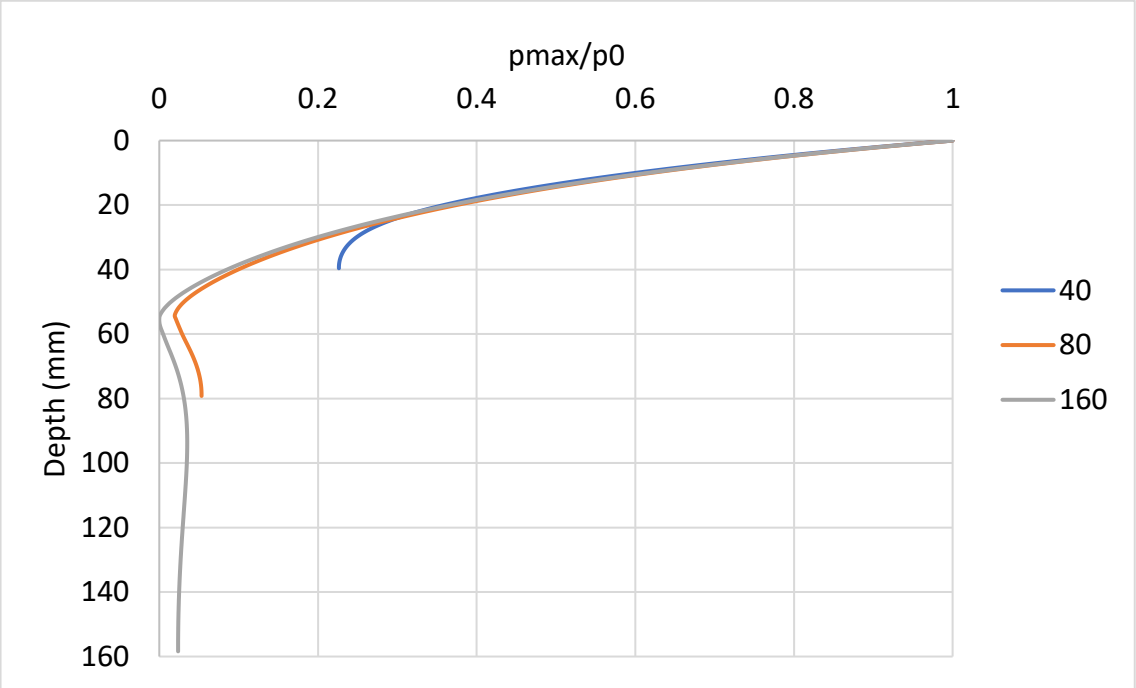

Figure 46 Maximum Normalized Pressure Distribution for various depths (40 mm, 80 mm, and 160 mm) (Same degree of saturation)

been carried out using 3 different depths (40 mm, 80 mm, and 160 mm). Figure 46 shows the maximum normalized pressure distribution for various depths. The vertical axis shows the real soil depth rather than the normalized soil depth. It is realized that the pressure distribution at the top of the soil layer is similar for all cases. The reason behind this result has been recognized as the use of the same degree of saturation for all cases.

Therefore, another 3 simulations with 3 different depths (40 mm, 80 mm, and 160 mm) have been carried out. However, in these cases, the amount of air has been kept constant rather than the degree of saturation. So, for a soil depth of 40 mm, the degree of saturation has been assumed as 89.4%. For a soil depth of 80 mm, the degree of saturation has been assumed as 94.7%. And, finally, for a soil depth of 160 mm, the degree of saturation has been assumed as 97.3%. Figure 47 shows the maximum normalized pressure distribution for various depths when inside the soil mediums the amount of air is same. According to this figure, it can be seen that the pressure response is getting better as the depth of soil increases when the air amount is same due to decreasing degree of saturation. As an example, in the present laboratory condition, if the soil depth was 160 mm rather than 80 mm, the pressure response of both coarse and fine grain soil would be better and relatively small leakage would be observed.

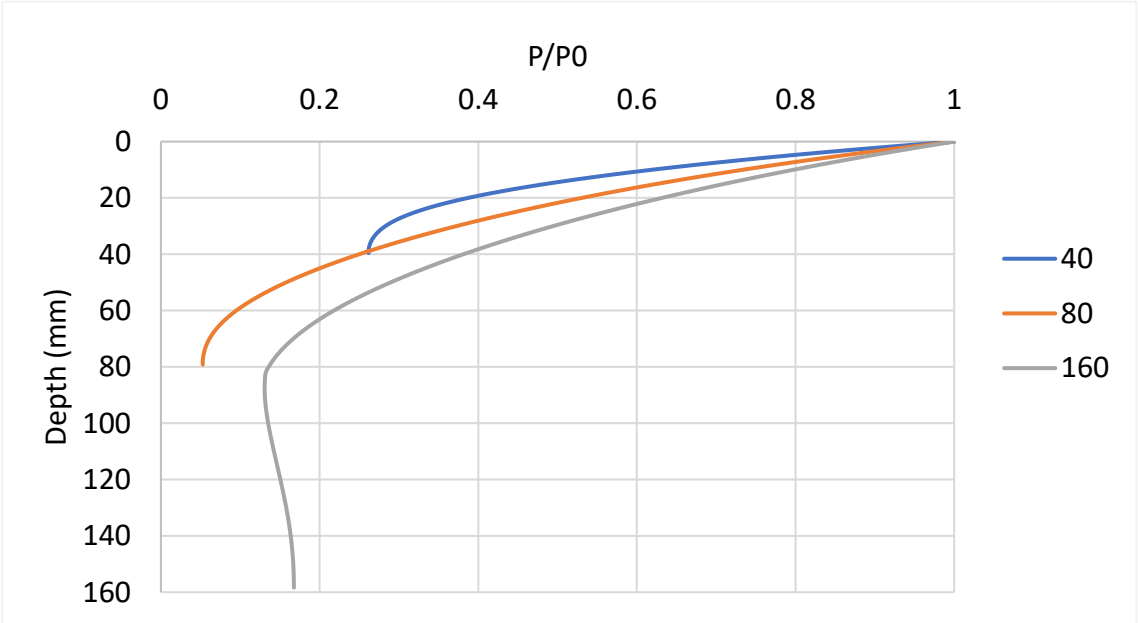

Figure 47 Maximum Normalized Pressure Distribution for various depths (40 mm, 80 mm and 160 mm) (Same amount of air)

2. The Effect of the Shear Modulus on the Pressure Response of Soils

In order to assess the effect of shear modulus on the wave-induced soil response to the pressure fluctuations, with the developed numerical model, 3 different simulations have been carried out using 3 different shear modulus values (2 MPa, 5 MPa, and 10 MPa). Figure 48 shows the maximum normalized pressure distribution for various shear modulus values. According to the figure, the shear modulus has some effects on the pressure response of the soils. Especially, at the bottom layer of the soil, if the shear modulus is large, the response of soil to the pressure fluctuations is poor. If the shear modulus is low, the pressure is transmitted better to the bottom of the soil medium. However, there is no clear difference in the pressure transmission at the top layer with varying shear modulus.

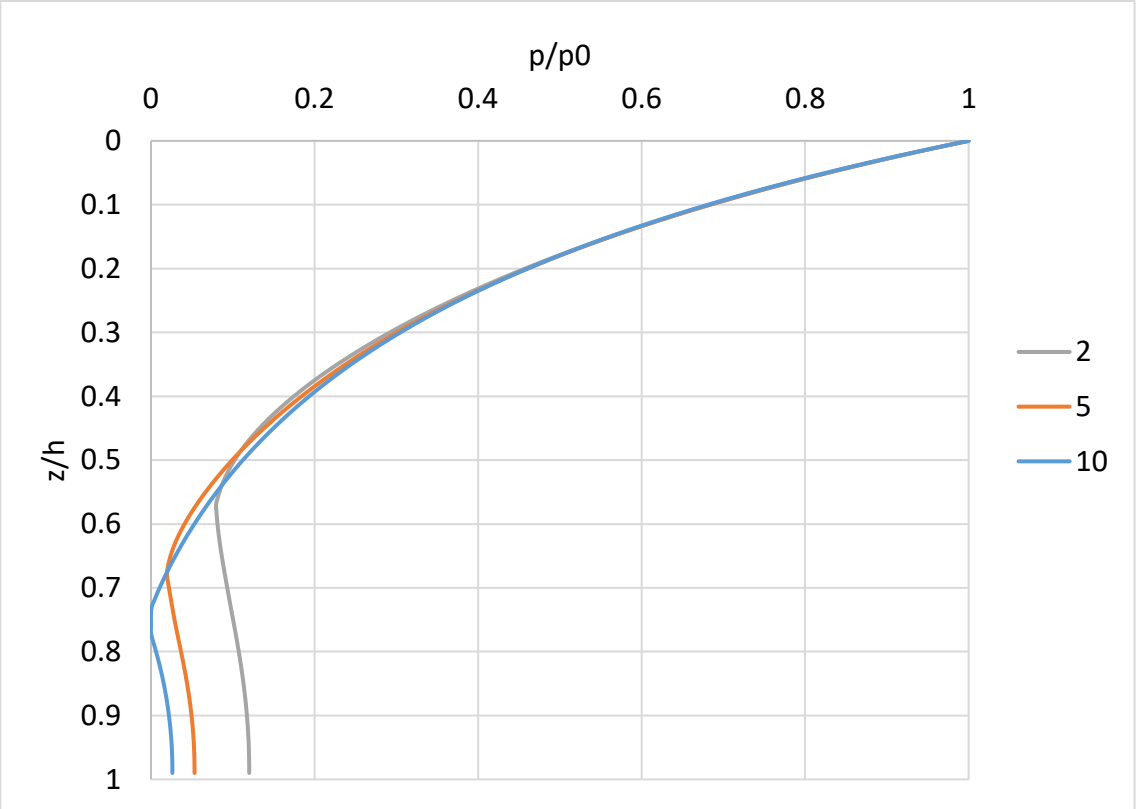

Figure 48 Maximum Normalized Pressure Distribution for various shear modulus values (2 MPa, 5 MPa, and 10 MPa)

3. The Effect of the Wave Period on the Pressure Response of Soils

In order to assess the effect of the wave period on the wave-induced soil response to the pressure fluctuations, with the developed numerical model, 3 different simulations have been carried out using 6 different wave periods (0.1 seconds, 0.5 seconds, 1 second, 2 seconds, 10 seconds, and 100 seconds). Figure 49 shows the maximum normalized pressure distribution for various wave periods. According to the figure, when the period of the wave is small, the transmission of the pressure is poor. However, when the period is very large, the pressure can be transmitted better to the soil medium. From a distinct perspective, the pressure has no time to be transmitted inside the soil medium, when the frequency of the wave is large.

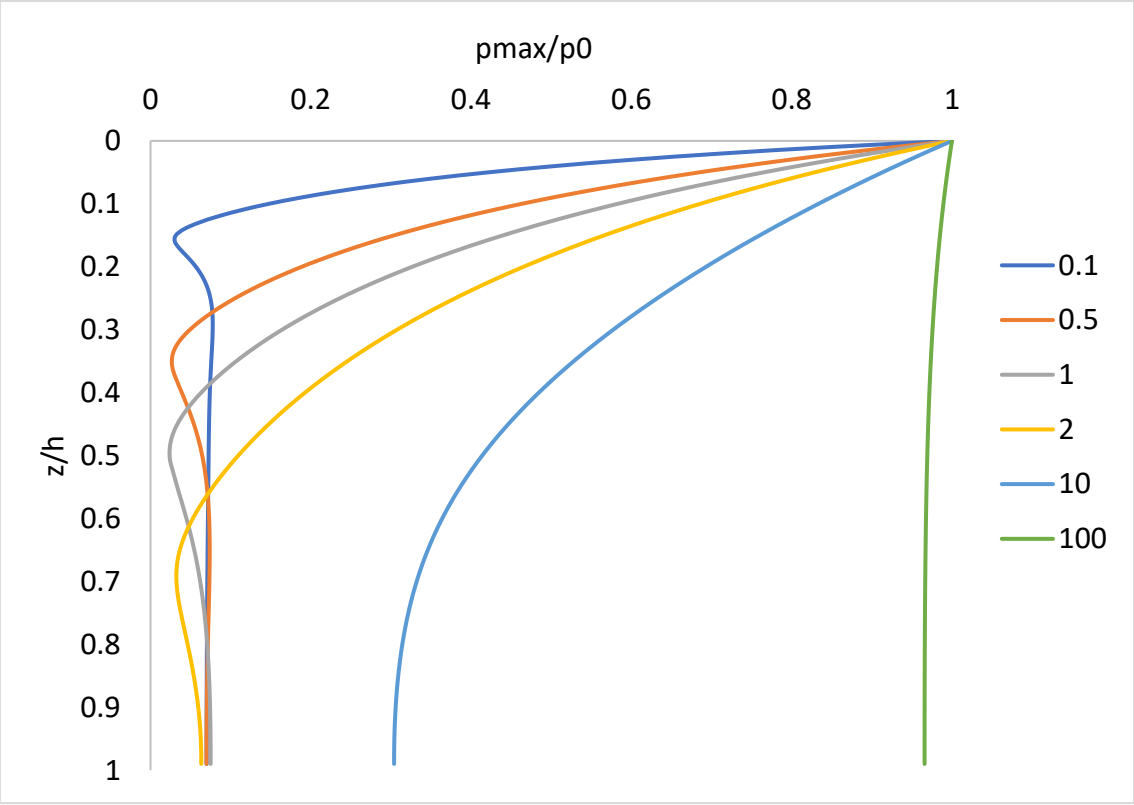

Figure 49 Maximum Normalized Pressure Distribution for various wave periods (0.1 sec, 0.5 sec, 1 sec, 2 secs, 10 secs and 100 sec)

V. DISCUSSION ON RESULTS

A. Comparison of QS Model and Laboratory Experiments

The results of the laboratory experiments on the leakage of sand through a small gap under oscillatory water flow have been compared to the results of the developed and validated numerical model on the wave-induced soil response to confirm the mechanism that leads to the acceleration of the leakage.

As the interpretation of the results of the laboratory experiments is that the pressure gradient near the top layer and the displacements are the driving factors on the sand leakage, the computed maximum pressure gradients at the top layer of the developed numerical model according to grain size and the degree of saturation have been compared to the measured leaked sand area from the laboratory experiments in Figure 50.

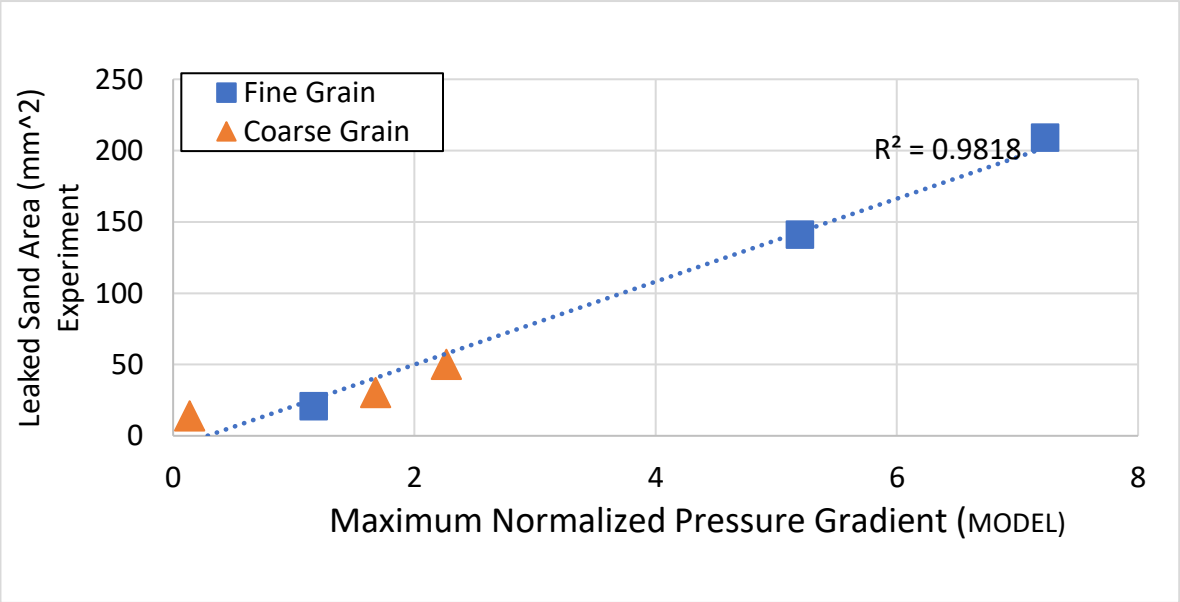

Figure 50 Comparison of maximum normalized pressure gradient at the top layer of the soil medium from the developed numerical model and the leaked sand area from the laboratory experiments

In Figure 50, the orange triangles show the relation between the leaked sand area and the maximum pressure gradient near the top layer of the coarse grain sand, while the blue squares show the case for the fine grain sand. Combining these, the line that has been fitted to the data shows very strong correlation. As proposed in the hypothesis of this study, in the leakage of sand for the laboratory experiments, the pressure gradient near the water-soil interface plays a significant role. The leaked sand area increases as the

pressure gradient increases. The pressure gradient increases with the poor pressure response of the soil depending on the wave and soil parameters.

Another factor on the leakage of sand is the displacements of the soil under pressure oscillations. It has been determined that two main parameters that induce the displacement. The first one is related directly to the compressibility of the air. The pressure oscillations near the balloons contracts or expands the balloons that will induce a displacement in the soil medium. To account this effect with a theoretical approach, the attenuated pore pressure near the air balloons has to be calculated by the developed numerical model. And, the relation between the displacements and the compressibility of air should be explained.

The other parameter that induces the displacement of soil medium is the pressure gradient. From the video recordings, it is realized that due to high-pressure gradients when the air is introduced, the soil medium is disturbed significantly under pressure fluctuations. Therefore, the effect of pressure gradient on the displacement of soil should be also considered. However, rather than the top layer, the difference in pressure of the whole layer from bottom to top has been considered as it disturbs the soil and induces the displacement. Also, as mentioned in the results of the laboratory experiments, the recorded displacements have been measured away from the gap. Since the displacements have been observed to be higher due to high-pressure gradient near the top layer and it is hard to find a standard point for the measurement.

For the displacements, to combine the effects of the two factors (the compressibility of air and the pressure difference from top to bottom), a regression analysis has been made with non-dimensional parameters representing these two factors. Firstly, the dimensionless parameter for the compressibility of air will be presented. As there is no heat exchange, the following equation can be written,

$$PV^{\gamma} \approx \text{constant} \qquad 49$$

So, for the contraction and expansion during the pressure oscillation, the following equation can be written

$$P_i V_i^{\gamma} = (P_0 + \Delta P) V_{cont}^{\gamma} = (P_0 - \Delta P) V_{exp}^{\gamma} \quad (50)$$

where P_i is initial pressure of air, V_i is initial volume of air, P_0 is the pressure of air under water in steady state, ΔP is the difference of maximum and minimum magnitudes of pressure fluctuations at a depth of 6 cm from the soil-water interface. Since, the balloons are located at the last 2 cm (between 6 cm - 8 cm). V_{cont} is volume of air when the air balloon is contracted when the magnitude of pressure fluctuation is maximum, and V_{exp} is volume of air when the air balloon is expanded when the magnitude of pressure fluctuation is minimum.

If the sum of volumes during the expansion and contraction is assumed to be,

$$V_{exp} + V_{cont} \approx 2V_i \quad (51)$$

Then, the volume difference can be calculated as,

$$\Delta V = V_{exp} - V_{cont} \approx \frac{2\Delta P V_i}{P_i} \quad (52)$$

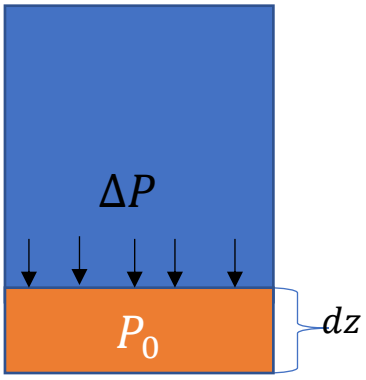

Figure 51 Hypothetical drawing for displacement due to compressibility of air

If the process of contraction and expansion is assumed to be in one-dimensional (Figure 51), then, the displacement due to the air compressibility, d_c can be found to be proportional to

$$d_c \propto \frac{2\Delta P V_i}{P_0 V_{container}} \quad (53)$$

where $V_{container}$ is the volume of the acrylic container and V_i is the initial volume of air introduced to the soil medium. So, the relation between the observed displacements

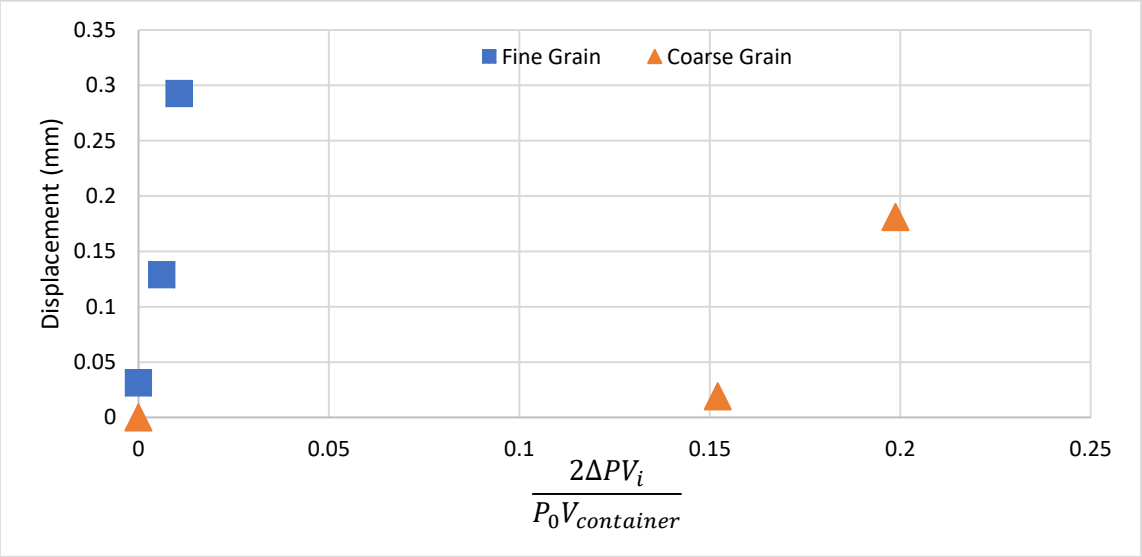

Figure 52 The relation between the displacement from the laboratory experiments and the dimensionless parameter for the compressibility of air

away from the gap from the laboratory experiments and the non-dimensional parameter by the compressibility of air is given in the Figure 52 for coarse and fine grain soil.

For the coarse grain sand, it has been already stated that the pressure transmission is very good. So, the pressure reaching the level of balloons is much higher for the coarse grain soil than the fine grain soil. Therefore, it is expected to have more contraction and expansion in the coarse sand. However, for the same air presence, the fine grain soil shows larger displacement in the laboratory experiments. Therefore, there should be another parameter which affects to displacements in the soil.

The pressure gradient between the top and the bottom of the soil is the second effective parameter on the displacements. It causes a disturbance on the soil medium. Therefore, Figure 53 shows the relationship between the displacements measured during the laboratory experiments and the normalized pressure difference between the top and bottom layer of soil in the maximum pressure distribution.

The pressure difference between the top and bottom of the soil layer, in fine grain soil, is much higher due to the poor response of the soil to pressure oscillations.

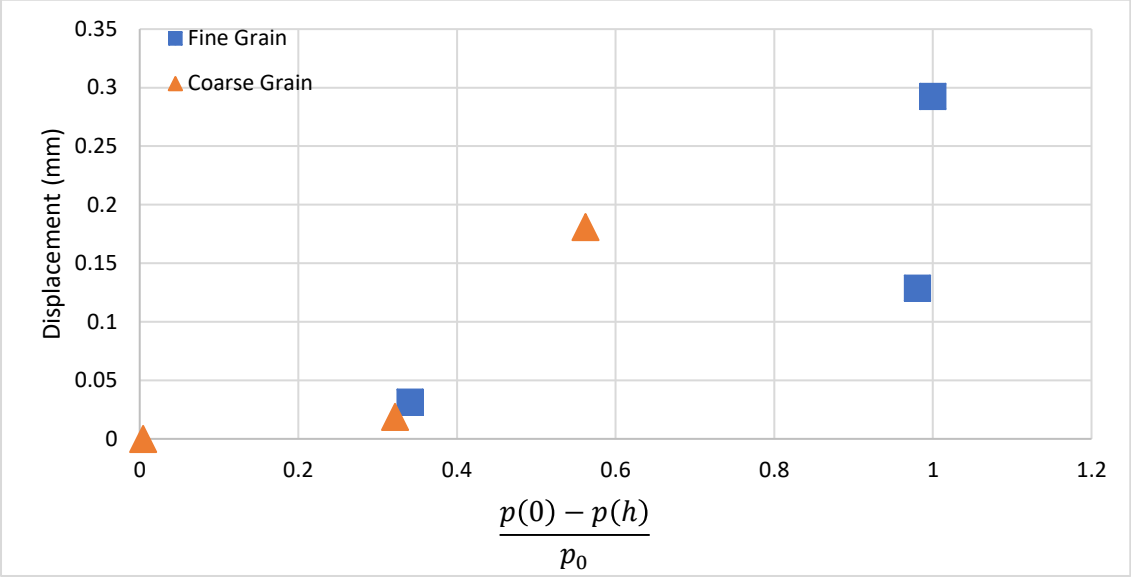

Figure 53 The relation between the displacement from the laboratory experiments and the dimensionless parameter for the pressure difference between top and bottom of soil layer

Using the two dimensionless parameters ($\frac{2\Delta PV_i}{P_0 V_{container}}$ and $\frac{p(0)-p(h)}{p_0}$), from the regression analysis, the following equation has been obtained.

$$\frac{d_s}{h} = C_1 + C_2\left(\frac{p(0)-p(h)}{p_0}\right) + C_3\frac{2\Delta PV_i}{P_0 V_{container}} \qquad 54$$

with the C_1, C_2 and C_3 are being the coefficients and h is the depth of soil medium. The values assigned to them from the regression analysis has been presented in the Table 11.

Table 11 The coefficients based on the regression analysis

C_1	-4.28×10^{-4}
C_2	3.07×10^{-3}
C_3	2.33×10^{-3}

Figure 54 shows the relation with the regressed equation and the normalized displacement values obtained from the laboratory experiments. In the horizontal axis, the regressed equation shows the combination of two effective non-dimensional parameters on the displacement. According to this graph, the displacement can be obtained indirectly with the dimensionless parameters

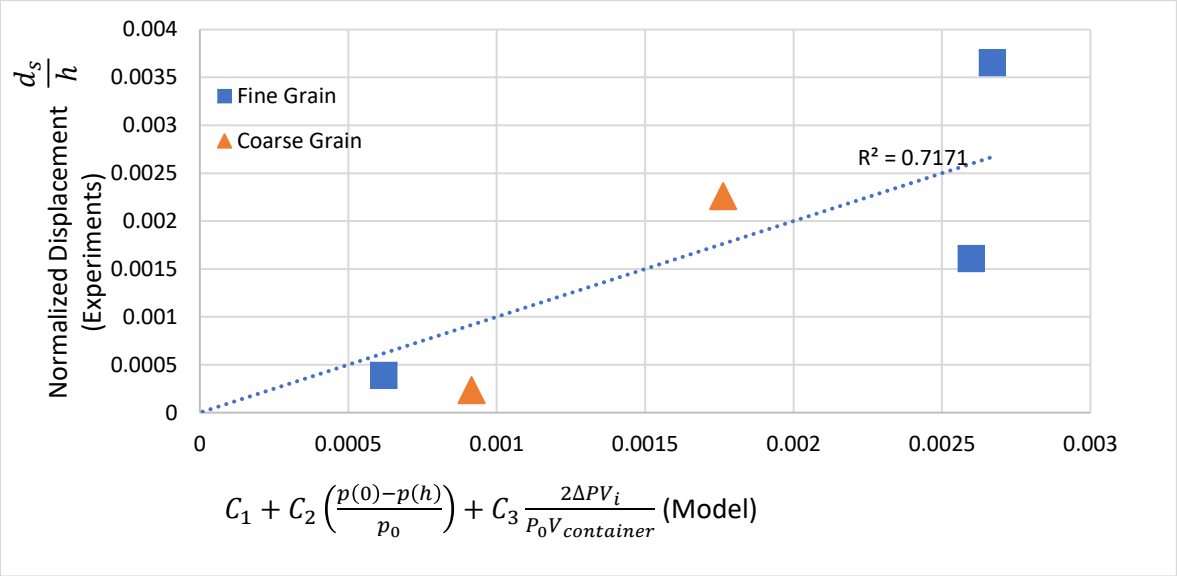

Figure 54 The relation with the regressed equation and the normalized displacement values

B. Topics Left for Further Studies

In this part of the dissertation, the faults, the inadequacies, and deficiencies about laboratory experiments and theoretical approach will be mentioned. To further explain the mechanism of void development in seawalls.

One of the most important shortcomings of these experiments is the direction of gravitational acceleration. In these experiments, gravity acts as resisting force. However, in a real seawall environment, according to the layout of the seawall, gravity will act as a driving force. However, in this study, the main purpose is to reveal the acceleration mechanism, rather than the estimating the sand leakage rate. Therefore, the experiments served to this purpose.

The discharge of rainfall and overtopped water through the permeable backfill may also contribute to the leakage of the seawall. Due to the increase of the pressure head on the landward side of the seawall, seepage from land towards sea side may generate and

with the seepage forces, the soil grains may leak through the imperfections of the seawall. However, this process has not been investigated in this study.

Another concern about these experiments is the location of the hole which causes the leakage of sand in the seawall is also very important. If the hole is located near the mean sea level, then the leakage may depend on also the wave velocities and breaking characteristics rather than just pressure oscillations. However, if the hole is in relatively deep water or protected from direct wave attack by the armor stones, the main driving force will be the pressure oscillations.

To grasp the air content in the backfill soil of a seawall needs comprehensive field study. However, there are some investigations on the size of air bubbles in marine soils. Still, it is very hard to measure the real air content in situ. As reported in Sumer (2014), some studies with geo-endoscopic cameras are promising. Also, indirectly, from pressure measurements, air content in seabed can be proven owing to poor pressure response of soil when the degree of saturation is below 100%.

In this study, air balloons have been used to simulate the void pockets in the backfill of a seawall. Therefore, it is considered that the air content in a seawall environment both very big comparing with grain size and concentrated inside the balloons. However, size and distribution of air bubbles may alter the soil mechanics in the seawall environment. Therefore, it is important to point out that what happens if the air bubbles distributed homogeneously into the soil medium. From compressibility standpoint, the distribution of air will not affect the general compressibility of the soil medium. However, laboratory experiments in this study have been carried out with placing balloons at the bottom of the container. Homogeneous distribution of air would change the absolute pressure of air bubbles. As a result, the compressibility may change slightly. From the permeability point, small air bubbles will decrease the hydraulic conductivity significantly by blocking the pore water flow through the sand grains. Therefore, the response of the soil will decrease and the pressure gradients causing the leakage of the sand will increase significantly.

VI. CONCLUSION AND RECOMMENDATIONS

A. Conclusion

This study has revealed the acceleration mechanism of void development in the seawalls. With increasing air content, large pressure gradients are generated near the soil-water interface which intensifies the leakage of sand. Getting more compressible with time, the backfill will lose the filler soil faster. This process has been confirmed through both laboratory and theoretical analysis. On a hypothetical time axis, the void development in the backfill of a seawall can be expected as the Figure 55. In other words, the void development in the backfill is to be expected an exponential line with the time as in Equation 12.

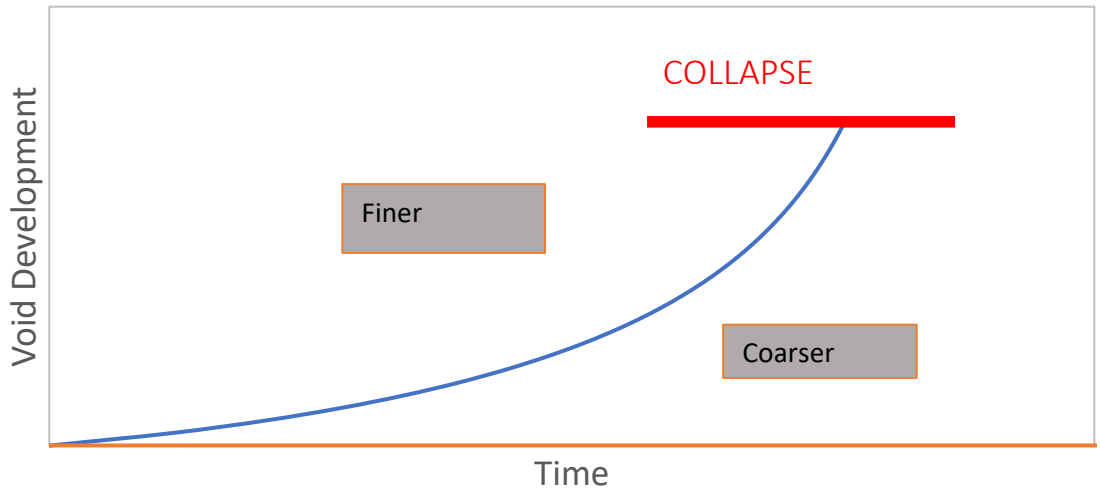

Figure 55 Void development in the backfill of a seawall with time

In fine grain soil, the void development is faster than in coarse grain soil. However, in any case, if voids start developing in a backfill, it is inevitable to have a failure in the seawall due to the enlargement of the voids following the leakage of backfill material.

Furthermore, in this study, the wave-induced pressure transmission in the soil has been modeled with the quasi-static assumption based on the poroelasticity equations in the one-dimensional domain. The model has been verified with laboratory experiments of earlier researchers. Also, the measurements of leakage from the laboratory experiments have been compared with the results of the developed numerical model. A good

correlation has been obtained with the comparison between the results of laboratory experiments and numerical model according to the argument of this study.

In the laboratory experiments, the displacement caused by the pressure oscillations has two mechanisms. The first one is the expansion and contraction of the balloons under the pressure oscillation. The second mechanism that causes the displacement in soil layer is the disturbance effect of pressure gradient on the stability of the soil medium. As the pressure gradient destabilizes the soil layer, it also contributes to the displacement of soil particles.

Both the laboratory experiments and the developed numerical model have confirmed that the pressure response is getting poorer as the permeability of soil decreases and as the compressibility of soil increases. As the pressure applied to the top of the soil surface cannot be transmitted to the bottom of the soil, the generated pressure gradient is large when the pressure response is poor. Consequently, the seepage forces on the soil grains induce large leakage of sand. With the developed model, the phase lag during the transmission of the pressure from the top to the bottom of soil has also been analyzed. Furthermore, the effects of soil depth, shear modulus, wave period on the wave-induced seabed response have been analyzed with the developed model.

The void development mechanism and the leakage of backfill through a small gap under pressure oscillations have been studied in this thesis. From a practical approach, if the backfill material leaks towards the sea, the subsidence or another type of failure is inevitable. Therefore, geotextile or the filter layers should be protected from the harsh environment. Therefore, protecting tools such as armor layers and toe protections are necessary to decrease the amplitude of pressure acting on the geotextile or filter layer. Also, in the case of a subsidence, the reason of subsidence should be unraveled. The geotextile layer or filter layer should be repaired and, if necessary, the toe scour and armor layer should be strengthened.

B. Recommendations

A field study is necessary to fully understand the mechanism of void development in seawalls. The laboratory experiments are affected by the scale of the generated forces. At the laboratory, the used soil is same that is found in the field. However, in a laboratory

environment, the forces are not as much as in the field. Furthermore, the behavior of sand leakage dependent on the compressibility of the soil which is almost impossible to arrange in the laboratory. However, it is hard to carry out a field study for this subject as the location of the void development of a backfill is not known before the failure. Besides, the amount of time necessary to cause such destruction is not clear. Therefore, a long-term, continuous monitoring until the destruction of a seawall is necessary. Also, with a short-term monitoring, the before, after and during storm conditions of the voids can be investigated.

Also, the content of the voids should be examined. As the voids might be filled with air or water, it is very important to account the air content from compressibility point of view. Also, the location of the voids is very important as how far they are located from the gap. Furthermore, the distribution of air content may have significant effects on permeability. It is expected to be lower permeability when the air is distributed homogeneously due to the blockage of pore water movement.

In the current laboratory experiments, the effects of gravity could not be assessed due to the arrangement of the equipment. In a real seawall environment, gravity can be one of the most important forces which contribute to leakage of backfill material. Therefore, a sound investigation on gravity effects on the leakage of backfill material is needed.

In the laboratory experiments, the generated water flow had only horizontal component. In a progressive wave, a vertical component may also affect the leakage rate. It can be another valuable study topic.

The effects of a gap on shear stress and pressure transmission should be investigated both experimentally and numerically. The conclusion about the effect of the gap in this study, when the gap is narrow, the shear stress cannot move sediments. Only the pressure difference can lift the sand. However, as the gap gets wider, the pressure difference loses its influence and shear stress becomes more effective. To fully understand the behavior of sand depending on the gap, more experiments are needed.

Also, the effects of rainfall and overtopping on the leakage should be investigated. Because they can also generate seepage flows which may contribute to the leakage of sand.

VII. REFERENCES

- Bierawski, L. G., Maeno, S., Gotoh, H., & Harada, E. (2002). DEM-FEM model of the outflow of backfilling sand from behind a seawall under wave motion. *Proc., 5th Int. Conf. on Hydro-Science and Engineering.*
- Biot, M. A. (1941). General theory of three-dimensional consolidation. *Journal of applied physics*, *12*(2), 155-164.
- Biot, M. A. (1956). Theory of propagation of elastic waves in a fluid-saturated porous solid. I. Low-frequency range. *The Journal of the Acoustical Society of America*, *28*(2), 168-178.
- Chowdhury, B., Dasari, G. R., & Nogami, T. (2006). Laboratory Study of Liquefaction due to Wave–Seabed Interaction. *Journal of Geotechnical and Geoenvironmental Engineering*, *132*(7), 842–851. https://doi.org/10.1061/(ASCE)1090-0241(2006)132:7(842)
- Craig, R. F. (2004). *Craig's soil mechanics*. CRC Press.
- Dong, L. P., Sato, S., & Liu, H. (2013). A sheetflow sediment transport model for skewed-asymmetric waves combined with strong opposite currents. Coastal Engineering, 71, 87–101. https://doi.org/10.1016/j.coastaleng.2012.08.004
- Harleman DRF, Melhorn PF, Rumer RR (1963). Dispersion-permeability correlation in porous media. Am. Soc. Civ. Eng., (NY), 89: 67-85.
- Hur, D.-S., Nakamura, T., & Mizutani, N. (2007). Sand suction mechanism in artificial beach composed of rubble mound breakwater and reclaimed sand area. *Ocean Engineering*, *34*(8–9), 1104–1119. https://doi.org/10.1016/j.oceaneng.2006.08.005
- Ishihara, K., & Yamazaki, A. (1984). Analysis of wave-induced liquefaction in seabed deposits of sand. SOILS AND FOUNDATIONS, 24(3), 85–100. https://doi.org/10.3208/sandf1972.24.3_85
- Jeng, D. S. (2003). Wave-induced sea floor dynamics. Applied Mechanics Reviews, 56(4), 407. https://doi.org/10.1115/1.1577359
- Jeng, D. S., & Cha, D. H. (2003). Effects of dynamic soil behavior and wave non-linearity on the wave-induced pore pressure and effective stresses in

porous seabed. Ocean Engineering, 30(16), 2065–2089. https://doi.org/10.1016/S0029-8018(03)00070-2

- Jeng, D. S., Barry, D. a., & Li, L. (2000). Water wave-driven seepage in marine sediments. *Advances in Water Resources*, *24*(1), 1–10. https://doi.org/10.1016/S0309-1708(00)00036-1
- Jeng, D.-S. (2013). Porous models for wave-seabed interactions, Jointly published by Shanghai Jiao Tong University Press, and Springer Heidelberg, London.
- Kirca, V. S. O., Sumer, B. M., & Fredsoe, J. (2013). Residual Liquefaction of Seabed under Standing Waves. Journal of Waterway Port Coastal and Ocean Engineering, 139(6), 489–501. https://doi.org/Doi 10.1061/(Asce)Ww.1943-5460.0000208
- Maeno, S., & Nago, H. (1983). Effect of Displacement Method on Sand Bed Liquefaction under Oscillating Water Pressure. Proceedings of the Japanese Conference on Hydraulics, 27(1), 621–626. https://doi.org/10.2208/prohe1975.27.621
- Maeno, Y. H., & Hasegawa, T. (1985). Evaluation of wave-induced pore pressure in sand layer by wave steepness. *Coast. Eng. Japan*, *28*, 31-44.
- Magda, W. (1996). Wave-induced uplift force acting on a submarine buried pipeline: Finite element formulation and verification of computations. Computers and Geotechnics, 19(1), 47–73. https://doi.org/10.1016/0266-352X(95)00036-A
- Magda, W., Maeno, S., & Nago, H. (1998). Wave-Induced Pore-Pressure Response on a Submarine Pipeline Buried in Seabed Sediments - Experiment and Numerical Verification -. Journal of the Faculty of Environmental Science and Technology. Okayama University, 3(1), 75–95.
- Mei, Chiang ; Foda, M. (1981). Wave-induced Responses in a Fluid Filled Poro-Elastic Solid with a Free Surface - A Boundary Layer Theory. Geophysical Journal. Royal Astronomical Society, 66, 597–631.

- Mizutani, N., Mostafa, A. M., & Iwata, K. (1998). Nonlinear regular wave, submerged breakwater and seabed dynamic interaction. Coastal Engineering, 33(2–3), 177–202. https://doi.org/10.1016/S0378-3839(98)00008-8
- Mory, M., Michallet, H., Bonjean, D., Piedra-Cueva, I., Barnoud, J. M., Foray, P., Abadie, S., Breul, P. (2007). A Field Study of Momentary Liquefaction Caused by Waves around a Coastal Structure. Journal of Waterway, Port, Coastal, and Ocean Engineering, 133(1), 28–38. https://doi.org/10.1061/(ASCE)0733-950X(2007)133:1(28)
- Mostafa, A. M., Mizutani, N., & Iwata, K. (1999). Nonlinear Wave, Composite Breakwater, and Seabed Dynamic Interaction. Journal of Waterway, Port, Coastal, and Ocean Engineering, 125(2), 88–97. https://doi.org/10.1061/(ASCE)0733-950X(1999)125:2(88)
- Nago, H. (1982). Liquefaction of highly saturated sand layer under oscillating water pressure. *Memoirs of the School of Engineering, Okayama University*, *16*(1), 91-104.
- Nakamura, T., Hur, D.-S., & Mizutani, N. (2008). Mechanism of Backfilling Sand Discharge from a Gap under Vertical Revetment. *Journal of Waterway, Port, Coastal, and Ocean Engineering*, *134*(3), 178–186. https://doi.org/10.1061/(ASCE)0733-950X(2008)134:3(178)
- Sakai, T., Mase, H., & Matsumto, A. (1988). Effects of inertia and gravity on seabed response to ocean waves. In: Modelling Soil-Water-Structure Interaction, pp. 61–66. A.A. Balkema, The Netherlands
- Sumer, B. M. (2014). Liquefaction Around Marine Structures:(With CD-ROM). World Scientific.
- Takahashi, S., Suzuki, K., Tokubuchi, K., & Shimosako, K. (1997). Experimental Analysis of the Settlement Failure Mechanism Shown by Caisson-Type Seawalls. In *Coastal Engineering 1996* (pp. 1902–1915). New York, NY: American Society of Civil Engineers. https://doi.org/10.1061/9780784402429.148
- Terzaghi, K. (1943). Theoretical soil mechanics. New York: Wiley.

- Tsotsos, S., Georgiadis, M., & Damaskinidou, A. (1989). Numerical analysis of liquefaction potential of partially drained seafloors. Coastal Engineering, 13(2), 117–128. https://doi.org/10.1016/0378-3839(89)90019-7
- Tsui, Y., & Helfrich, S. C. (1983). Wave-Induced Pore Pressures in Submerged Sand Layer. *Journal of Geotechnical Engineering*, *109*(4), 603–618. https://doi.org/10.1061/(ASCE)0733-9410(1983)109:4(603)
- Ulker, M. B. C., & Rahman, M. S. (2009). Response of saturated and nearly saturated porous media: Different formulations and their applicability. *International Journal for Numerical and Analytical Methods in Geomechanics*, *33*(5), 633–664. https://doi.org/10.1002/nag.739
- Wheeler, S. J. (1986). *The stress-strain behaviour of soils containing gas bubbles* (Doctoral dissertation, University of Oxford).
- Verruijt A (1969), Elastic storage of aquifers, Flow Through Porous Media, RJM De Wiest (ed), Academic Press, New York, 331–376.
- Zen, K., & Yamazaki, H. (1990). Mechanism of wave-induced liquefaction and densification in seabed. *Soils and Foundations*, *30*(4), 90–104. https://doi.org/10.3208/sandf1972.30.4_90
- Zienkiewicz, O. C., Chang, C. T., & Bettess, P. (1980). Drained, undrained, consolidating and dynamic behaviour assumptions in soils. *Geotechnique*, *30*(4), 385-395.
- Zonguldak'ta deniz kıyısındaki kaldırım ve yol çöktü. (2015, 6 25). Retrieved from CNN TURK: http://www.cnnturk.com/